Study of the microbial competition between homoacetogens and hydrogenotrophic methanogens in aerobic mixed cultures for acetate production from H2/CO2 : an experimental and modelling approach

Léa Laguillaumie

Université Fédérale
Toulouse Midi-Pyrénées

THESIS

For the award of a

DOCTORATE OF THE UNIVERSITY OF TOULOUSE

Issued by Institut National des Sciences Appliquées de Toulouse

---

Defended by

Léa LAGUILLAUMIE

On 9 September 2022

Study of the microbial competition between homoacetogens and hydrogenotrophic methanogens in anaerobic mixed cultures for acetate production from H2/CO2: an experimental and modeling approach.

PhD School: **MEGEP - Mécanique, Energétique, Génie civil, Procédés**

Department: **Génie des Procédés et de l'Environnement**

Research Laboratory:

TBI - Toulouse Biotechnology Institute, Bio & Chemical Engineering

Supervised by

Etienne PAUL and Claire DUMAS

The jury members
Mr. Théodore BOUCHEZ, Directeur de recherche INRAE, PROSE, France – Reviewer
Mr. Ramon GANIGUE, Professor Ghent university, Belgium – Reviewer
Mr. Mohammad TAHERZADEH, Professor Borås university, Sweden – Reviewer
Mrs. Hariklia GAVALA, Associate professor DTU, Denmark – Examiner
Mr. Nicolas ROCHE, Professeur Université Aix-Marseille, France – Jury president
Mr. Jean-Philippe DELGENES, Directeur de recherche INRAE, LBE, France – Examiner
Mr. Etienne PAUL, Professeur INSA, TBI, France – PhD Supervisor
Mrs. Claire DUMAS, Chargée de recherche INRAE, TBI, France – PhD Co-supervisor
Mr. Matthieu PEYRE-LAVIGNE, Ingénieur de recherche, CRITT GPTE, France – Invited

Abstract

Capturing carbon dioxide (CO_2) is a major challenge for developing a low-carbon economy. In addition, the reduction of CO_2 allows the synthesis of platform molecules for the chemical and energy industry. Anaerobic mixed cultures contain homoacetogenic microorganisms (HAC) capable of reducing CO_2 to acetate. However, one of the obstacles to their use is the understanding and control of their functional diversity. In particular, managing the competition between HACs and hydrogenotrophic methanogens (HMs) that convert CO_2 into methane is crucial to produce acetate.

The study contributes to bring new knowledge on the competition between HAC and HM. For this, notions of mass transfer between the gas phase where the substrates are located, and the liquid phase which contains the microbial catalysts (G/L), as well as kinetic and thermodynamic aspects of biological reactions have been integrated.

Microbial competition was studied using data from an *ex situ* biological methanation reactor of H_2/CO_2, in mixed and thermophilic culture. In parallel, microbial growth modeling work specific to each microorganism was carried out in order to study their behaviour in batch and continuous reactors. Maintaining a G/L mass transfer rate higher than the gas consumption rate appeared decisive to promote the growth of HACs. These modeling results, coupling microbial kinetics and thermodynamics of reactions, made it possible to identify favourable environments for HAC selection. They were then confronted with an experimental plan in order to study the system in real conditions.

As part of the experimental plan, batch and then continuous reactors at 25 °C and 35 °C were set up. In batches, the lifting of the limitation by the transfer of gas, as well as the lowering of the temperature to 25 °C made it possible to select mixed anaerobic cultures for the HAC function by eliminating the methanogens, after four successive batches of 4 to 6 days each.

In continuous reactors, the effect of pH between 5 and 7 and dilution rate between 0.1 and 1 d^{-1} has been studied. At neutral pH, a significant acetate productivity of 0.296 $molC.L^{-1}.d^{-1}$ could be observed over several residence times. Moreover, lowering the pH to 5 did not eliminate the HMs. On the other hand, a zone of critical dilution rate of the HMs could be identified between 0.25 and 0.38 d^{-1}, while the HACs were maintained in the reactor up to the maximum tested value of 1 d^{-1}.

Interestingly, the model showed that these reactors were not limited by the G/L mass transfer, but by the reaction thermodynamics, thus setting a maximum acetate concentration, which imposes the gas consumption rate. These results demonstrate the potential of using continuous reactors to wash out methanogens and select HAC on H_2/CO_2 in anaerobic mixed cultures. Thanks to a work of optimization of the culture medium for the HAC, the mixed culture could be enriched up to 75 % in *C. autoethanogenum*, after the addition of vitamins in the culture medium. At 25 °C, the production of ethanol and the elongation in butyrate and hexanoate could be observed, although minor.

During this study, an adaptable model allowing to describe the microbial competition was developed. It made it possible to show the different types of limitations of the system: the G/L mass transfer, the thermodynamics of the reactions, or the nutrients of the liquid phase. Understanding the system has allowed the development of techniques for enriching mixed cultures with HAC. These results constitute a database for the optimization of the production of platform molecules from H_2/CO_2, without recourse to chemical or thermal inhibitions of HMs.

Acknowledgements

I would first like to thank my supervisors Pr. **Etienne Paul** and Dr. **Claire Dumas** for entrusting me with this thesis work. Having the opportunity to work with you has been an extraordinary professional and personal experience. I learned a lot from our scientific discussions and I always felt supported throughout this unique adventure. Today, I am very proud to have built my research mind alongside you.

I sincerely thank Associate Professor **Hariklia N. Gavala** and Associate Professor **Ioannis V. Skiadas** for giving me the opportunity to carry out part of this thesis within their research team at the Technical University of Denmark (DTU). Your scientific experience in the field of gas fermentation helped me a lot, and it has been a great pleasure to work with you. I really enjoyed my stay with you and I am very grateful for your welcome and your kindness. I would also like to thank **Cesar** and **Malthe** for welcoming me and helping me during my experiments in DTU lab, as well as **Antonio** for all the scientific discussions we had and his help with data analysis.

I particularly thank Dr. **Matthieu Peyre-Lavigne** for his great contribution and support in the modeling tasks of this thesis. Matthieu, thank you for always making yourself available, and for all the moments we shared, our scientific, but also non-scientific discussions, in the morning over coffee, at lunchtime over crosswords.

I would like to thank the team of engineers at EAD9 without whom this thesis work could not have been carried out. Thank you for your help with the analysis of my samples, the construction of my reactor, and for all the technical problems that I may have encountered, and which you resolved.

I am endlessly grateful to all the members of the team **EAD9** for all these beautiful years spent inside and outside the lab. We had the chance to organise nice events all together, which helped to maintain a team spirit and a cohesion between us all. I will never forget the football and basketball sessions, badminton and volleyball at INSA, the traditional canoe and Christmas events, the “auberges espagnoles”, the journeys together during conferences… Obviously, this list cannot be exhaustive. Thank you everyone for making my daily work life a celebration.

I want to address a special thanks to the PhD students I had the chance to work with: **Sidonie**, my thesis partner since we started together, evolving in the lab alongside you inspired and pushed me a lot; **Emilie**, you were a cornerstone when I arrived, your seriousness in the lab, and your enthusiasm for hanging out with other doctoral students always amazed me; **Mattéo**, Thank you for all our discussions about our existential scientific problems (μ=D), and for all the improbable things I learned thanks to you; **Irene**, you were a resource person in all respects, both technically in the lab and during our evening outings, thank you for being my unconditional partner for dancing and laughing until the end of the night; **Paolina**, our

friendship is one of the greatest things that could have happened to me, and I will never be able to thank you enough for the love, joy and support you brought me when you came into my life; **Morgane**, you have greatly contributed to my ecological awareness, your activism inspires me enormously, thank you for all these beautiful moments shared; **Sylvain**, thank you for all the wonderful evenings we spent playing board games, I discovered lots of them thanks to you; **Mathilde**, thank you for your help and welcome when I arrived in the team, it was so comfortable to know that whatever my question, you could answer it; **Beatriz**, Thank you for always throwing yourself fully into your projects, thanks to you we were able to give birth to our most beautiful audiovisual pieces; **Aldo**, thank you for the good Mexican dishes I was able to taste, and all the good time we spent together.

Loïc, thank you for being by my side throughout my thesis, and even before, for always supporting me. Spending time with you makes me feel lighter, happier. I look forward to our future projects together, you are the best partner, I love you.

Of course, I would like to thank my best and unconditional friends **LéMaChloAnLauCaLé**. Our friendship made me become the woman I am today. Over all these years we have experienced so many beautiful things together, and I can't wait for those to come. Thank you for always listening to my moods, always giving me good advice, and allowing me to let go during our countless evenings rebuilding the world, I love you.

Anaïs, I can't tell how much I love you because you are the best sister anyone could have in the world. My sister process, I know that whatever happens to me I can always count on you.

I would like to thank my parents. **Dad**, **mom**, you have always believed in me, you have always encouraged me during my thesis, and your love has carried me every single day since I was born. Thanks to you, I became who I am, and I can never thank you enough, I love you.

Scientific communications, teaching and interns supervision

Published articles in peer review journals:

Laguillaumie L., Peyre-Lavigne M., Grimalt-Alemany A., Gavala H.N., Skiadas I.V., Paul E., Dumas C. Controlling the microbial competition between hydrogenotrophic methanogens and homoacetogens using mass transfer and thermodynamic constraints. Journal of Cleaner Production, Volume 414 (2023). https://doi.org/10.1016/j.jclepro.2023.137549.

Laguillaumie, L., Rafrafi Y., Moya-Leclair E., Delagnes D., Dubos S., Spérandio M., Paul E., Dumas C. Stability of Ex Situ Biological Methanation of H2/CO2 with a Mixed Microbial Culture in a Pilot Scale Bubble Column Reactor. Bioresour technol 354, 127180 (2022). https://doi.org/10.1016/j.biortech.2022.127180

Rafrafi, Y., **Laguillaumie, L.** & Dumas, C. Biological Methanation of H2 and CO2 with Mixed Cultures: Current Advances, Hurdles and Challenges. Waste Biomass Valor 12, 5259–5282 (2021). https://doi.org/10.1007/s12649-020-01283-z

Communications in national and international conferences:

« Enrichment method in successive batches for homoacetogens isolation within a microbial mixed culture grown on H2/CO2 » - **Laguillaumie L.**, Grimalt-Alemany A., Peyre-Lavigne M., Skiadas I., Gavala H., Paul E., Dumas C. - WasteEng (Copenhagen, Denmark) **2022**. ***Oral presentaiton.***

« Compétitions microbiennes dans le cadre de la valorisation du biogaz en méthane et acide acétique » - **Laguillaumie L.**, Grimalt-Alemany A., Peyre-Lavigne M., Skiadas I., Gavala H., Paul E., Dumas C. JRI Biogaz et Méthanisation (Lyon, France) **2022**. ***Oral presentation.***

« Enrichment of chemolithotrophic microbial mixed cultures (MMC) in a H2/CO2 fermentation CSTR for value-added chemicals synthesis. » - **Laguillaumie L.**, Rafrafi Y., Dubos S., Bounouba M., Moya-Leclair E., Paul E., Dumas C. - IWA Resource Recovery (Ankara, Turquie) **2021**. ***Oral presentation - visioconference (due to covid).***

« Orientation of biogas recovery towards the production of methane or organic acids in anaerobic mixed cultures biogas, methane, organic acids, anaerobic digestion » - L. Laguillaumie, Y. Rafrafi, E. Paul, E. Mengelle, S. Dubos, M. Bounouba, D. Delagnes, **C. Dumas** - Sardinia symposium (Cagliari, Italy) **2021**. ***Oral presentation.***

« Methane or organic acids production? Identification of key parameters for driving biological methanation processes. » - Rafrafi Y., Laguillaumie L., Contreras V., Lefebvre X., Mengelle E., Delagnes D., Dubos S., Bounouba M., Paul E., Spérandio M., Palmade S., Guerre

V., **Dumas C.** WasteEng2020 (Copenhagen, Denmark) **2021**. ***Oral presentation – visioconference.***

« Stratégies d'orientation de la valorisation du biogaz vers la production de méthane ou d'acides organiques en culture mixte anaérobie. » - **Léa Laguillaumie**, Yan Rafrafi, Etienne Paul, Evrard Mengelle, Simon Dubos, et al. Journées Recherche Innovation Biogaz et Méthanisation 2020, Sep **2020**, Toulouse, France. ⟨hal-02967413⟩. ***Poster and flash oral presentation.***

Teaching: 184h at INSA Toulouse

2021-2022:	Chemistry of aqueous solutions (18h) Mass transfer processes (international master degree) (12h)
2020-2021:	Chemistry of aqueous solutions (36h) Biological reactors (24h)
2019-2020:	Chemistry of aqueous solutions (54h) Microbiology (8h)
2018-2019:	Thermodynamics (24h)

Interns supervision

2021: Aurélien Catalan,	« Gaseous fermentation of H2/CO2 for the production of acetate in anaerobic biological reactor » University of Toulouse III Paul Sabatier Master degree of physico-chemical processes for chemistry, environment and energy
2019: Constance Laloye,	« Development of a methodology for the analysis of active metabolic paths in microbial consortia: application to biological methanation » INSA Lyon Master degree of biochemistry and biotechnologies

Table of contents

List of figures

List of tables

General introduction

1 The resource CO_2

In the context of the climatic emergency, the objective set at COP21 in Paris in 2015 (Paris Agreements) is to keep the increase in global temperature below 1.5-2 °C by 2050 or 2100 according to the scenarios developed. To do this, greenhouse gas (GHG) emissions and the use of carbon or fossil energy sources such as coal, oil and natural gas must be reduced, and a part of these resources must even remain unextracted (Welsby et al., 2021).

CO_2 represents about three quarters of GHG emissions (40 Gt in 2018), its percentage in the atmosphere is increasing because the flows of anthropogenic emissions are greater than the flows absorbed in the natural carbon cycle (Ministère de la transition écologique et solidaire, 2020). This disturbance creates an imbalance, at the origin of the observed climatic transformations. Two main levers are necessary to achieve the set objectives. The first is to reduce anthropogenic CO_2 emissions by developing a new economic model based on rational and sober consumption. The second is to compensate incompressible CO_2 emissions with sustainable carbon sinks, and to develop a renewable energy mix. All of this, which is called circular economy, or low-carbon economy, must meet several criteria to ensure the sustainability of the system, which are: the maximum energy and material efficiency of the sectors, their economic viability, and access to a comfortable way of life for the whole of world's population.

Scientific efforts are developing in two main areas to support this transformation of the global economy. First, the acceleration of the development of already functional technologies to respond as quickly as possible to the current state of emergency. This part of the work must be carried out in close collaboration with industrial partners in the transport, agriculture, building, industry and energy sectors, which are the sectors that emit the most GHGs, representing 86% of emissions in

France in 2018 (Ministère de la transition écologique et solidaire, 2020). Second, the research and study of less mature technologies, aimed at exploring new methods of energy production and material recovery. Indeed, the most efficient of these technologies can then be developed in the context of longer-term low-carbon economy scenarios.

To date, the compensation of CO_2 emissions represents a very high cost for manufacturers, due to its capture and storage. However, CO_2 has direct applications, in the food sector in particular, but for which it must be 99.99 % pure and subject to numerous regulations as to its origin (Grim et al., 2020). Thus, CO_2 waste has been considered as a key carbon resource, which, when it cannot be used directly, can be transformed and reused in other sectors such as chemistry (synthesis of materials, or fine chemistry for the synthesis of active ingredients) or energy (synthesis of energy vectors such as methane, or fuels such as ethanol). Indeed, CO_2 is a globally available, non-toxic, stable carbon resource, and could make it possible to respond to many economic, technical and societal obstacles in the context of economic transformation. In France in 2014, for example, the chemical and the fuel industries were 95 % and 80 % based on fossil resources respectively (Tlili et al., 2014).

Overall, if all organic chemistry was based on CO_2 chemistry instead of oil chemistry, 2 $Gt.yr^{-1}$ of CO_2 could be recycled (Tlili et al., 2014). It is therefore a restricted route, but one that can contribute to reducing GHG emissions and especially the extraction of fossil resources for the chemical industry. In addition, the products of this sector have significant added value, which could benefit to certain processes that have not yet been industrialized for economic reasons. The major scientific challenges of this recovery route are based on the fact that it would be necessary to completely transform the chemistry industry to move from oxidation processes of petroleum-derived hydrocarbons to CO_2 reduction processes. However, CO_2 chemistry already has industrialized applications in organic chemistry, mainly oxidation reactions such as carboxylations (Dumergues, 2016).

The production of fuels from CO_2 is a much larger market, but it also faces other scientific hurdles, particularly in terms of energy efficiency, because the reduction of CO_2 in fuels requires large amounts of energy. Nevertheless, this path cannot be ruled out since in low-carbon scenarios, the energy mix is based on a majority of renewable resources and could therefore make it possible to couple the reduction of CO_2 with the use and storage of this type of energy. This is the case, for example, in the "Power-To-Gas" sector, which makes it possible both to store and to use surplus or intermittent renewable electricity, and to produce hydrogen by water electrolysis. Coupled with the reduction of CO_2, this process also allows to produce methane, and this constitutes the methanation process (Benjaminsson et al., 2013).

2 Challenges for CO_2 chemistry

Currently, about 140 $Mt.yr^{-1}$ of CO_2 are chemically transformed, and the production of urea (precursor of agricultural fertilizers) represents 96-98 % of this flow. The other pathways are therefore largely in the minority, among them there is for example the production of methanol (5 $Mt.year^{-1}$) by hydrogenation, or of salicylic acid (0.17 $Mt.year^{-1}$) by carboxylation (Dumergues, 2016).

As mentioned above, one of the main obstacles to the development of CO_2 chemistry is the energy efficiency of the processes, since a lot of energy is needed to reduce CO_2. Thus, facilities geographically close to the CO_2 source must be preferred, to avoid the costs, energy and GHG emissions associated with the compression and transport of gas.

Then, at the reaction scale, research focuses on the design and development of catalysts that reduce the energy required to activate the reaction. An ideal catalyst would be non-toxic, simple to manufacture and widely available, stable, inexpensive, and recyclable. It should also be able to withstand varying levels of purity and CO_2 concentrations, in order to reduce the costs and energy spent on gas purification (Grim et al., 2020). Thus, this thesis project is included in the context of

developing efficient and sustainable catalysts for the reduction of CO_2 into chemicals and fuels.

3 Biological CO_2 reduction

Different energy sources can be used to reduce CO_2. Light, and in particular solar energy, is naturally used by photosynthetic organisms to reduce CO_2 converting it into biomass. Thus, open ponds, or photobioreactors exist at industrial scale to capture the very low CO_2 concentration from the atmosphere. Photochemistry is inspired by these biological catalysts, and in particular the enzyme RuBisCO (Ribulose Biphosphate Carboxylase Oxygenase), which is responsible for the reduction of CO_2 in these systems, to develop catalysts which use solar energy and carry out more specific reactions. Electricity is another energy source that can be used to supply electrons to the CO_2 reduction reaction. This route is also interesting to recover excess electricity, since the electricity cannot be stored directly. Electrochemical and bioelectrochemical processes can be developed, or the electrolysis of water can be carried out upstream in order to provide H_2 to reduce CO_2. Indeed, the chemical energy contained in certain molecules, such as H_2, can also be used to reduce CO_2. In nature, methanogenic microorganisms thus reduce CO_2 to methane, and homoacetogens to acetate. The enzymes carrying out the reduction of CO_2 in these microorganisms are dehydrogenases such as Fdh (Formiate dehydrogenase) or COdh (carbon monoxide dehydrogenase), which initiate the Wood-Ljungdahl metabolic pathway. The latter allows the production of an acetyl-CoA molecule thanks to the key enzyme acetyl-CoA synthase (Acs) which makes a C-C bond between two carbons coming from two CO_2 molecules. For chemists, this path is a source of inspiration since the creation of C-C bonds is a major challenge to get out of petrochemistry, where C-C bonds are broken through oxidative processes instead. However, the C-C bond is rich in energy, so the chemical processes for its creation operate under conditions of high pressure and temperature (200-500 °C, 1-1000 bar). For example, the Fischer-Tropsch generates hydrocarbons from carbon monoxide and hydrogen with metal catalysts

(Guillou, 2005). Research in chemical catalysis therefore strives to both optimize catalysts in order to reduce pressure and temperature conditions, and to reduce the use of noble metals, which are often better catalysts.

Biocatalysts, whether whole microorganisms or their isolated enzymes, are of great interest because they operate under mild conditions of pressure and temperature. Biotechnology thus makes it possible to lower the energy costs of the processes. Biocatalysts are generally non-toxic, and relatively simple to produce and recycle. Although, the development of bioprocesses for the reduction of CO_2 encounters scientific, technical and economic challenges.

Likewise, the development of mixed microbial cultures (MMCs) catalysts is interesting. Indeed, microbial consortia offer many advantages such as the possibility to combine different biological functions in the same reactor, but also functional redundancy which confers to microbial consortia their adaptability to variations of environmental parameters (Paul et al., 2021; Agler et al., 2011). Moreover, MMCs do not require the sterilization of the equipment before use, which is a considerable advantage, especially for the development of continuous reactors, which are often subject to contamination and require strict conditions of sterility in pure cultures.

However, the often low productivities and the cost of H_2 to reduce CO_2 are limitations to the economic profitability of biological CO_2 reduction processes (Figure 1). Energy efficiency is also a major issue, studied in the context of dedicated life cycle analyses establishing the scenarios according to which these processes are relevant or not. For instance, the price of H_2 from organic waste (dark fermentation) is high (Figure 1), and the choice of the H_2 source is important to ensure the economic viability of the processes. The improvement of processes in terms of energy, and the development of high-performance catalysts are therefore the major scientific stakes addressed by the research on biological CO_2 reduction processes.

Diversifying the portfolio of products synthesized from CO_2 is also a key objective, both to meet

the challenges of the chemical sector and to increase the economic profitability of processes through the production of high value-added molecules.

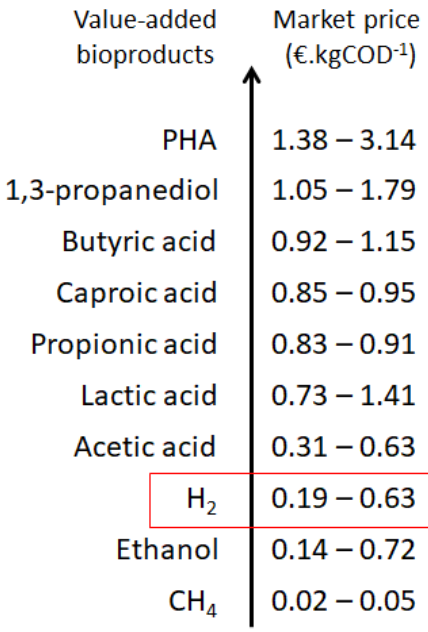

Figure 1: Market price of different chemicals obtained from the valorisation of organic wastes with mixed microbial cultures, and which could also be produced from CO_2 reduction(Salehizadeh et al., 2020; Moscoviz et al., 2018). PHA: Polyhydroxyalkanoates.

Among those molecules of interest, acetate is a platform molecule with many applications, such as the production of solvents, paints and coatings, polymers for the packaging industry, or terephthalic acid (PTA) for the textile industry. Although these sectors must be largely redesigned as part of the transformation of the economy, acetic acid will still be used for the production of polymers and materials in particular, but also for certain medical and food applications. Acetate also has an interesting added value, and represents a market of 16 Mt in 2020, *i.e.* a transformation potential of 23 $Mt.year^{-1}$ of CO_2 (Mordor Intelligence, 2020). About 10 % of the world's acetate is biologically sourced for vinegar production, and the rest is produced by catalytic carbonylation of methanol at high pressures and temperatures. Thus, the combination of an increase in the proportion of acetate produced biologically on the one hand, and the use of a renewable carbon

source such as CO_2 on the other hand, constitutes a promising path to reduce the use of petrochemicals and to promote CO_2 chemistry.

4 Objectives of the thesis project

The thesis is part of the development of efficient catalysts for the valorisation of CO_2. Thus, the objective of this thesis work was to reduce CO_2 to acetate, by controlling MMC catalysts. The work is part of the fields of microbiological engineering and MMCs engineering. The effect of culture conditions on microbial communities and the functional orientations of MMCs are at the center of the work, along with kinetic and thermodynamic considerations of biological reactions. Indeed, the microorganisms reducing CO_2 to acetate being anaerobic, the reactions operate close to thermodynamic equilibrium, which requires to evaluate the energetic limitations of the biological reactions involved.

The microbial competition between homoacetogens (HAC) and hydrogenotrophic methanogens (HM) quickly appeared as the major lock to be controlled, therefore this study focused on this competition. In order to control microbial competitions, it is necessary to understand its origin, then to have a detailed knowledge of the different microorganisms involved. Particularly from a metabolic, kinetic and energetic point of view, but also their nutritional requirements, and optimal growth or production conditions. In the context of the recovery of gaseous substrates, the understanding of physical processes such as the mass transfer, and their impact on biological reactions, is also necessary for a thorough understanding of the system. A systemic approach of reactors and biological reactions is therefore necessary.

CHAPTER 1: Literature review

1 Microbial mixed culture engineering for CO_2 reduction

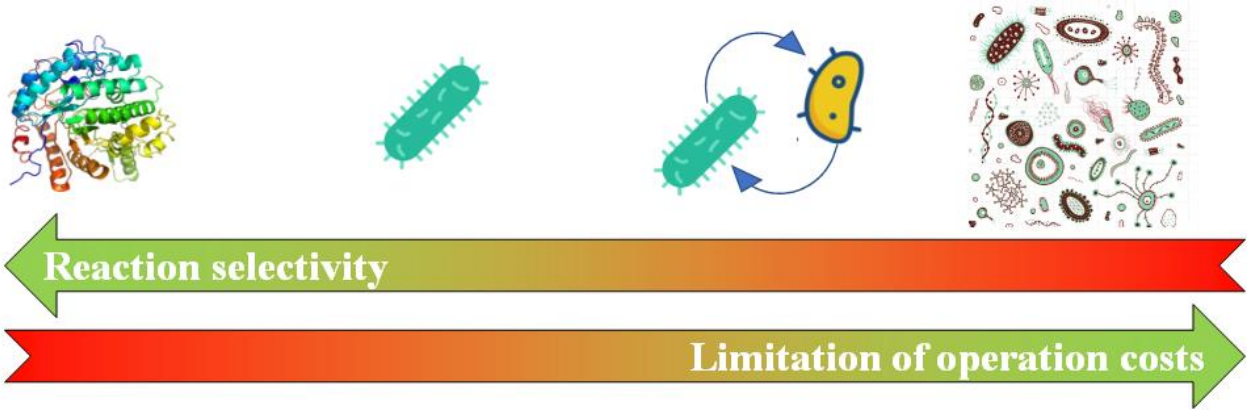

	Enzymes	Pure cultures	Co-cultures	Mixed cultures
Benefits and applications	Fine chemistry Functionalization Product purity Unfeasible reactions with classical organic chemistry	Operational conditions System variability and behaviour prediction Product purity Productivity Metabolism study Metabolic engineering	Interspecies cooperation Multi-step reactions Product complexity Product quality Productivity Metabolic engineering	Wide range of substrates High metabolic potential Functional redundancy and operational conditions adaptation Synergies and ecological equilibrium Growth of uncultured microorganisms Non-sterile conditions Continuous processes Ubiquitous, cheap Wastes management
Challenges	Enzyme screening, purification, development, and production before utilization	Microorganisms isolation Sterile conditions need and contamination risk Restricted substrate range Continuous processes	Microorganisms isolation Sterile conditions need and contamination risk Continuous processes	Consortium engineering Product diversity Stability and reproducibility of specialized cultures Difficult scientific investigations

Figure 2: Characteristics of different types of biocatalysts.

In nature, CO_2 reduction is carried out by photoautotrophic organisms, but also chemoautotrophic organisms. In the first case, the energy source is sunlight, while in the second one, energy comes from chemicals such as sugars or hydrogen. The energetic efficiency is ensured by biocatalysts, the enzymes, enabling to lower the activation energy needed to initiate the reactions, which can be carried out under mild conditions. Enzymes for CO_2 reduction manage to activate the CO_2 and H_2 molecules in their catalytic site, either through electronic interactions (in metallic complexes containing for example Co, Fe or Ni) or by electrostatic interactions with specific amino acids. In both cases, the bonds of the CO_2 are strongly polarized, which activates the reaction (Tlili et al., 2014; Fontecave, 2015). Biocatalysis consists of the use of isolated enzymes, isolated

microorganisms (pure cultures), a combination of known microorganisms (co-cultures), or microbial consortia (mixed cultures) (Figure 2).

This work focuses on the use of MMCs. These biocatalysts are on the rise, as they present numerous benefits, both to improve energetic and economic efficiencies of processes, and to carry out reactions that could not be achieved in a single reactor. Sterile conditions are not required, which is interesting for industrial scale and continuous process development. Also, the use of MMCs allows working with uncultivable microorganisms, *i.e.* microorganisms that could not be isolated in laboratory. Indeed, a lot of microbial interactions exist between microorganisms in natural environments, which explains why the majority could not be isolated (Basile et al., 2020; Lewis et al., 2010), therefore, there should be numerous potential interesting candidates in MMCs that could help to improve existing bioprocesses productivities. Additionally, metabolic redundancy among the multitude of microorganisms contained in MMCs is an advantage, as it allows adaptability and robustness of the process facing substrate or physical parameters changes. The cumulation of those similar functions between different communities also contributes to reach higher rates and productivities in some cases when using MMCs (Paul et al., 2021).

MMCs have two main fields of applications. The first one is the achievement of a wide range of reactions in a single process involving very diverse but complementary biochemical functions. It is for example widely used in wastewater treatment, or organic wastes management. The principle is based on microbial interactions and synergies to consume multiple and diverse substrates. The use of MMCs for this type of applications allows to develop stable ecosystems in bioprocesses. Hence, anaerobic digestion (AD) is an outstanding process which combines both the advantage of handling high diversity and variability of substrates but also of producing a single valuable product, methane, naturally recovered in the gas phase. This particularity, also linked to thermodynamics, explains the convergence to methane in anaerobic environments. Indeed, methane contains the lowest free energy per electrons, so the whole chain of reactions is naturally

driven by its production and extraction from the liquid to the gas (Hanselmann, 1991; Moletta, 2008; Agler et al., 2011). The column of Winogradsky in sediments, or granular sludges in waste water treatment plants, are other examples of stable MMCs systems performing multiple complementary reactions according to a spatial distribution of microorganisms depending on substrate gradient concentration (Esteban et al., 2015; Gao et al., 2011).

Another strategy though, is conversely to constraint the MMC with very specific environmental conditions. This way, decreasing the biodiversity toward few major communities and promoting an exclusive biochemical function. This strategy is based on natural selection of the microbes along generations, selecting the more suitable candidates to survive in the given conditions among as much as initial biodiversity as possible. This is interesting to carry out specific reactions with high product selectivity. In anaerobic environment, this kind of strategy allows to produce naturally other chemicals than methane, especially in the liquid phase, by controlling the process parameters. Nevertheless, the high initial biodiversity of MMCs results in many biochemical functions coexisting. MMC engineering consists in applying process and physical-chemical parameters that will give the advantage to microorganisms of interest, and in the same time weaken the undesired activities. There are a lot of different strategies to specialize a MMC, but all of them consists in applying certain conditions to constraint microorganisms (selection pressure). MMC specialization is accompanied with a loss of biodiversity. The specialization strategy must be designed from a thorough knowledge of functional microbes: their interactions with their environment and other microbes; their metabolisms, and especially carbon, nitrogen, phosphate, energy requirements etc.; their growth kinetic and energetic properties, and also those of other microbes that interact or compete with them. From this knowledge, it is generally possible to identify a high selective factor, that is a specific feature of the functional microbes, differentiating them from concurrent.

Microbial interactions are central in MMCs and need to be understood when implementing a

MMC specialization strategy. Some of them could benefit to the process and should remain if they improve the functional performances, while others compromise it and should be eliminated. Some interactions between microbes are beneficial for one or both of them (*e.g.* commensalism, mutualism interactions), or detrimental (*e.g.* amensalism, predation, competition interactions) (Basile et al., 2020; Paul et al., 2021). However, the study of microbial interactions is a difficult task considering the multiple interactions that exist in a single MMC. Co-cultures are often used to study specifically the interactions between two microbes of interest (Westerholm et al., 2019; Girbal et al., 1997; Lee and Zinder, 1988; Archer and Powell, 1985).

In the framework of this work, the main issue when implementing a biological reactor with MMC to reduce CO_2 to acetate, is the competition between the microorganisms of interest, the HAC, with HM. In order to carry out a MMC management strategy to promote HAC, a review of both communities in competition was required. In next section are reviewed HAC and HM features, in terms of growth kinetic, thermodynamic and energetic considerations, metabolism, and nutrient requirements.

2 MMC growth representation

2.1 Kinetic model of Monod

The kinetic model of Monod (1942) is an extension of Michaelis-Menten law to describe microbial growth according to substrate availability. As all chemical reactions, there is one reactant, or substrate, that is stoichiometrically limiting the biological reactions. Hence, microbial growth can be described according to this limiting substrate concentration with a Monod limitation term, introducing Ks. Ks is a half-saturation constant, corresponding to the substrate concentration when the specific growth rate is half the maximal specific growth rate of a microorganism. Inhibition terms can also be added, introducing an inhibition constant K_I as described in equation A. Growth rate is also a function of pH and temperature, and microorganisms doesn't have the same range of optimal conditions, neither have the same sensitivity to parameters variation. Microbial growth is an autocatalytic reaction, meaning that biomass (catalyst) is a product of the reaction. In conventional models, decay is integrated to growth rate, to represent the observed growth rate and be in capacity to confront simulations to real conditions. Decay is generally a first order kinetic, with k_d the decay constant.

The conversion rate equation including Monod limitation terms can described as follow:

$$r_{X(T,pH)} = \left[\mu_{max(20°c,pH7)} \left(\frac{C}{K_C + C} \times \frac{e^-}{e^- + K_{e^-}} \times \frac{N}{N + K_N} \times \frac{K_I}{K_I + S} \times \frac{K_{I.P}}{K_{I.P} + P} \dots\right) \times f(T, pH \dots)\right] \times X - k_d X \quad \text{(A)}$$

Where r_X is the microbial growth rate, μ_{max} is the specific maximal growth rate. C, e^- and N are the carbon, electron, and nitrogen sources concentrations respectively. K_I is a substrate inhibition constant, $K_{I,P}$ is a product inhibition constant, k_d is the decay coefficient, and X is the biomass concentration. Other inhibition terms exist, for example the Haldane kinetics (B) to describe

acetate substrate inhibition of acetoclastic methanogens (Vavilin et al., 2000), or VFA product inhibition terms (C) and (D) for acidogenic bacteria (Pratt et al., 2012).

Haldane kinetics: $$r_X = \mu_{max} \times \frac{AcH}{K_{AcH} + AcH + AcH \times \left(\frac{AcH}{K_{i_{AcH}}}\right)^p} \quad (B)$$

where AcH is the concentration of the non-dissociated form of acetic acid, and p is the degree index generally set to 1.

Non-competitive product inhibition term: $$\frac{1}{1 + \frac{AcH}{K_{AcH}}} \quad (C)$$

Where K_{AcH} is the acetate concentration for which growth is 50 % inhibited.

Thermodynamic inhibition term: $$\max\left(0, \left(1 - \left(\frac{AcH}{K_{AcH}}\right)^n\right)\right) \quad (D)$$

Where K_{AcH} is the maximal threshold concentration above which growth is 100 % inhibited, for n = 1 the inhibition function is linear, for n > 1 the function is convex.

2.2 Microbial competition in kinetic models: the resource ratio competition

Microbial competitions can express themselves in different ways. Some microbes compete for space, others can produce inhibiting substances for their competitors, or fix an essential substrate, and even accumulate and store it. Here the focus is made on the competition for the previously described limiting substrate. The resource ratio competition model consists in defining the competition according to the substrate availability, and the substrate consumption rates of both competitors. Hence, microorganisms can adopt two different strategies to have the advantage over their competitors. The first type of competitors are r-strategists, meaning that they have high specific growth rates, or high specific consumption rates. They will grow faster and become dominant. Conversely, K-strategists are microbes with a better substrate affinity, meaning that the bioavailability of the substrate is higher for them than for their competitors. This competition representation is based on substrate concentration, in particular around the cells, and can be

described with Monod equations with proper parameters of the different competitors (*i.e.* μ_{max} and K_S). Here, the culture mode is determinant, as it can give the advantage to the r- or to the K-strategists. Classically in a single liquid phase batch mode, the r-strategists outcompete the others, due to high initial substrate concentrations, while in chemostat, substrate concentration remains low which promotes K-strategists. However, the hydraulic retention time (HRT) constrains the microorganisms to a minimal growth rate, which can also affect the outcome of the competition by washing out slow growing microbes ("Bioprocess Engineering Principles - 2nd Edition," n.d.). Working with two phases, liquid and gas, brings some particularities, especially since the substrates are gaseous. Then, even in closed mode, the substrate is supplied according to a flux, corresponding to the gas to liquid mass transfer rate, and the maximal concentration of the substrate in the liquid is limited by gas solubility. Hence, the competition is highly dependent on the gas mass transfer rate that fixes a substrate maximal delivery rate, and the maximal capacity of the biological reactor. H_2 has the lower solubility, and is therefore often the limiting substrate when working with H_2/CO_2 substrate. Additionally, working with gaseous substrates opens on new process control modes, as the substrate management is decoupled from the growth management. Gas phase can be opened or closed, so as the liquid phase, and all these choices will affect the competition features and its outcome. A thorough understanding of the culture mode effect on microbial competitions are therefore central to design an efficient MMC specialization strategy.

With this theory, it is possible to predict the outcome of a competition for a substrate, provided that the culture broth is homogeneous, and that cells are in suspension. However, some biological phenomenon can complexify this representation. For example, the capacity of certain microorganisms to attach on the walls, which often enables slow growing microbes to maintain themselves in a continuous process (biofilm formation). Microorganisms can also attach together and then create a proximity between different types of microorganisms that have syntrophic

interactions, meaning that the products of the ones are only available as substrate for the attached communities but not for eventual suspended equivalents. This has been reported in the case of interspecies H_2 transfer, which corresponds to a spatial proximity between hydrogen producers (*e.g.* hydrolytic and acidogenic bacteria) and hydrogen consumers (*e.g.* methanogenic archaea) in AD reactors (McInerney and Bryant, 1981; Basile et al., 2020). The outcome of a competition can also be described according to thermodynamics of the reactions, especially in anaerobic systems. Hence, numerous researchers developed thermodynamic or bioenergetic models to describe the dynamic behaviour of MMCs.

2.3 Thermodynamic consistency of anaerobic MMCs dynamic models

Numerous classical MMC models are based on Monod equations, like ASM and ADM models (Henze et al., 2000; Batstone et al., 2002). In these models are represented different microbial activities with proper growth and decay rates, with additional limitation or inhibition terms as previously described. However, more recently, researchers included other dimensions to these models, in particular thermodynamics considerations. Indeed, some inhibitions and limitations are originated from thermodynamics, hidden in empirical parameters, often estimated through the model. Thus, thermodynamic consistent models were developed to better represent dynamic behaviour of anaerobic MMCs by considering thermodynamic limitations and improve the Monod representation.

Thermodynamic consistency of biological reactions mainly consists in considering the free energy change of the reactions (ΔrG), reflecting its feasibility in the given environmental conditions. The versatile behaviours of MMC, but also at the metabolic level of some microorganisms such as acetogens, is directly linked to the maximal energy released by the reaction (ΔrG). ΔrG depends on substrates and product concentrations, including protons and pH, and temperature:

$$\Delta rG = \Delta rG^{\circ} + RT \times \ln\left(\frac{\prod p\ {a_p}^{\nu p}}{\prod s\ {a_s}^{\nu s}}\right) \quad (kJ.reaction^{-1}) \qquad \text{(E)}$$

ΔrG° is the Gibbs free energy change of the reaction in standard conditions (25 °C, 1 bar, 1 M), calculated from the standard enthalpy of formation of the reactants
R is the ideal gas constant
p, the products of the reaction considered
s, the substrates of the reaction considered
ν, the stoichiometric coefficient of the reactant in the reaction considered
a is the activity of soluble compounds.

Cells require a minimal energy harvesting from the catalytic reactions to enable their functioning. This minimal energy is called conserved energy ΔG_C. ΔG_C depends on the ATP yield of the catabolic route. Jin et Bethke (2007), hence proposed the calculation of a thermodynamic factor, not only considering the ΔrG, but also the conserved energy in the cell to represent the thermodynamic feasibility of a biological reaction:

$$F_T = \begin{cases} 1 - \exp\left(-\frac{\Delta G_A - \Delta G_C}{\chi RT}\right), & \Delta G_A \geq \Delta G_C \\ 0, & \Delta G_A \leq \Delta G_C \end{cases} \qquad \text{Dimensionless} \qquad \text{(F)}$$

ΔG_A is the negative of ΔrG of the global reaction of the metabolic path considered
$\Delta G_C = Y_{ATP} \times \Delta G_P$ is the conserved energy by the cell
Y_{ATP} is the ATP yield of the metabolic path
ΔG_P is the ΔG of the reaction of phosphorylation of an ADP molecule into an ATP molecule commonly between 40 and 50 kJ/reaction for anaerobic microorganisms (Jin and Bethke, 2007)
χ is the average stoichiometric number of a metabolic path

F_T is comprised between 0 and 1, and can be integrated into growth rates equation for thermodynamic consistency of kinetic models (Grimalt-Alemany et al., 2020). F_T = 0 describes thermodynamic unfeasibility of the reactions, while F_T = 1 describes kinetic control of the reactions, meaning that ΔrG is low enough for the cell to harvest enough energy for functioning. Intermediary F_T describes a thermodynamic limitation of the reaction due to energetic limitation. Other models have been developed with even further thermodynamic considerations to describe anaerobic systems, no longer considering multiple microbial communities, but a single metabolic

network, containing all metabolic paths known in a given system (Rodríguez et al., 2008). Then, the metabolic routes integrated in the model are driven by energetics and thermodynamics rather than kinetic features of microorganisms. These models assume that a natural selection occurs in favour of the reaction from which the cells harvest the maximal energy. These studies allowed for example to better predict product profile during glucose anaerobic fermentation, by defining variable growth yields, or growth rates, according to available energy in the system (Rodríguez et al., 2006a). This model also integrates an intracellular compartment and product transport mechanisms in the energetic balances Same authors also proposed to describe butyrate and acetate yields as function of H_2 partial pressure and pH, and hence better reflect the MMC behaviour and products profile according to these parameters, with a variable stoichiometry (Rodríguez et al., 2006b). In another model, it is proposed to represent growth in two steps, the first one being the reversible activation of the cell by accumulating energy to reach an energetically transitory state, and the second step being the irreversible division of the cell (Desmond-Le Quéméner and Bouchez, 2014). Hence, the growth rate is defined as dependent of this activation energy contained in a harvesting volume around the cell. These thermodynamic models are interesting for anaerobic MMCs representation, because by definition they integrate and represent microbial growth and competitions, on an energetic basis. They also consider thermodynamic product and pH inhibitions.

3 Produce acetate from CO_2 with MMCs is mainly about managing the competition between homoacetogens and hydrogenotrophic methanogens.

Homoacetogens are good candidates for the reduction of CO_2 to chemicals, as they produce acetate, the first intermediate for liquid products synthesis. They are one of the microorganisms carrying out the Acetyl-CoA reductive pathway (or Wood Ljungdahl Pathway, WLP), a highly efficient route fixing two CO_2, inherited from the earliest stages of life on earth. However, their

discovery dates from the 1930s, since when new homoacetogens keep being identified, isolated, and characterized. Interestingly, homoacetogenesis is not a phylogenetic trait, because HAC are found in different phyla. HAC can use a wide range of electron donors and acceptors, such as nitrate, but also organic reduced compounds such as ethanol (Figure 3).

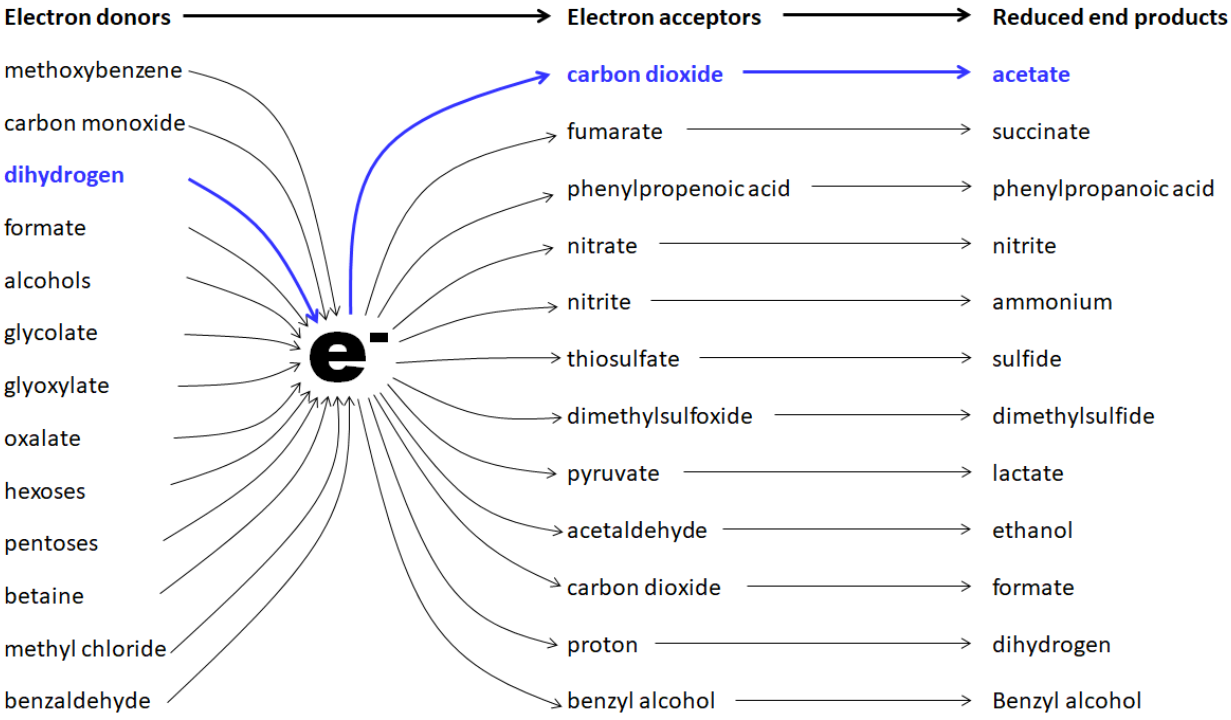

Figure 3: Electron donors and acceptors that homoacetogens can use, and corresponding released reduced products. Adapted from Drake et al. (2008).

Homoacetogens use WLP as a catabolic route producing acetate. Other anaerobic microorganisms are encoding the WLP, including hydrogenotrophic methanogens and sulphate reducers. CO_2 reduction with anaerobic MMCs is interesting because if CO_2 is the only carbon source, the selection pressure is high, as few microorganisms can grow under autotrophic and anaerobic conditions. Still, in anaerobic and autotrophic MMCs, depending on the available substrates, different communities can coexist (Table 1). Hence, it is important to know the different interactions between these populations, which mainly are competitions for the same substrate as they are all able to reduce CO_2, and syntrophic interactions for example between acetate producers

and consumers. If the medium doesn't contain electron acceptors other than CO_2 (no Fe^{3+}, NO^{3-}, SO_4^{2-} or S^0 or organic compounds), then the communities in competition are hydrogenotrophic methanogens (HM) and homoacetogens (HAC), because both use H_2 to reduce CO_2 with similar metabolic path: the acetyl-CoA pathway. In these conditions, sulphate reducing bacteria (SRB) should not be able to grow. However, it is always necessary to supply the medium with a sulphur source, which could help SRB to maintain themselves in the MMC. Acetate consuming reactions such as syntrophic acetate oxidation (SAO) and acetoclastic methanogenesis (AM) might also appear as long as acetate is accumulated in the medium.

Carbon source	*Electron donor*	*Electron acceptor*	*Metabolic route*	*Products*
	H_2	NO_3^-	Denitrification	N_2 H_2O
	H_2	S^0	Sulfo-reduction	H_2S
	H_2	SO_4^{2-} $S_2O_3^{2-}$	Sulfate-thiosulfate reduction	H_2S H_2O
CO_2	**H_2**	**CO_2 CO**	**Hydrogenotrophic methanogenesis Homoacetogenesis**	**CH_4 H_2O Acétate H_2O**
	CH_4	SO_4^{2-}	Anaerobic oxidation of methane	CO_2 HS^-
	NH_4^+	NO_3^- NO_2^- Fe^{3+}	Anaerobic oxidation of ammoniac	N_2 H_2O Fe^{2+}
	S^{2-} S^0 $S_2O_3^{2-}$	NO_3^-	Denitrification, Sulfo-oxidation	N_2 SO_4^{2-}

Table 1: Diversity of autotrophic metabolisms in anaerobic conditions, adapted from Jan (2012).

To inhibit methanogenesis, different strategies may work. It is possible to apply heat treatment to the microbial consortium with the aim of eliminating communities that are not able to sporulate, which is the case of methanogens. Generally, the application of temperatures from 70 to 90 ° C during 15 to 30 min is required (Grimalt-Alemany et al., 2018; Omar et al., 2018). A revitalization work must then be done to exploit the MMC. This strategy has the advantage of efficiently eliminating methanogenic populations in most cases, even if some authors still observe the recovery of methane production after treatment (Liu et al., 2018). Some authors like Omar et al. (2018), were even able to observe a methane over CO_2 yield of 100% after heat treatments at 70

or 90 ° C for 30 min. This methane production recovery is likely due to contamination of the process, which remains a risk which could be avoided by controlling the competition with process parameters. In addition, this technique can also rule out non-sporulating hydrogenotrophic bacteria which may be of interest for the desired activity. In particular, *A. woodii*-like acetogens are non-spore-forming bacteria (Schuchmann and Müller, 2014).

Another strategy, widely used at laboratory-scale studies, is the addition of chemical inhibitors of methanogenesis. The most commonly used is 2-bromoethanesulfonate (BES), but there are others such as mercaptoethanesulfonate (MES) or lumazine (Liu et al., 2011). MES and BES mimic methyl-CoM and thus block the enzyme of the last stage of methanogenesis (Figure 4). These inhibitors therefore make it possible to inhibit any type of methanogenesis. BES is used at different concentrations depending on the studies, from 10 to 50 mM and even 100 mM (Wang et al., 2017; Luo et al., 2018; Omar et al., 2018; Shen et al., 2018). It is interesting to note that the concentrations chosen do not seem to depend on the time of the experiment nor on the temperature, and are rarely justified or discussed. However, during long cultivation times it is necessary to regularly add BES because its efficiency decreases over time, and it can be degraded in the system (Luo et al., 2018; Zhang et al., 2013b; Steinbusch et al., 2011). Chemical inhibitors are convenient for specific lab experiment, though they are not an economically viable solution to scale up processes (Agler et al., 2011).

It is proposed in this work to undertake MMC engineering to overcome the methanogens and selectively produce chemicals (*i.e.* acetate). In the next sections, the case of using MMCs to reduce CO_2 into chemicals in anaerobic conditions will be specifically treated. In this context, handle the competition of homoacetogens with methanogens is the main challenge. For this reason, both communities will be reviewed, regarding their natural occurrence and habitat, metabolism and kinetic features. Thermodynamic features will also be addressed, considering the low energy generation of anaerobic reactions.

3.1 Natural habitats and requirements of homoacetogens and hydrogenotrophic methanogens

Homoacetogens (HAC) and hydrogenotrophic methanogens (HM) are found in numerous natural environments, mostly anaerobic, such as animals gut microbiota, sediments, hydrothermal sources etc. (Jan, 2012; Karekar et al., 2022). In natural environments, only 10 % of acetate is produced in autotrophy, and homoacetogenesis is rarely observed. Indeed, HM are the main autotrophic organisms in anaerobic environment. Yet, isolation and characterization of heterotrophic acetogens often lead to the conclusion that these microorganisms are able to grow in autotrophy (Karekar et al., 2022). Acetogens microorganisms have developed along evolution the capacity to consume a wide range of substrates. This strategy is commonly observed in nature, especially when carbon sources concentrations are low. Furthermore, anaerobic reactions deliver low energy, and microorganisms developed numerous catabolic routes to exploit a maximum of energy from their environment (Egli, 2010). Hence, they are also able to use numerous of electron donors and acceptors. Conversely, methanogenesis is one of the most exergonic anaerobic reactions which results in higher metabolic rates and lower substrates thresholds (Cord-Ruwisch et al., 1988; Kotsyurbenko et al., 2001). This explains why HM very often have the advantage in nature over HAC, that turn to heterotrophic growth. However, there are specific conditions that benefit to HAC over HM, such as suboptimal pH and temperatures, and high H_2 concentrations (Karekar et al., 2022; Conrad et al., 1989; Jarrell and Kalmokoff, 1988).

3.2 Kinetic features and metabolism of homoacetogens and hydrogenotrophic methanogens

3.2.1 The Acetyl-CoA reductive pathway

The acetyl-CoA reducing pathway, also known as the Wood-Ljungdahl pathway (WLP), is used by methanogens, but also homoacetogenic bacteria and sulphate reducing bacteria and archaea. Acetyl-Coenzyme A is a thioester, which is the activated form of acetate in the metabolism. This molecule is highly energetic and has a central role in metabolism. Many catabolic pathways converge on acetyl-CoA, which then initiates anabolic mechanisms such as the production of lipids, or the production of energy by phosphorylation at the substrate level. WLP allows autotrophic microorganisms to fix carbon from C1 compounds and also provides the energy needed for cell growth and development.

The WLP is a linear path composed of two branches. The methyl branch, synthesises a methyl group (CH3) after reduction of a CO2. The carbonyl branch, provides the carbonyl group (C=O) after CO2 reduction to CO. The methyl and carbonyl groups thus formed condense together to synthesize acetyl-CoA. Acetyl-CoA is further transformed into cell component in anabolism pathways. The difference between WLP in methanogens and in homoacetogens is mostly about the methyl branch mechanism and enzymes. Also, ATP formation is different: methanogens deviate the methyl group produced in the methyl branch, for a last reduction step and release of methane and ATP (Figure 4); while homoacetogens use the dephosphorylation of Acetyl-CoA for the synthesis of an ATP which releases acetate. Some microorganisms encoding the WLP can use other substrates: methylotrophs have the ability to directly incorporate methyl C1 compounds (methanol, methanethiol, methylamine) for the formation of the methyl group; carboxydotrophs have the ability to incorporate CO (Prakash et al., 2014; Schuchmann and Müller, 2014; Berg et al., 2010; Ragsdale and Pierce, 2008).

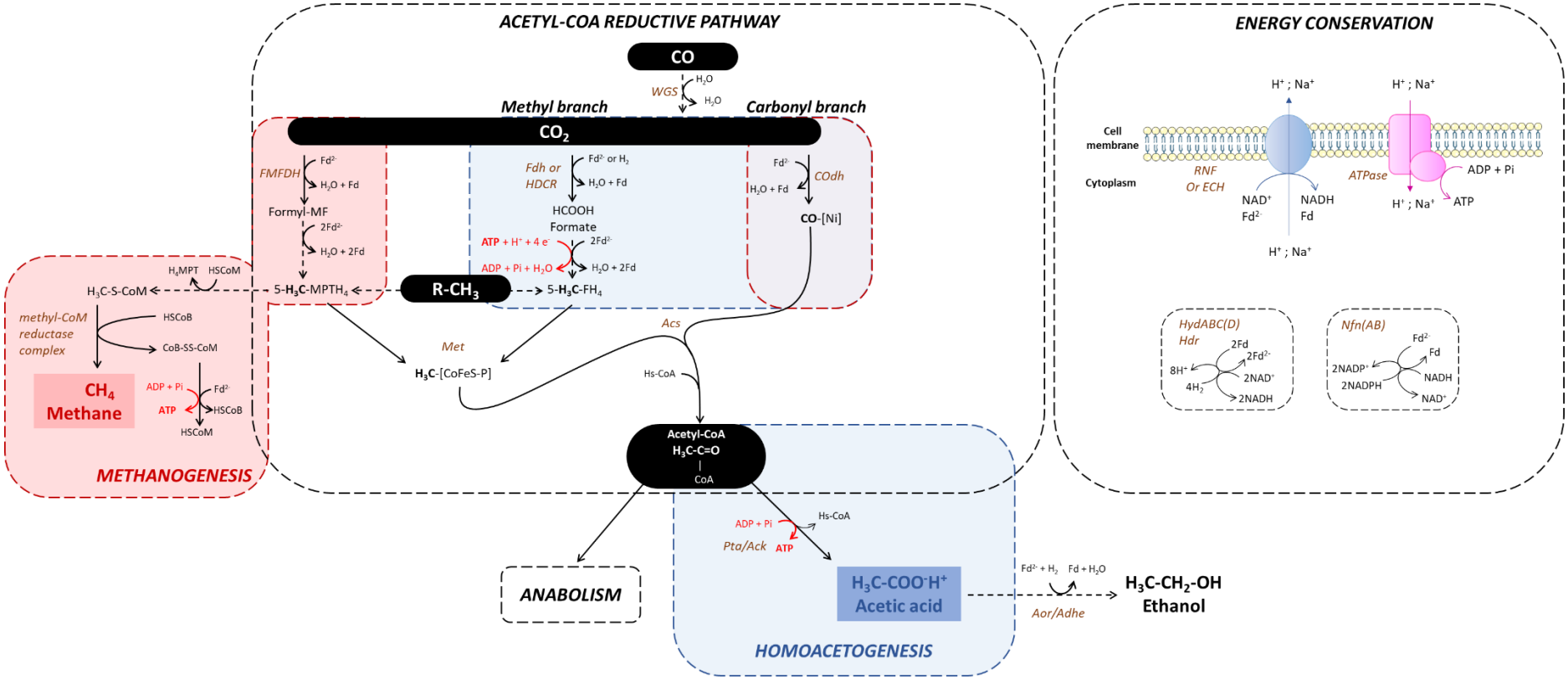

Figure 4: Wood-Ljungdahl pathway in methanogenic archaea and homoacetogenic bacteria (Prakash et al., 2014; Schuchmann and Müller, 2014). Fd ferredoxin, Ech ferredoxin–H2 oxidoreductase, Hyd and Hdr electron-bifurcating hydrogenases, Nfn ferredoxin–NAD$^+$ oxidoreductase, WGS water gas shift reaction, FMFDH formylmethanofuran dehydrogenase, Fdh formate dehydrogenase, HDCR hydrogen-dependent CO_2 reductase, Met methyltransferase, COdh/Acs carbon monoxide dehydrogenase-acetyl-CoA-synthase complex, MF methanofuran, H_4MPT tetrahydromethanopterin, Pta phosphotransacetylase, Ack acetate kinase, Aor aldehyde:ferredoxin oxidoreductase, Adhe aldehyde/alcohol dehydrogenase.

3.2.2 Methanogenesis

Methanogens are strict anaerobes, and belong to the archaea phylum *Euryarcheota*, and the orders *Methanococcales*, *Methanobacteriales*, *Methanomicrobiales*, *Methanopyrales*, *Methanocellales*, *Methanomassiliicocales* and *Methanosarcinales*. They are found in environments where their substrates (H_2, CO_2, CO, acetate, methyl compounds, NH_4^+, H_2S) are available. Hence, they are often associated to anaerobic organic matter degradation, in animals' intestinal tracts and sediments for instance. They are also found in geothermal springs such as hydrothermal vents (Bellini et al., 2022; Karekar et al., 2022; Jan, 2012). Two types of methanogenic communities are prevalent: hydrogenotrophic and acetoclastic. Hydrogenotrophic methanogens use H_2 and CO_2 as sole energy and carbon sources, which reverts to a chemolithoautotrophic metabolism. All but *Methanomassiliicoccales* orders cited are capable of hydrogenotrophic methanogenesis. On the other hand, acetoclastic methanogens use acetate as energy and carbon source defined as a chemoorganoheterotrophic metabolism. The genera able to use acetate for a methanogenic metabolism are identified as *Methanosarcina* and *Methanothrix*. However, acetoclastic methanogens can be flexible, as some species such as *Methanosarcina barkeri* have been found to use either H_2 or acetate according to their respective availability (Lambie et al., 2015). Methylotrophs and carboxydotrophs are able to use either methyl compounds or carbon monoxide respectively.

Acetoclastic methanogenesis consists in firstly producing acetyl-CoA from acetate on the expense of ATP (activation), and secondly hydrolysing the activated acetate (acetyl-CoA) to produce CO_2 and a methyl group for methane formation. In *Methanosarcina*, acetate activation is undertaken with acetate kinase and phosphotransacetylase, whilst in *Methanothrix* activation is performed by COdh/Acs complex (carbon monoxidedehydrogenase-acetyl-CoA-synthase complex) (Jetten et al., 1992). Moreover, COdh is highly oxygen-sensitive due to the presence of a metallic core composed of nickel, and Fe-S clusters (ferredoxins) (Ragsdale and Pierce,

2008; Jeoung and Dobbek, 2007). This enables to carry out low energy electron exchanges, which was impossible with the conventional NAD(P)H/NAD(P)$^+$ couple (E0' = -320 mV). Indeed, the redox potentials of the CO_2/$HCOO^-$ and H_2/H^+ couples are -432 and -414 mV respectively (Thauer et al., 1977).

3.2.3 Homoacetogenesis

Several homoacetogenic models have been described, with enzymatic and bioenergetic differences: *Acetobacterium woodii*, *Clostridium ljungdah*lii and *Moorella thermoacetica* (formerly known as *Clostridium thermoaceticum*). In *A. woodii*, the first CO_2 reduction reaction is catalyzed by a hydrogen-dependent CO_2 reductase complex (HDCR) directly involving an H_2 molecule for reduction. In the other two models, on the other hand, this reaction is carried out by a formate dehydrogenase (Fdh) using reduced cofactors, either with oxidation of a ferredoxin and H_2, or with oxidation of a ferredoxin and NADPH (Schuchmann and Müller, 2014). The different models also do not have the same energy conservation mechanisms. Whereas in *A. woodii* and *C. ljungdahlii* it is a ferredoxin-NAD^+ oxidoreductase (Rnf) complex which allows the translocation of H^+ or Na^+ through the plasma membrane, in *M. thermoacetica* it is a hydrogenase complex with conservation of energy (Ech) which allows this transfer. ATPase then makes it possible to produce ATP with the transferred ions. Bioenergetic studies generally assume that three transferred ions are necessary for the production of an ATP molecule (Grimalt-Alemany et al., 2019). However, this could vary depending on the microorganisms and enzymes involved. These enzymatic particularities according to the microorganisms generate bioenergetic differences and modify the overall balance of the reaction in terms of ATP yield in particular. Thus, there is generation of 0.3 and 0.5 moles of ATP per mole of acetate produced in the models *A. woodii* and *M. thermoacetica* respectively. In the *C. ljungdahlii model*, on the other hand, the ATP balance is not certain because different genes coding for three different Fdh have been sequenced, the reducing equivalents used by these Fdh are different: H_2 or Fd or NADPH/Fd.

For anabolism, *i.e.* if the pathway stops at acetyl-CoA to synthesize cell components, the pathway has a negative bioenergetic balance of -0.7 ATP (Bertsch and Müller, 2015). *C. ljungdahlii*, *C. autoethanogenum* and *C. ragsdalei* have 99 % similar 16S rRNA. Their optimal

pH for growth is 5-5.5 and they are all able to synthesize ethanol from syngas or H_2/CO_2. Acetate reduction to ethanol is carried out in the cytoplasm by the enzyme aldehyde:ferredoxin oxidoreductase (Aor). *C. autoethanogenum* is used as a pure culture at industrial scale for ethanol production (Simpson et al., 2007), and some studies are dedicated to the understanding of its bioenergetic features and how energy is conserved in the cells (Liew et al., 2016; Valgepea et al., 2018; Heffernan et al., 2020). Table 2 summarizes potential biological reactions occurring in reactors fed with H_2/CO_2, with their ATP yields and Gibbs free energy of reactions. The use of H_2/CO_2 by the cells induces strong energetic limitations compared to the use glucose or CO for example. Indeed, H_2 provides less electrons, making difficult to maintain a sufficient pool of reduced cofactors (Baleeiro et al., 2019). The most studied product in gas fermentation is ethanol, indeed this molecule is the only one to be produced at industrial scale from gaseous substrates to date. The production of ethanol is possible from H_2, as long as it goes through acetate and ATP production, so that it is reduced by Aor (Figure 4). In fact, direct production from H_2/CO_2 leads to a negative ATP balance (Table 2). Most acetogens have an Aor, except *A. woodii*-like HAC, and the production of ethanol with *A. woodii* has not been reported. To overcome energetic limitation, it is possible to use co-substrates such as glucose (Park et al., 2019) or CO (Heffernan et al., 2020). Hence, biomass concentration and productivities increase. This kind of co-fermentation can be implemented in biorefineries for example, using organic wastes co-products or syngas as co-substrates for example.

Reaction	ATP Yield	ΔrG°' (kJ/reaction)	Enzymes or Pathway	Microorganisms
Acetyl-CoA reductive pathway				
$4H_2 + 2CO_2 \rightarrow$ Acetyl-CoA	-0.7		WLP	
Homoacetogenesis				
AcetylCoA $\rightarrow Acetate^- + H^+ +$ CoA-SH	1		Pta/Ack	Homoacetogens
$4H_2 + 2CO_2 \rightarrow Acetate^- + H^+ + 2H_2O$	0.3	-95		
Ethanol production				
$6H_2 + 2CO_2 \rightarrow$ Ethanol $+ 3H_2O$	-0.1	-105		Homoacetogens except *A. woodii* type
$Acetate^- + H^+ + 2H_2 \rightarrow$ Ethanol $+ H_2O$	0.3	20	Aor	
Chain elongation				
$3Acetate^- + 3\ H^+ + 5$Ethanol $\rightarrow 4Butyrate^- + 4H^+ + 3H_2O + 2H_2$	1		Bcd	*C. kluyveri, E. limosum, C. carboxidovorans*
Ethanol $+ Acetate^- \rightarrow Butyrate^- + H_2O$		-39		
$12H_2 + 4CO_2 \rightarrow$ Butanol $+ 7H_2O$	1.2 - 1.8			*C. kluyveri, C. carboxidovorans*
Ethanol $+ Butyrate^- \rightarrow caproate^- + H_2O$		-39		
Methanogenesis				
$4H_2 + CO_2 \rightarrow CH_4 + 2H_2O$	0.5	-131	WLP	Hydrogenotrophic methanogens
$Acetate^- + H^+ \rightarrow CO_2 + CH_4$	0.5	-36	COdh/Acs	Acetoclastic methanogens
Sulfate reduction				
2Ethanol $+ SO_4^{2-} \rightarrow 2Acetate^- + H^+ + HS^- + 2H_2O$		-133		Sulfate reducing bacteria (SRB)
$Acetate^- + SO_4^{2-} \rightarrow HS^- + 2HCO_3^-$		-47		
$4H_2 + H^+ + SO_4^{2-} \rightarrow HS^- + 4H_2O$		-152		
$SO_4^{2-} + HCOO^- + H^+ \rightarrow HS^- + 4HCO_3^-$		-147		
Competitive oxidation				
$Acetate^- + H^+ + 2H_2O \rightarrow 4H_2 + 2CO_2$	0.3	95		Syntrophic acetate oxidizing bacteria (SAOB)

Table 2: Biological reactions occurring in MMCs grown on H_2/CO_2. ATP yield, ΔrG°' (25 °C, pH 7), enzymes and microorganisms involved in the reactions.(Baleeiro et al., 2019; Diender et al., 2015; Hu et al., 2011). WLP : Wood Ljungdahl pathway; Pta: phosphotransacetylase; Ack: acetate kinase ; Aor: aldehyde:ferredoxin oxidoreductase; Bcd: butyryl-CoA dehydrogenase; COdh/Acs: carbon monoxide dehydrogenase-acetyl-CoA-synthase complex.

3.2.1 Kinetic features of hydrogenotrophic methanogens and homoacetogens.

A review of kinetic parameters of common cultured HAC and HM was carried out during this work (Table 3 and Table 4). The major part of these kinetic parameters has been determined in batch reactors, and with gaseous substrates containing CO. Indeed, few studies have been carried out on H_2/CO_2. Also, mass transfer limitation is not analysed in most of these studies. However, it should be mentioned if the cultures were mass transfer limited or not, as if they were, it is not possible to determine maximal performances of microorganisms.

A first observation on that data collected is that there is a high variability among the results found. This could be explained by different things. Apparent K_{H2} is dependent on gas to liquid mass transfer of the system used, especially when it is estimated from the residual concentrations in the gas phase. Hence, high K_{H2} values obtained by some authors can be explained be mass transfer limitations, and not necessarily the actual concentration thresholds that the microorganisms can handle when for instance consuming H_2 directly produced in the liquid phase by hydrogenogens (Pavlostathis and Giraldo-Gomez, 1991). Culture media used in each of these studies is also slightly different, because there is not a single normalized culture medium for MMC growing on gaseous substrates. As culture media composition can have an effect on microorganisms' performances, their characterization can only be applicable to the same conditions, which makes it difficult to predict the behaviour of a microorganism, and even more a MMC under new culture conditions

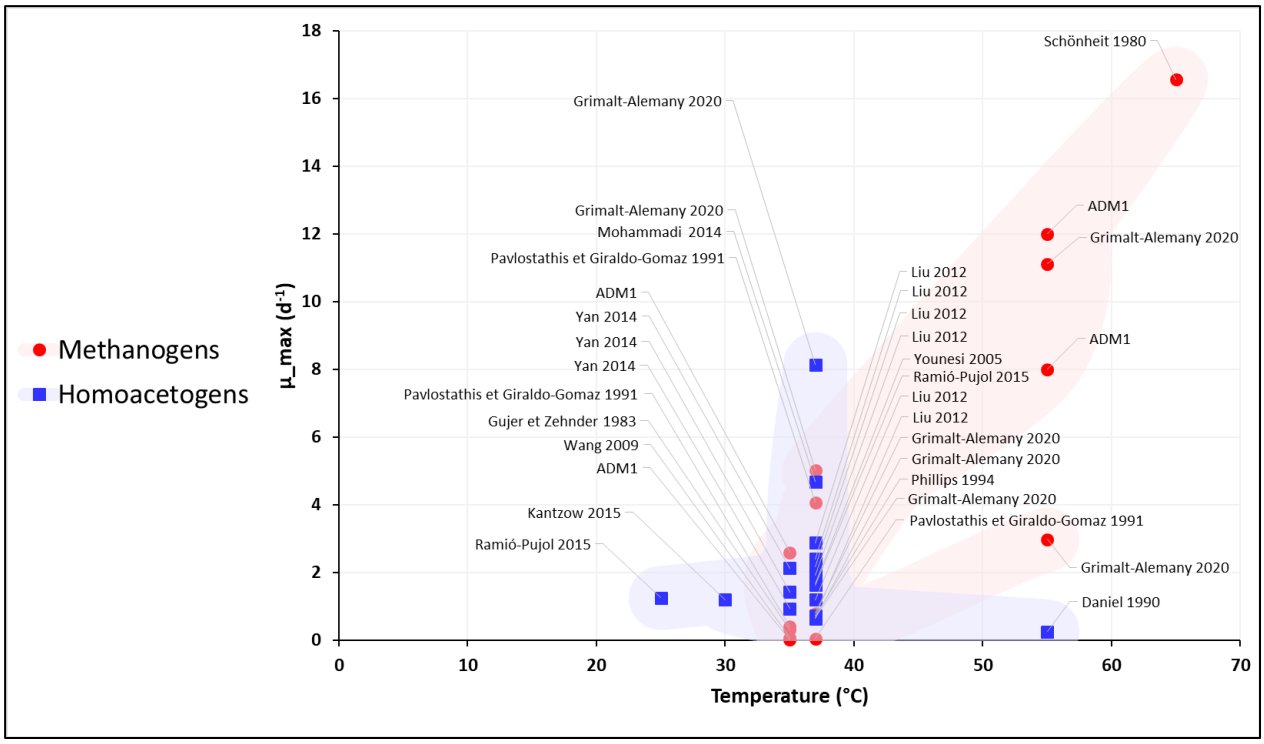

Figure 5: Maximal specific growth rates identified in the literature for Hydrogenotrophic methanogens and homoacetogens at different temperatures. Additional information concerning growth conditions of each study is available in Table 3 and Table 4.

Nevertheless, some tendencies are observed from this collection of parameters. Figure 5 represents the maximal specific growth rates (μ_{max}) of HAC and HM identified from various published results under different conditions of pH, temperature, substrates and reactors. Corresponding $Y_{X/H2}$, K_{H2} (when measured or estimated), and microorganisms involved, are detailed in Table 3 and Table 4. First observation is that μ_{max} of HAC under thermophilic conditions have rarely been characterized, so are μ_{max} of HM under psychrophilic temperature. Indeed, only few thermophilic HAC have been isolated such as *Moorella thermoacetica* (whose ancient name was *Clostridium thermoaceticum*).

Furthermore, HM have much higher μ_{max} under thermophilic temperatures than under mesophilic temperatures, and under mesophilic conditions HM have similar μ_{max} than HAC. Consistently, Grimalt-Alemany *et al.* (2019) showed that in a MMC grown at 55 °C, HM outcompeted HAC, and syngas ($CO/H_2/CO_2$, 20:65:15) was directly converted into methane. In the other hand, some controversial results under H_2/CO_2 from Fu *et al.* (2019), showed that

HAC followed by AM was the prevailing path at 60 °C while direct HM prevailed at 30 °C, and that HAC without subsequent AM prevailed at 15 °C. This difference can be explained by the different nature of the substrates, as in the first case the gas contained CO, which leads to variable toxicity effects on microbial communities, and also different energetic features of the metabolism as discussed previously (Nagarajan et al., 2013). Indeed, another study carried out with H_2/CO_2 showed similar results as Fu *et al.* (Conrad et al., 1989): the authors observed that in MMC enrichments at 17 °C, HAC outcompeted HM, while at 30 °C HM outcompeted HAC. The authors also identified a critical temperature determining the outcome of the competition around 20 – 25 °C. This inversion is based on the minimal H_2 threshold that the microorganisms can handle according to temperature, which is directly linked to the half-saturation constant K_{H2} that become lower for HAC under psychrophilic temperatures. K_{H2} fixes the H_2 threshold, which is linked to free energy change of the reaction. Indeed, there is a H_2 concentration below which the ΔrG become positive, and this is also linked to the electron acceptor used (Cord-Ruwisch et al., 1988): the higher Gibbs free energy change of reaction (ΔrG), the lower H_2 threshold. This explains that SRB have lower H_2 thresholds than HM and HAC, because sulphate reduction is more energetic than CO_2 reduction (Weijma et al., 2002). In the case of HM and HAC, the electron acceptor is the same (CO_2), but the ΔrG of reactions is in favour of HM because CH_4 is more reduced than acetate. Also, acetate accumulated in the liquid, contributing to increase ΔrG along the reaction, while CH_4 is stripped to the gas phase. Kotsyubenko *et al.* (2001) studied specifically the competition between different HMs and HACs isolated from low-temperature environments at 4 °C to 30 °C. They identified that H_2 thresholds were lower for HM except for temperature below 10 °C, and that this threshold, as well as the μ_{max} of all the strains increased with temperature. However, the increase of the μ_{max} of HM was more pronounced, suggesting that increasing temperature will benefit more to HM. According to these studies and the parameters collected, temperature appears as an important

environmental parameter influencing the outcome of the competition between HM and HAC, and that lowering temperature could be a first prerequisite for promoting HAC. Furthermore, the composition of the gas used (*i.e.* syngas or H_2/CO_2) is also important and can change the conditions of the competition because of bioenergetic and toxicity specificities. Among all these studies, only few considered CO_2. This is probably due to the fact that the cultures were conducted in batch mode, meaning that H_2 is always the limiting substrate during the first stage of the experiments, when the parameters are calculated. However, CO_2 can be limiting in other conditions, due for example to a high H_2/CO_2 ratio, or in continuous processes because of CO_2 loss in the liquid. Hence, kinetic parameters such as K_{CO2} could be needed to represent growth of MMC under certain conditions, but have not been well defined yet.

Homoacetogens	T	pH	μ_{max} (d^{-1})	$Y_{X/H2}$ $gCOD_X.gCOD_{H2}^{-1}$	Ks_{H2}	Substrate	Product	Culture mode	References
Clostridium carboxidivorans P7	25	6	**1.25**			CO:H_2:N_2:CO_2 32:32:28:8	Acetate, butyrate, caproate, Ethanol, butanol, hexanol	Batch	(Ramió-Pujol et al., 2015)
Clostridium carboxidivorans P7	37	6	**1.63**			CO:H_2:N_2:CO_2 32:32:28:8	Acetate Low ethanol titter	Batch	(Ramió-Pujol et al., 2015)
Enriched MMC	37	6	**0.68**	**0.042**		CO:H_2:N_2:CO_2 32:32:28:8	Acetate	Batch	(Grimalt-Alemany et al., 2020)
C. ljungdahlii	37	5.9	**4.68**		0.412 atm	CO/CO_2/H_2/Ar 30:30:30:10	Acetate + Ethanol	Batch	(Mohammadi et al., 2014)
C. ljungdahlii	37	-	**1.68**			CO/CO_2/H_2/Ar 55:10:20:15	Acetate + Ethanol	Batch	(Younesi et al., 2005)
A woodii	35	5.5	**0.94**		$5.2x10^{-4}$ M	Glucose	Acetate	Batch	(Yan et al., 2014)
Acetobacterium woodii	30	7	**1.20**			H_2/CO_2/N_2 40:17:43	Acetate	Continuous	(Kantzow et al., 2015)
Clostridium carboxidivorans P7	37-40	5-7	**2.88**			H_2/CO_2	Acetate, butyrate Ethanol, butanol	Batch	(Liou et al., 2005)
Clostridium carboxidivorans P7	37-40	5-7	**3.84**			CO/CO_2	Acetate, butyrate Ethanol, butanol	Batch	(Liou et al., 2005)
Clostridium scatologenes SL1	30-37	5.4-7.5	**2.88**			H_2/CO_2	Acetate, butyrate Ethanol, butanol	Batch	(Liou et al., 2005)
Clostridium scatologenes SL1	30-37	5.4-7.5	**4.80**			CO/CO_2	Acetate, butyrate Ethanol, butanol	Batch	(Liou et al., 2005)
Clostridium scatologenes ATCC 25775	37-40	5.4-7	**0.96**			H_2/CO_2	Acetate, butyrate Ethanol, butanol	Batch	(Liou et al., 2005)
Clostridium scatologenes ATCC 25775	37-40	5.4-7	**2.16**			CO/CO_2	Acetate, butyrate Ethanol, butanol	Batch	(Liou et al., 2005)
Alkalibaculum bacchi CP11	37	8	**0.72**			CO/CO_2/H_2/N_2 20:15:5:60	Acetate + Ethanol	Fed-batch	(Liu et al., 2012)
Alkalibaculum bacchi CP11	37	8	**1.92**			CO/CO_2/H_2 40:30:30	Acetate + Ethanol	Fed-batch	(Liu et al., 2012)
Alkalibaculum bacchi CP13	37	8	**1.20**			CO/CO_2/H_2/N_2 20:15:5:60	Acetate + Ethanol	Fed-batch	(Liu et al., 2012)
Alkalibaculum bacchi CP13	37	8	**2.40**			CO/CO_2/H_2 40:30:30	Acetate + Ethanol	Fed-batch	(Liu et al., 2012)
Alkalibaculum bacchi CP15	37	8	**2.16**			CO/CO_2/H_2/N_2 20:15:5:60	Acetate + Ethanol	Fed-batch	(Liu et al., 2012)
Alkalibaculum bacchi CP15	37	8	**2.88**			CO/CO_2/H_2 40:30:30	Acetate + Ethanol	Fed-batch	(Liu et al., 2012)
MMC modeling	37	7	**8.14**		$2.31x10^{-6}$ M	H_2/CO/CO_2 65:20:15	Acetate	Batch	(Grimalt-Alemany et al., 2020)
Enriched MMC	37	7	**0.64**	**0.048**		H_2/CO/CO_2 65:20:15	Acetate	Batch	(Grimalt-Alemany et al., 2020)
Acetogenium kivui **ATCC 33488**	55	6.5	**0.26**	**0.081**		H_2/CO_2/N_2 30:30:40	Acetate	Batch	(Daniel et al., 1990)

Table 3: Homoacetogens (HAC) kinetic parameters according to Monod model for microbiological growth and their conditions of obtention.

Homoacetogens	T	pH	μ_{max} (d^{-1})	$Y_{X/H2}$ $gCOD_X.gCOD_{H2}^{-1}$	Ks_{H2}	Substrate	Product	Culture mode	References
Clostridium ljungdahlii	37	4.5	**0.71**	0.033		$H_2/CO_2/CO/Ar$ 20:10:55:15	Acetate + Ethanol	Continuous	(Phillips et al., 1994)
***Clostridium thermoaceticum* ATCC 39073**	55	6.5	**0.028-0.081**	0.041		$H_2/CO_2/N_2$ 30:30:40	Acetate	Batch	(Daniel et al., 1990)

Table 3 (continued).

Hydrogenotrophic methanogens	T	pH	µmax (d^{-1})	$Y_{X/H2}$ ($gCOD_X.gCOD_{H2}^{-1}$)	Ks_{H2}	Substrate	Product	Culture mode	References
	35	-	**0.02**		$1.1x10^{-6}$ M		CH_4	ADM1 model	(Batstone et al., 2002, p. 1)
	35	-	**2.6**		$5.6x10^{-6}$ M		CH_4	ADM1 model	(Batstone et al., 2002, p. 1)
	55	-	**8**		$3.1x10^{-7}$ M		CH_4	ADM1 model	(Batstone et al., 2002, p. 1)
	55	-	**12**				CH_4	ADM1 model	(Batstone et al., 2002, p. 1)
MMC	35	7	**0.07**			VFA	CH_4	Continuous	(Wang et al., 2009)
Methanobrevibacter arboriphilus	35		**2.7**			H_2/CO_2	CH_4	Batch	(Gujer and Zehnder, 1983)
Methanobrevibacter smithii	37		**4.07**	0.064		H_2/CO_2	CH_4	Batch	(Pavlostathis and Giraldo-Gomez, 1991)
Methanospirillum hungatei JF-1	37		**0.05**	0.030		H_2/CO_2	CH_4	Batch	(Pavlostathis and Giraldo-Gomez, 1991)
representative values for AD at 35 °C	35		**0.4**	0.042		H_2/CO_2	CH_4	Batch	(Pavlostathis and Giraldo-Gomez, 1991)
Methanobacterium thermoautotrophicum	65	7	**16.56**	0.035	CO_2 10 % H_2 20 %	H_2/CO_2 80:20	CH_4	Batch	(Schönheit et al., 1980)
modeling	37	7	**5.03**		$1.56x10^{-6}$ M	$H_2/CO/CO_2$ 65:20:15	CH_4	Batch	(Grimalt-Alemany et al., 2020)
modeling	55	7	**11.11**			H2/CO/CO2 65:20:15	CH_4	Batch	(Grimalt-Alemany et al., 2020)
Enriched MMC	37	7	**0.8**	0.064		$H_2/CO/CO_2$ 65:20:15	CH_4	Batch	(Grimalt-Alemany et al., 2020)
Enriched MMC	55	7	**2.98**	0.045		H2/CO/CO2 65:20:15	CH_4	Batch	(Grimalt-Alemany et al., 2020)

Table 4: Hydrogenotrophic methanogens (HM) kinetic parameters according to Monod model for microbiological growth and their conditions of obtention.

3.2.2 State of the art of gaseous substrates conversion to acetate with MMCs.

Gas conversion to value-added chemicals such as acetate is a rising research topic. There have been many studies in pure cultures, from lab scale experiment, to commercialization (Liew et al., 2016). Studies with MMCs are infrequent, and most of them are carried out with syngas containing CO. Table 5 summarises major results from the literature, of the conversion of H_2/CO_2 or $CO/H_2/CO_2$ into acetate and other biochemicals such as ethanol. With MMCs, the main scientific issues addressed are the reactor design, and the screening of optimal environmental parameters. Most of the studies are carried out in serum bottles for conditions screening purposes. Hollow fibber membrane reactors are often chosen for continuous experiments because they allow biomass fixation in the fibres, enhancing the substrate availability for microorganisms, and biomass retention while extracting continuously the products. Extracting continuously the products allow to reach higher productivities, because products inhibition is overcome (Wang et al., 2017). However, product concentration in the liquid is lower, inducing to find a compromise between concentration and productivities depending on downstream processes. Operation pH is generally below 7, most of the time 6. Indeed, it has been shown that acetate productivities decreases with pH decrease, while ethanol and butyrate productivities increases simultaneously (Ganigué et al., 2016, 2015). Finally, MMCs are mainly enriched with microbial communities of the genus *Clostridium* under mesophilic conditions, and *Thermoanaerobacterium* under thermophilic conditions.

As discussed before, methanogenesis competition is handled with BES or heat treatments in these studies, and there were no attempts yet to engineer the MMCs with process parameters to avoid methanogenesis under H_2/CO_2 and naturally promote HAC.

reactor design	mode	HRT (d)	inoculum	duration (d)	T (°C)	pH	P_{CO}	P_{H2}	P_{CO2}	Acetate molC.L^{-1}	Acetate molC.L^{-1}.d^{-1}	BES (mM)	Heat shock	Microbial analysis	References
HFMBR	Batch		mesophilic anaerobic digestate	165	35	6.0	0.45	0.7		0.140		10		*Clostridium sp.*	(Shen et al., 2018)
	Batch			60	55	6.0				0.650				*Thermoanaerobacterium sp.*	
						6.0				0.930					
						5.5				0.310	0.210				
	Continuous	1.5		40		6.0				0.690	0.470				
						6.5				0.820	0.560				
HFMBR	Batch		anaerobic sludge	53	35	6.0	0.45	0.7		0.650		10		*Clostridium sp.* 30 % *Syntrophomonas sp.* 20 %	(Wang et al., 2018)
	Continuous	5.5		30							0.020				
		3.3		30							0.010				
		1		7							0.000				
HFMBR	Batch		anaerobic digestate	98	25	6.0		0.6	0.4	1.000	0.029	yes		*Clostridium sp.* and Pr*evotella*	(Wang et al., 2018)
	Batch			58						0.330	0.009				
HFMBR	Batch		anaerobic digestate	46	55	6.0		0.6	0.4	1.350	0.068	10		*Thermoanaerobacterium sp.* 66 % *Thermohydrogenium sp.* 12 %	(Wang et al., 2017)
				71						1.410	0.068				
	Continuous	0.5		7						0.140	0.285				
		1		10						0.350	0.356				
		2.5		12						0.640	0.261				
Stirred tank reactor	Batch		waste water anaerobic digestate	109	37	4.5	0.64	0.6	0.2	0.080		20		*Clostridium sp.*	(Ganigué et al., 2015)
HFMBR	Batch		mesophilic anaerobic methane producing culture	26	35	5.0		0.6	0.4	0.420	0.020	10		*Clostridium sp. C. ljungdahlii C. drakei*	(Zhang et al., 2013b)
	Continuous	9		35						0.110	0.013				
HFMBR	Batch			80	35	6.0		0.6	0.4	0.250		10		*Clostridium sp. C. ljungdahlii C. kluyveri*	(Zhang et al., 2013a)

Table 5: Major literature studies of gaseous substrate conversion into acetate and other liquid products with MMCs. HFMBR: Hollow fibre membrane reactor; HRT: hydraulic retention time; C: concentration in g.L^{-1}; P: productivity in mmolC.L^{-1}.d^{-1}.

4 PhD scope

This thesis project has the objective of studying the microbial competition between HM and HAC, with the ambition of selectively producing acetate from H_2/CO_2 through consortium engineering strategy. A first challenge was to evaluate the feasibility of such process. From the literature review, different scientific needs were highlighted. First, a great variability in kinetic parameters reported for HM and HAC was observed. This demonstrates that HM and HAC are diverse metabolic groups. This is an advantage considering functional redundancy potential of MMCs regarding CO_2 reduction, as some HAC and HM can be selected under a wide range of operating conditions. However, this disparity in the kinetic parameters values is also due to the difficulty of experimentally measuring them (Pavlostathis and Giraldo-Gomez, 1991). They are also highly reactor- and conditions-dependent, making difficult their use for the prediction and the understanding of the microorganism's behaviour under other conditions and with other types of reactors.

What have been learned though from the literature, is that in nature methanogens could not be isolated from psychrophilic environments (Jarrell and Kalmokoff, 1988), while HAC could. Hence, temperature could play an important role in the selection of HAC when decreased. Another redundant observation is that high H_2 partial pressures generally enhance acetate production in natural environments but also in anaerobic bioreactors (Karekar et al., 2022; Agneessens et al., 2017). Additionally, pH has a strong effect on product profile in MMCs. In particular, pH decrease along acetate production promotes carboxylates reduction into alcohols and chain elongation (Ganigué et al., 2015). Thereby, these key parameters identified in the literature were the starting points of the investigations carried out in this thesis work.

One of the objectives of this work was to identify points of attention, generally applicable, in order to better apprehend the outcome of the competition in different growing conditions. This

should bring some insights to implement H_2/CO_2 biological conversion into acetate, but also to specialize MMCs biocatalysts for this specific function, with the challenge of not resorting to chemical inhibitors or heat treatments. The scope of this work is also to provide knowledge about homoacetogens behaviour in MMCs, they are found in other systems such as biological methanation, dark fermentation and anaerobic digestion reactors, and still remain poorly studied and understood in MMCs. Some applications require to promote HAC, while others need to avoid the reactions. In both cases, a thorough knowledge of this microbial community is essential for the development of anaerobic MMC biotechnologies (Basile et al., 2020).

In order to meet these objectives, different approaches of modeling and experimental works have been undertaken, and complement each other's. In chapter 3, the acetate production from H_2/CO_2 was analysed with data from a thermophilic biological methanation reactor. Data were analysed to identify what promoted VFA production in this system, and refine the statements formulated from the literature. A modeling work joined this analysis, based on kinetic parameters reviewed from the literature. The model was developed with AQUASIM, to represent growth of HM and HAC. This preliminary work allowed to make some assumptions regarding the microbe's behaviours, and to hypothesize the outcome of the competition according to different operating conditions such as temperature, reactor culture modes, and substrate limitation state. Physical-chemical aspects such as pH, acid-base dissociation and gas to liquid mass transfer were considered in the analysis and in the model, as well as growth kinetics and thermodynamics.

Then, experimental campaigns were designed and conducted to confront the modeling predictions to real conditions. This work aimed at exploring and demonstrating the feasibility of using consortium engineering methods for acetate production from H_2/CO_2 and HM elimination. First, the competition was studied in batch mode in chapter 4. The effect of the

temperature between 25 °C and 35 °C, and of the mass transfer limitation, were specifically studied and are discussed regarding the previous statements formulated in chapter 3 about the outcome of the microbial competition. This work in batch experiments also aimed at providing a cultivation method, based on successive batches, to specialize MMCs with HACs.

Finally, in chapter 5, an experimental campaign in continuous stirred tank reactors (CSTRs) is presented. Going through continuous reactors was chosen to bring a new selection pressure: the dilution rates. From this regard, it is an interesting tool to study microbial competitions as dilution rate fixes the minimal specific growth rate required for the microorganisms to maintain themselves in the reactor. Hence, it is also a tool for microbial selection in MMCs. In this chapter, the effect of pH, temperature and dilution rate (D) are studied regarding the microbial competition, especially whether or not HM remained active. Some optimisation of the culture medium is also included in this part of the work.

These results obtained through modeling, and different experimental systems (chapters 4 and 5) provide diverse and complementary information about the behaviour of HM and HAC in anaerobic MMCs. The confrontation and the discussion of the different results contribute to bring insights for CO_2 reduction bioprocesses development.

CHAPTER 2: Materials and methods

1 Dynamic model on AQUASIM

A kinetic model has been developed on Aquasim 2.1g (Reichert, 1994) in order to study the microbial competition within the consortium, according to kinetics and thermodynamics features. The model is based on ADM1 existing processes, and have been adapted for the project. The model includes dynamic microbial growth in accordance with Monod equation; dynamic physical-chemical processes of weak acid dissociation, acid-base equilibria, and gas to liquid mass transfer (Figure 6). In the model, microbes metabolize the dissolved gas. Homoacetogens produce Acetate and proton, instantaneously equilibrated according to pH. To simplify the model, only a gas and a liquid compartment are represented. Even if all the biological reactions discussed are supposed to occur in the cytoplasm, no intracellular compartment is represented in this model.

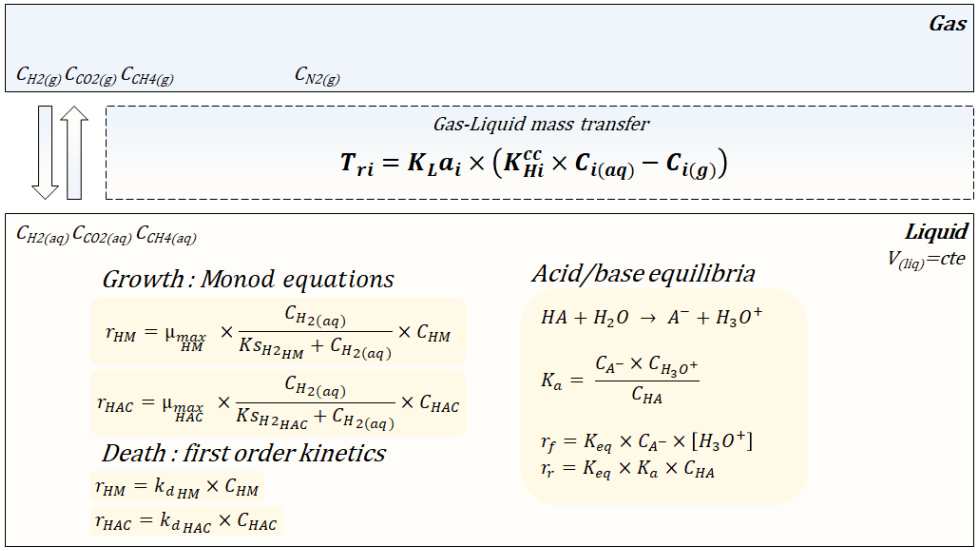

Figure 6: Scheme of the main physical-chemical and biological reactions considered in the dynamic model.

1.1 Gas phase

No reactions occur in the gas compartment, and it is described as a homogeneous mixture of perfect-gases. Four state variables are represented in the gas phase: H_2, CO_2 CH_4 and N_2.

1.2 Liquid phase

The liquid phase is described as an ideal aqueous solution. Ionic strength *I* (G) of the mineral medium has been calculated as 0.026 M, which is lower than conventional physiological range (0.05 – 0.25 M) (Amend and Shock, 2001).

$$I = \frac{1}{2}\sum m_i z_i^2 \qquad \text{(G)}$$

m: molality of the component i
z: charge of the component i

For this reason, ionic strength is considered as 0 so quantities used was not corrected according to ionic strength into the model. Additionally, in the framework of the simulation of batch experiments in serum bottles, low concentrations of acetate and biomass was reached, so solutes are considered as infinitely diluted. However, when higher concentrations of acetate and biomass are reached, this hypothesis should be reconsidered, and the physicochemical quantities have to be corrected according to ionic strength and dissolved organics concentrations.

1.3 Gas solubility in aqueous solution

Gas solubility in pure water at a given temperature depends proportionally on the partial pressure of the compound in the gas phase. The proportionality factor is called Henry's law constant. In real environments, Henry's law constant also depends on temperature, ionic strength and dissolved organic compounds. For the reason expressed in previous section 1.2., Henry's law constants will be corrected according to temperature only. There are different manners to express the Henry's law constant, with different units. Especially, two main types of Henry's law constant can be found: Henry's law solubility constants (H) describe the ratio

between aqueous quantity over gaseous quantity (aq/g) of the compound considered at equilibrium; reversely, Henry's law volatility constants (K_H) refer to the ratio of gaseous quantity over aqueous quantity (g/aq) of the compound at equilibrium. Different variants in the two previously described types exist with different units as well as dimensionless constants. A terminology and description of these different Henry's law constants has been well established by R. Sander (2015), as well as a compilation of the constant values and will be used in the following sections. Depending on how the equilibrium of the two phases is described, the use of one or another variant of Henry's law constant is needed to ensure unit consistency.

1.4 Gas to liquid mass transfer rate definition

Only H_2, CO_2 and CH_4 mass transfer are described in the model, as N_2 is not involved in the reactions of interest. In the model, the gas to liquid mass transfer rate is described as follow according to AQUASIM manual:

$$I_i = q_{ex,i} \times \left(f_i \times C_{i,aq} - C_{i,g}\right) \text{ in mol.L}^{-1}\text{d}^{-1} \quad \text{(H)}$$

With $C_{i,aq}$ and $C_{i,g}$ the soluble aqueous and gaseous concentrations of compound i, $q_{ex,i}$ the exchange coefficient and f_i the conversion factor allowing the description of phase transition. In the case of I_i being the gas to liquid mass transfer rate ($T_{r,i}$) of compound i, $q_{ex,I}$ is the volumetric transfer coefficient $k_L a_i$ in d^{-1} and f_i is a dimensionless Henry's law volatility constant (K_{Hi}^{cc}) expressed as the ratio of concentrations in the gas over the liquid at equilibrium state. Finally, the mass transfer rate is described as follow:

$$T_{ri} = K_L a_i \times \left(K_{Hi}^{cc} \times C_{i,aq} - C_{i,g}\right) \quad \text{(I)}$$

As temperature strongly affects gas solubility, a correction of the Henry's law constant according to temperature is included in the model as follow (Sander, 2015):

$$K_{Hi}^{cc} = \frac{1}{H_i^{cp}(T) \times RT} \quad \text{(J)}$$

$$H_i^{cp}(T) = H_i^{cp}(T^\theta) \times \exp\left(\frac{-\Delta_{sol}H}{R} \times \left(\frac{1}{T} - \frac{1}{T^\theta}\right)\right) \quad \text{(K)}$$

where:

	$H_i^{cp}(T^\theta)$, M.atm^{-1}	$\frac{-\Delta_{sol}H}{R}$, K
H_2	0.00078020250	500
CO_2	0.03343725000	2400
CH_4	0.00141855000	1600

And T^θ = 298.15 K

1.5 Biological reactions

The model includes two growth processes describing methanogenic archaea (X_{HM}) and homoacetogenic bacteria (X_{HAC}) biomasses production rates (Table 6), and biomass composition is considered as $C_5H_7NO_2$.

1.5.1 Stoichiometric equations of growths:

$$X_{hm}: \nu_{H_2}H_2 + \nu_{CO_2}CO_2 + \nu_{NH_4^+}NH_4^+ \rightarrow \nu_X C_5H_7NO_2 + \nu_{CH_4}CH_4 + \nu_{H_2O}H_2O + \nu_{H^+}H^+$$

$$X_{hac}: \nu_{H_2}H_2 + \nu_{CO_2}CO_2 + \nu_{NH_4^+}NH_4^+ \rightarrow \nu_X C_5H_7NO_2 + \nu_{C_2H_4O_2}C_2H_4O_2 + \nu_{H_2O}H_2O + \nu_{H^+}H^+$$

Hydrogen is considered as the limiting substrate in any case due firstly to its low solubility and secondly because CO_2 is supplied in excess compared to H_2 according to the stoichiometric ratio of the reactions. Thus, only Monod term for H_2 is included in growth rates and CO_2 limitation is neglected.

1.5.2 Decay rates

The model includes two decay processes describing methanogenic archaea and homoacetogenic bacteria biomass decomposition into composite materials X_C as it is described in ADM1 (Table

6), with k_{dec} set to 0.02 for HAC and HM. Note that in the framework of this project, the heterotrophic growth on composite material is considered as negligible and was not included.

Processes ↓	**State variables (mol.L^{-1})**										**Rates (mol.L^{-1}.d^{-1})** ↓
	C_{Xc}	C_{Xh2}	C_{Xhac}	$C_{H2,liq}$	$C_{CH4,liq}$	C_{ac-}	$C_{H2O\ produced}$	$C_{IC,liq}$	$C_{IN,liq}$	C_{H+}	
Growth of X_{HM}		$Y_{XHM/H2}$		-1	1 - $Y_{XHM/H2}$		$\sum_{i=IC_{CO2},X_{HM},CH_4} O_i\nu_i, X_{HM}$	$-\sum_{i=X_{HM},CH_4} C_i\nu_i, X_{HM}$	- $Y_{XHM/H2}$	$Y_{XHM/H2}$	$k_{mol,HM} \times \frac{C_{H2}}{C_{H2}+K_{s,HM}} \times X_{HM}$
Growth of X_{HAC}			$Y_{XHAC/H2}$	-1		1 - $Y_{XHAC/H2}$	$\sum_{i=IC_{CO2},X_{HM},CH_4} O_i\nu_i, X_{HAC}$	$-\sum_{i=X_{HAC},C_2H_4O_2} C_i\nu_i, X_{HAC}$	- $Y_{XHAC/H2}$	$Y_{XHAC/H2}$	$k_{mol,HAC} \times \frac{C_{H2}}{C_{H2}+K_{s,HAC}} \times X_{HAC}$
Decay of X_{HM}	1	-1									$k_{dec,HM} \times X_{HM}$
Decay of X_{HAC}	1		-1								$k_{dec,HAC} \times X_{HAC}$

Table 6: Biochemical rate coefficients (ν_i) and kinetic rate equations for growth and decay processes included in the model.

1.6 Acetic acid dissociation and acid-base equilibria

Acid-base equilibria are considered and integrated to the model. This enables the calculation of pH, and the simulation of different forms of soluble CO_2. Dissociation constant of each acid-base couple are defined according to temperature, except for acetate which is fixed. For each equilibrium, two processes are created for the forward and reverse reactions. For each HA/A^- equilibrium:

$$HA + H_2O \leftrightarrow A^- + H_3O^+$$

$$K_a = \frac{C_{A^-} \times C_{H_3O^+}}{C_{HA}} \quad \text{(L)}$$

$$r_f = K_{eq} \times C_{A^-} \times C_{H_3O^+} \quad \text{(M)}$$

$$r_r = K_{eq} \times K_a \times C_{HA} \quad \text{(N)}$$

f stands for forward reaction and r reverse reaction. K_{eq} was arbitrary fixed to 10^{12} for increasing the kinetics of the reaction and simulate an instantaneous equilibrium. Fictive anions and cations were implemented into the model to ensure electroneutrality.

Electroneutrality is verified by:

$$balance\_charge = (NH_4^+) + (H_3O^+) + (cat^+) - (Ac^-) - (HCO_3^-) - 2 \times (CO_3^{2-}) - (OH^-) - (an^-) = 0$$

pH can be calculated as follow:

$$pH = -\log[C_{H_3O^+}] \quad \text{(O)}$$

Processes ↓	State Variables (mol.L^{-1})									Rates (mol.L^{-1}d^{-1}) ↓
	C_{acH}	C_{ac}	C_{IC_co2}	C_{IC_hco3}	C_{IC_co3}	C_{NH4+}	C_{NH3}	C_{H}	C_{OH}	
f_acH_ac	-1	1						1		$K_{eq} \times Ka_{acH} \times C_{acH}$
r_ac_acH	1	-1						-1		$K_{eq} \times C_{ac^-} \times C_{H^+}$
f_CO2_HCO3			-1	1				1		$K_{eq} \times Ka_{CO_2} \times C_{CO_2}$
r_HCO3_CO2			1	-1				-1		$K_{eq} \times C_{HCO_3^-} \times C_{H^+}$
f_HCO3_CO3				-1	1			1		$K_{eq} \times Ka_{HCO_3^-} \times C_{HCO_3^-}$
r_CO3_HCO3				1	-1			-1		$K_{eq} \times C_{CO_3^{2-}} \times C_{H^+}$
f_NH4_NH3						-1	1	1		$K_{eq} \times Ka_{NH_3} \times C_{NH_4^+}$
r_NH3_NH4						1	-1	-1		$K_{eq} \times C_{NH_3} \times C_{H^+}$
f_H_H2O_OH								1	1	$K_{eq} \times K_w$
r_OH_H2O_H								-1	-1	$K_{eq} \times C_{OH^-} \times C_{H^+}$
Balance_an								balance_charge	-balance_charge	$K_{eq} \times C_{an^-}$
Balance_cat								-balance_charge	balance_charge	$K_{eq} \times C_{cat^+}$

Table 7: Rate coefficients and kinetic rate equations for acid-base reactions in the model.

Variables	Value
K_{eq}	10^{12}
Ka_{acH}	1.7378008×10^{-5}
Ka_{NH_3}	$0.637 \times \exp\left(-\frac{6209}{T_K}\right)$
Ka_{CO_2}	$5.02 \times 10^{-5} \times \exp\left(-\frac{1462.7}{T_K}\right)$
$Ka_{HCO_3^-}$	$7.83 \times 10^{-8} \times \exp\left(-\frac{2213}{T_K}\right)$
K_w	$2.8 \times 10^{-5} \times \exp\left(-\frac{6485}{T_K}\right)$

Table 8: Dissociation constants of acid-base equilibria included in the model (Roustan, 2003). T_K is the temperature in Kelvin.

1.7 Gibbs free energy of reactions and thermodynamic factor

Thermodynamic calculations are included into the model to evaluate the feasibility of the biological reactions. Four reactions are considered:

Hydrogenotrophic methanogenesis:	HM	$4H_2 + CO_2$	→	$CH_4 + 2H_2O$
Homoacetogenesis:	HAC	$4H_2 + 2CO_2$	→	$C_2H_4O_2 + 2H_2O$
Acetoclastic methanogenesis:	AM	$C_2H_4O_2$	→	$CH_4 + CO_2$
Syntrophic acetate oxidation:	SAO	$C_2H_4O_2 + 2H_2O$	→	$4H_2 + 2CO_2$

AM stands for acetoclastic methanogens as described in ADM1, and SAO for syntrophic acetate oxidation. These two biological reactions might be considered in the system as long as acetate is produced. Growths of these microbes are not included into the model. However, the calculations of Gibbs free energy (ΔrG) and thermodynamic factor (F_T) as described by Jin et Bethke (2007) are included for all the reactions to evaluate their feasibility and the eventual thermodynamic limitations of HM and HAC.

1.7.1 Dynamic calculation of the Gibbs free energy of reaction (ΔrG)

ΔrGs are calculated dynamically into the model, to evaluate the feasibility of four reactions of interest (HM, HAC, AM, SAO) along the process according to the following equation:

$$\Delta rG = \Delta rG° + RT \times \ln\left(\frac{\prod_p (P_g \times H_g)^{\nu} \times {C_l}^{\nu}}{\prod_r (P_g \times H_g)^{\nu} \times {C_l}^{\nu}}\right) \quad \text{(P)}$$

ΔrG° is calculated from the ΔfG° of the substrates and products from (Table 9), R is 0.0083144598 $kJ.mol^{-1}.K^{-1}$, P are the partial pressures of gaseous reactants, H are the solubility Henry's law constant of gaseous reactants, C are the concentration of solutes reactants. Activities in the standard equation (E) were replaced by soluble concentrations, assuming the liquid phase is an ideal aqueous solution (Jin and Bethke, 2007). The dissociated form of weak acids such as acetate are considered in the equation of ΔrG, as well as proton to integrate pH dependence of ΔrG in the calculation.

Compound	State	ΔfG° ($kJ.mol^{-1}$)
Hydrogen	H_2 (aq)	17.6
	H_2 (g)	0
Carbon dioxide	CO_2 (aq)	-385.98
	CO_2 (g)	-394.36
Methane	CH_4 (aq)	-34.33
	CH4 (g)	-50.72
Acetate	CH_3COO^-	-369.31
Acetic acid	CH_3COOH	-396.45
Water	H_2O	-237.19

Table 9: Gibbs free energy of formation (ΔfG°) of the different reactants. Blue highlights represent the value considered in the calculations (Alberty, 2005).

1.7.2 Dynamic calculation of the thermodynamic factor (F_T)

F_T was calculated from equation (F), with values summarized in Table 10.

	HM	HAC	AM	SAO
ΔrG° (kJ/reaction)	-131	-82	-49	+82
Y_ATP (molATP/reaction)	0.5	0.3	0.5	0.3
ΔGp (kJ/reaction)	45	45	45	45
ΔGc (kJ/reaction)	22.50	14.85	22.50	14.85
X	2	1	2	1

Table 10: Thermodynamic parameters used for the calculation of the ΔrG of the different reactions considered in the experimental conditions (Grimalt-Alemany et al., 2020).

2 Experimental set up

2.1 Pilot-scale methanation process

Experiments were carried out prior to the PhD project in a 20 L bubble column reactor of height and internal diameter of 1.200 m and 0.145 m respectively. The liquid phase ran in batch mode, whereas gas were continuously sparged from the bottom to the top of the column through porous fritted with a porosity between 100 and 160 µm. Headspace was recirculated at 120 $NL.L^{-1}.d^{-1}$. H_2:CO_2 ratio is 4:1, according to reaction stoichiometry (1).

The culture medium was composed of NH_4Cl 1 $g.L^{-1}$; KH_2PO_4 0.5 $g.L^{-1}$; $MgCl_2$, $6H_2O$ 0.1 $g.L^{-1}$; $CaCl_2$, $2H_2O$ 0.05 $g.L^{-1}$; Na_2SO_4 0.1 $g.L^{-1}$; $NaHCO_3$ 0.13 $g.L^{-1}$; Na_2S, $9H_2O$ 2 $g.L^{-1}$. Phosphate buffer is also used (K_2HPO_4 2.05 $g.L^{-1}$; KH_2PO_4 0.59 $g.L^{-1}$).

The inoculum came from household wastes, duck manure and bovine manure industrial AD plants. They were mixed, centrifuged, and suspended in fresh medium.

Amounts of hydrogen, carbon dioxide and methane are measured with a gas chromatograph (HP 5890 Series II). Amounts of acetate, propionate, butyrate, isobutyrate, valerate, isovalerate and hexanoate are measured with a gas chromatograph (VARIAN 3900 GC). Vector gas is N_2.

Soluble proteins has been quantified with bicinchonique acid (BCA) method. It is a spectrophotometric method based on complexation of BCA-Cu^{2+} with proteins. A standard curve has been done with bovine serum albumin (BSA) solutions from 0 to 1 $gBSA.L^{-1}$. A working solution was prepared with 5 mL solution A (BCA solution GBiosciences) and 100 µL solution B (Copper solution GBiosciences). Wells of a microplate were filled with 25 µL of sample and 200 µL of working solution. Standard range was realized in triplicates and samples were measured twice. Microplate was incubated 15 min at 55 °C. Absorbance was measured in a spectrophotometer (Multiskan Ascent Thermo Electron Corporation). Microplate was shaked 10 s at 480 rpm before absorbance reading at 570 nm.

2.2 Successive batches enrichments

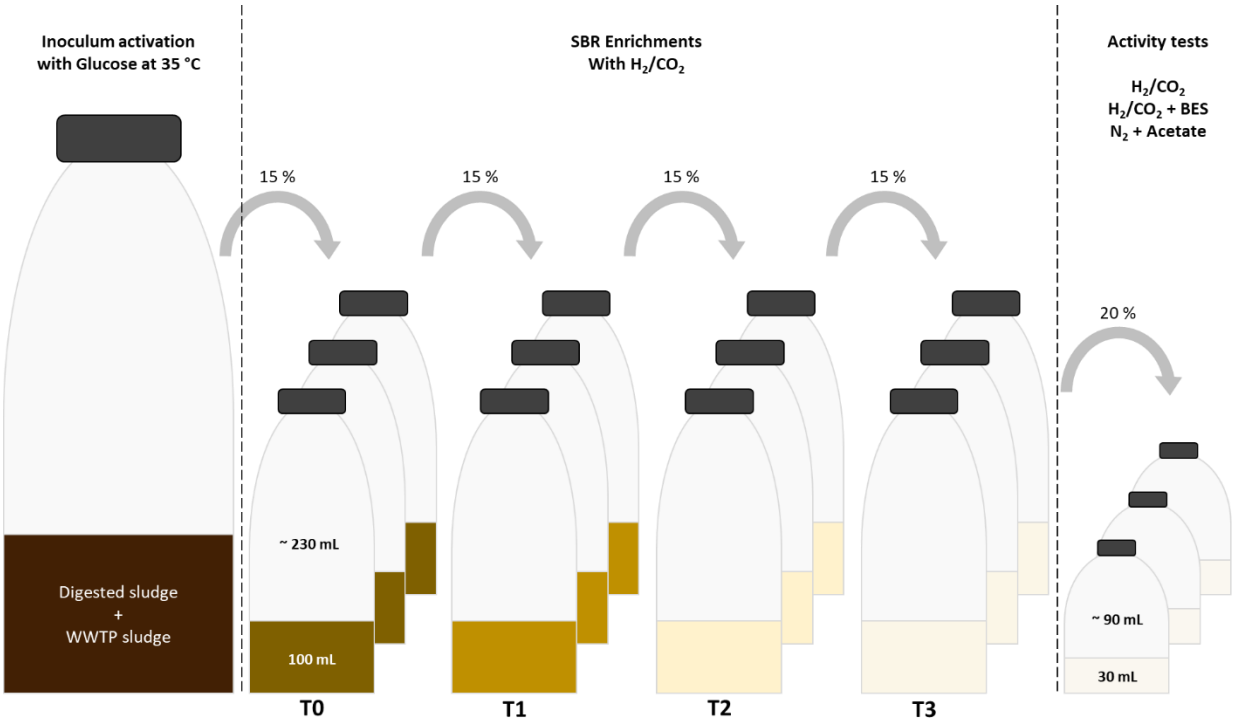

Figure 7: Graphical explanation of the successive batches enrichments carried out in this work.

Successive batches (SBs) were performed in triplicates in 330 mL serum vials at 25 °C and 35 °C. The flasks were filled with 85 mL of growth medium, sealed with rubber stoppers and screw plugs and flushed 15 min with N_2 before the addition of 15 mL of active inoculum. 75 mL of CO_2 and 150 mL of H_2 were added in the flasks to reach a final relative pressure of 1 bar, H_2 and CO_2 partial pressures of 0.66 ± 0.03 and 0.33 ± 0.03 respectively. The pH was measured externally at 6.30 ± 0.05 after inoculation with raw activated inoculum (T0), and 6.05 ± 0.03 after inoculation with enriched cultures (from T1 to T3). Once gas consumption is observed, liquid and gas composition are analysed (see analytical methods section). Four successive batches were operated (T0-T3), selecting at each step the most active mixed culture to inoculate the next triplicate of batches. The vials were prepared the same way at the beginning of each batch.

2.3 Methanogenic, homoacetogenic, and acetotrophic activity tests

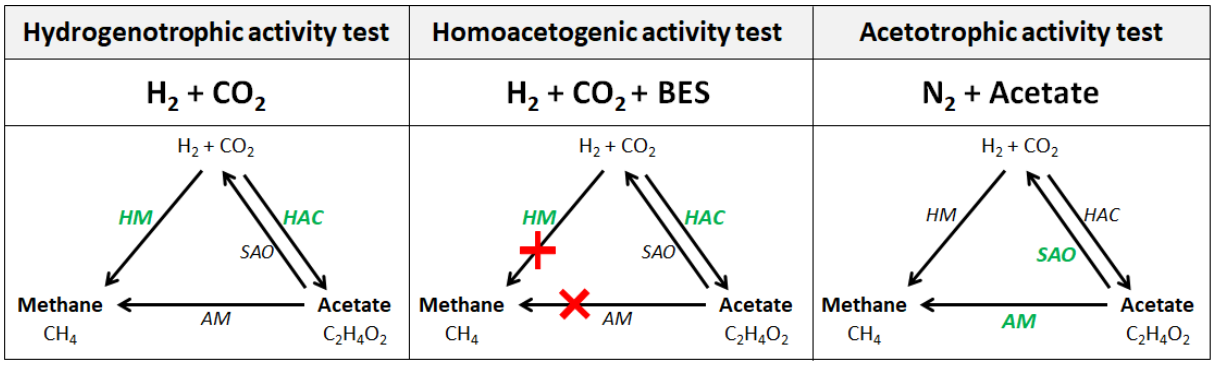

Figure 8: Graphical explanation of the activity tests carried out on the MMCs selected during the SB experiments. In green and black the feasible and unfeasible routes according to thermodynamics at initial state of the test respectively. Red crosses represent the inhibitory effect of BES on methanogenesis.

To assess the enriched microbial activities, tests were carried out in 120 mL serum vials with 30 mL of liquid volume. Vials were filled with 24 mL of fresh medium, sealed with rubber stoppers and screw plugs and flushed 10 min with N_2 before the addition of 6 mL of enriched culture T3 (20 % v/v). Triplicates of three different conditions were carried out. The first condition was H_2/CO_2, 30 mL of CO_2 and 60 mL of H_2 were injected in the vial. The second condition was H_2/CO_2 + BES, 15 mM of BES were added to the culture broth, 30 mL of CO_2 and 60 mL of H_2 were injected in the vials. The third condition was N_2/Acetate, 20 mM of acetate were added to the culture broth, without H_2/CO_2 injection. The vials were incubated at the temperature at which the inoculum (T3) had been grown.

2.4 Continuous stirred tank reactors (CSTR), liquid and gas opened

2.4.1 CSTR at 35 °C in TBI

2.4.1.1 Gas phase monitoring

2.4.1.1.1 Gas-liquid mass transfer characterization

The mass transfer coefficient (k_La) of the reactor was determined in water at 35 °C according to reoxidation method (Roustan, 2003). The water was flushed with nitrogen until the dissolved oxygen was close to zero. Then, the system was opened in order to diffuse air in the same conditions as H_2/CO_2 during the experiments. Three successive measurements were carried out. The dissolved oxygen dynamics and the linearization curves are presented in Figure 9.

$$\ln\left(\frac{(C^*-C_{t0})}{(C^*-C_{tx})}\right) = k_L a \times (tx - t0) \qquad \text{(Q)}$$

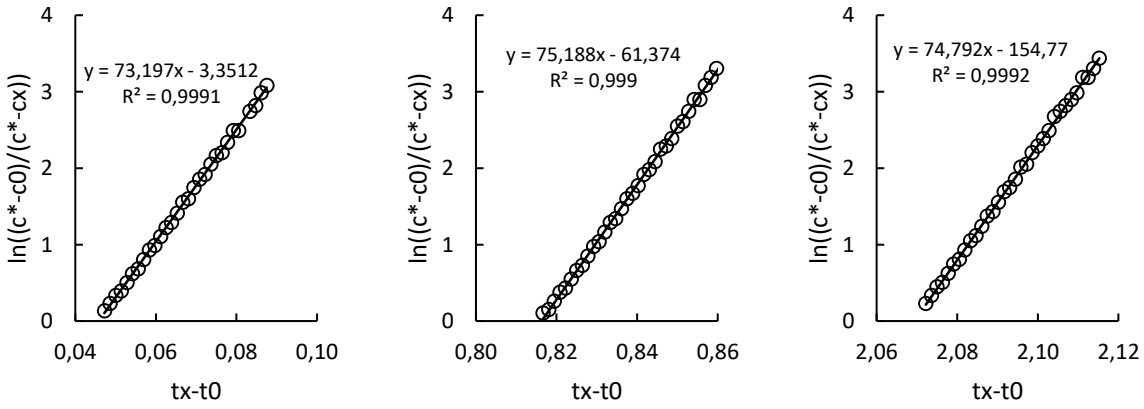

Figure 9: Linearization of reoxygenation curves to determine k_La in triplicate in the CSTR developed at TBI.

Finally, the mass transfer coefficient for O_2 was 74 ± 1 h^{-1} and O_2 was solubility of 6.92 ± 0.02 $g.L^{-1}$. The correction for H_2, CO_2 and CH_4 are calculated with gas diffusivity as follow (Roustan, 2003):

$$k_L a_i = k_L a_{O2} \times \sqrt{\frac{D_i}{D_{O2}}} \qquad \text{(R)}$$

With D_{O2} = 2.1 x 10^{-5} $cm^2.s^{-1}$, D_{H2} = 4.5 x 10^{-5} $cm^2.s^{-1}$, D_{CO2} = 1.9 x 10^{-5} $cm^2.s^{-1}$ and D_{CH4} = 1.5 x 10^{-5} $cm^2.s^{-1}$.

	O_2	H_2	CO_2	CH_4
k_La (d^{-1})	1776	2616	1704	1512
Solubility at 35 °C($mmol.L^{-1}$)	0.2	0.7	23.8	1.1
Maximal transfer rate ($mmol.L^{-1}.d^{-1}$)	386	1827	40556	1584

Table 11: Calculations of k_La of other gases, and maximal transfer rate of the system for the different gases considered.

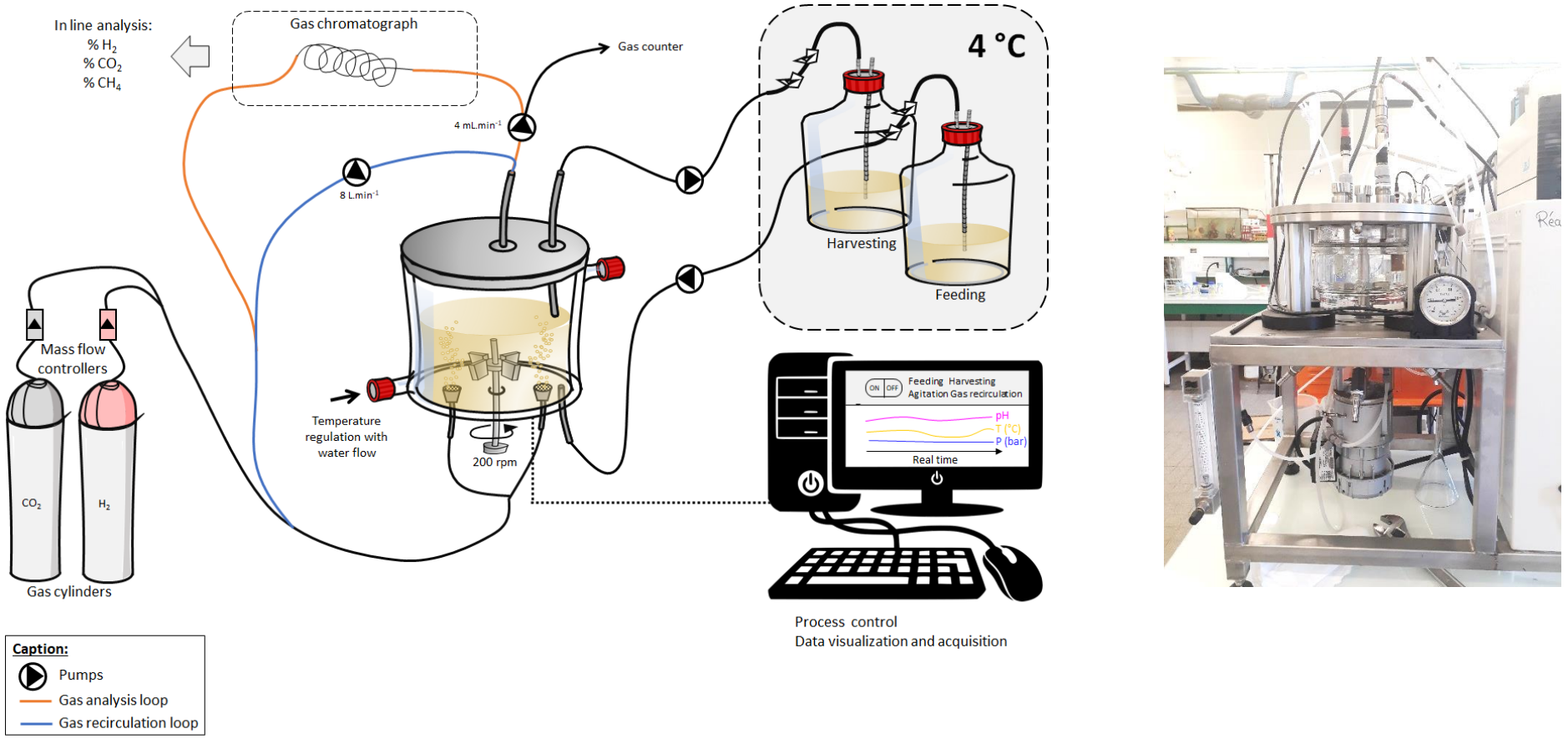

Figure 10: Scheme and picture of the continuous gas fermentation process implemented for the conversion of H_2/CO_2 to acetate in TBI.

2.4.1.1.2 Gas phase volume measurement

Dead volume of the reactor was measured in the conditions of the CSTR assays. The reactor was filled with 2 L of fresh medium inoculated with 10 % (v/v) of sludge. Temperature was set to 35 °C, reactor was closed and the gas leaks were controlled so the reactor could maintain an overpressure of 0.2 bars during 1h. Successive known volumes of N_2 were injected with a 60 mL syringe in the reactor. Pressure increase as a function of the volume injected was plotted to evaluate the gas phase volume (Figure 11) as follow:

$$V_{gas} = P_{atm} \times \frac{1}{\frac{\Delta P}{\Delta V}} \quad \text{(S)}$$

With P_{atm} = 1.0227 bar the 9th of December 2019 in Toulouse ("Toulouse-Blagnac (Haute-Garonne - France) | Relevés météo en temps réel - Infoclimat," n.d.).

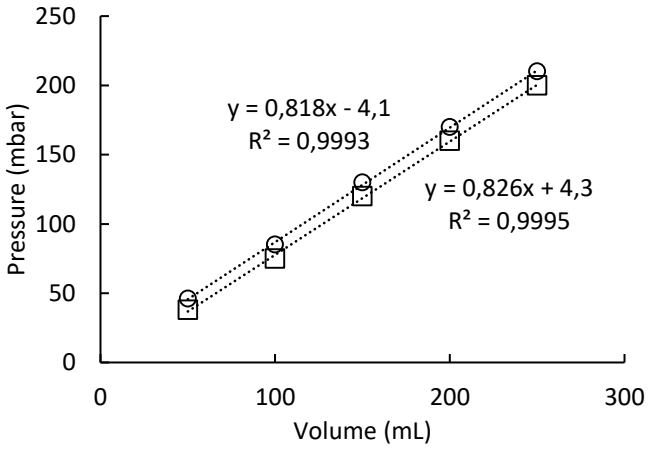

Figure 11: Pressure increase in the reactor closed as a function of gas volume injected to evaluate the gas phase volume of the reactor.

Finally, the gas phase volume was 1.24 ± 0.01 L in the conditions of the assays.

2.4.1.1.3 Gas mass flow controllers

Gas feeding was ensured with gas mass flow controllers (EL-FLOW SELECT F-201CV, Bronkhorst, France) connected to H_2 and CO_2 gas cylinders. H_2 and CO_2 flows were set to 0.06

$L_{20°C}.min^{-1}$ and 0.03 $L_{20°C}.min^{-1}$ respectively. These mass flow controllers were originally used with air and were calibrated for H_2 and CO_2. Their range were 2 $NL.min^{-1}$. The gas flowed continuously, and the output flow was measured with a gas meter (Ritter Drum-type TG 0.5).

2.4.1.1.4 GC continuous analysis

The gas phase was continuously circulated in a closed loop at 4.4 $mL.min^{-1}$ and cross a gas chromatograph (Trace 1300, Thermo Scientific) equipped with a column Rxi-1ms (Restek) of 30 m and 0.32 mm of internal diameter. A loop for H_2 detection in N_2 as carrier gas and PFPD detection, and another loop for CO_2 and CH_4 in He as carrier gas and TCD detection were implemented. Gas was analysed every 10 min.

2.4.1.2 Liquid phase monitoring

2.4.1.2.1 Continuous operations

The mineral medium bottle was store in a fridge at 4 °C and anaerobic conditions all along its consumption. The feeding flow was set according to the HRT needed. The feeding flow was ensured with a peristaltic pump working intermittently because of the low flows applied. Harvesting of the culture broth was carried out with a sampling cannula placed on the surface of the liquid to maintain a constant volume. The harvesting flow was set higher than the feeding flow, and occurred at the same intermittent time as feeding phases. The feeding and harvesting bottles were weighed every day to monitor the actual liquid flow and consider the harvesting of the volume equivalent to the base addition to regulate pH. Liquid sampling was carried out during the feeding/harvesting times, once or twice a day.

2.4.1.2.2 Microbial mixed culture origin and physical-chemical composition

The MMC used is a mixture of three sludges from anaerobic digestors. One treats cattle slurry on a dairy farm, another treats duck slurry and the last treats organic food wastes. The first two were sieved at 0.5 mm in order to eliminate as many solid particles as possible and to keep only the liquid phase and suspended microorganisms. The last was sieved at 50 mm due to its high viscosity. 8 L of each were mixed and placed at 4 °C.

pH of total fraction	8.2
pH of soluble fraction	8.3
Total COD $g.L^{-1}$	34.1
Soluble COD $g.L^{-1}$	3.8
TSS $g.L^{-1}$	26.9
VSS $g.L^{-1}$	18.5
NH_4^+ $g.L^{-1}$	2.85 ± 0.15
AGV $g.L^{-1}$	Acétate 0,36 Propionate 0,02 Iso-butyrate 0,04 Corresponding to 0.43 $gCOD.L^{-1}$ of soluble COD

Table 12: Composition and characteristic of the inoculum.

2.4.2 CSTR at 25 °C in DTU

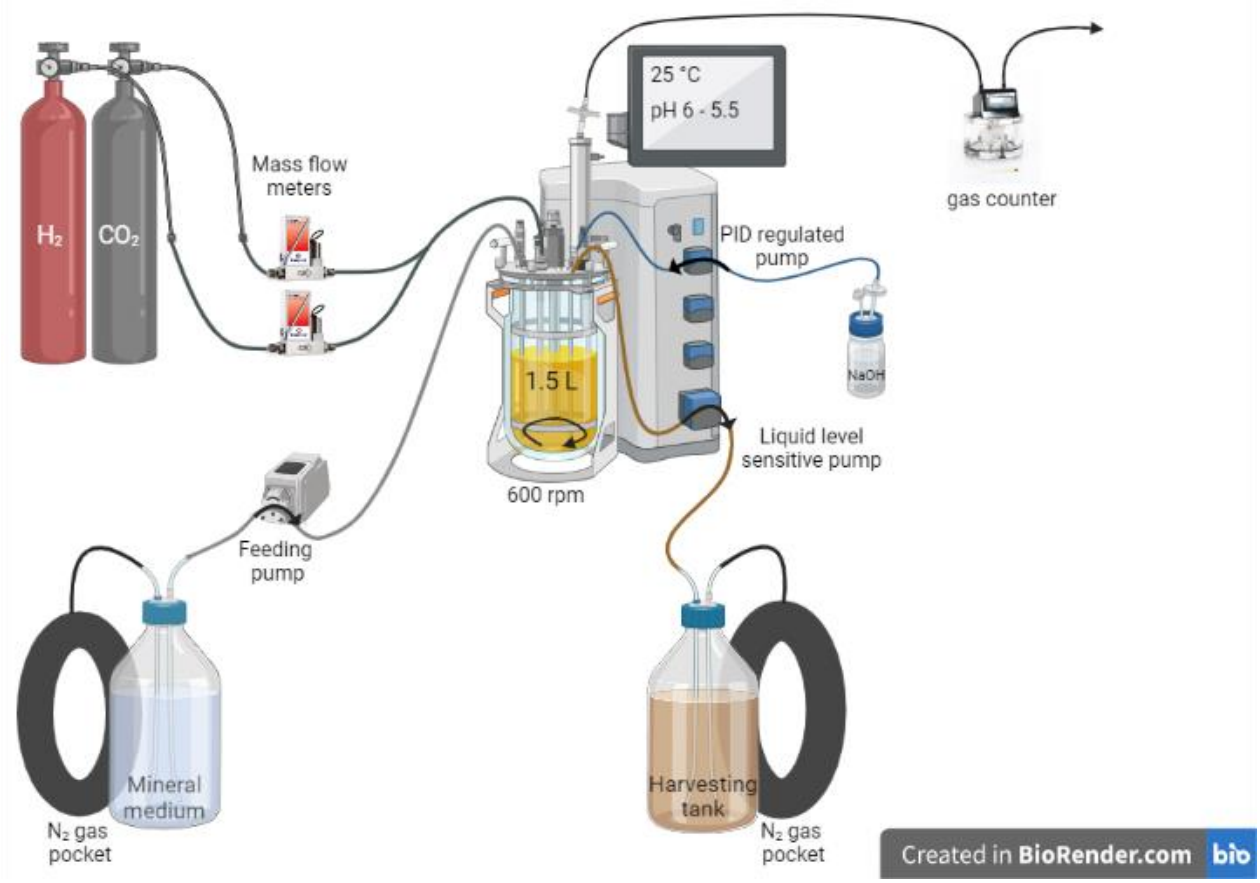

Figure 12: Reactor set up for the CSTR test at 25 °C.

A CSTR has been set up for the enrichment of the MMC with HAC, and the production of acetate in a single process (Figure 12). The reactor used was a 2L stirred tank reactor (uniVessel Glass, Sartorius) placed under a ventilated hood. The tank was equipped with two impellers, sparger at the bottom, and filled with 1.5 L of culture broth. The stirring speed was set at 600 rpm, and the temperature at 25 °C with a heating jacket. The process was set and monitored using a Biostat B controller (Sartorius Stedim Biotech). For safety reasons, H_2 inflow was controlled using a mass flow meter (El-Flow Select, Bronkhorsts) while CO_2 inflow was ensured through the controller. The output gas flow rate was calculated from a gas counter (Ritter MGC-1 V3.4) and a timer once a day. The feeding solution was composed of the mineral medium described in section 2.3. and connected to nitrogen pocket to ensure anaerobic

conditions. Feeding rate was continuous and set with a peristatic pump. Harvesting was ensured using a level sensor activating a high-speed peristatic pump of the controller. The reactor was equipped with a pH/ORP probe (Mettler Toledo InPro 325 X i), an optical oxygen sensor (Hamilton VisiFerm DO 225 ECS) and a temperature sensor. pH was regulated with 1M solutions of NaOH and HCl with PID method with the controller. pH was measured externally in order to calibrate the probe when necessary (once a week).

2.5 Growth media

2.5.1 Growth medium for the successive batches, the activity tests and the CSTR at 25 °C (DTU)

The growth medium was prepared from the four following solutions: salts (NH_4Cl, 50 $g.L^{-1}$; NaCl 10 $g.L^{-1}$; $MgCl_2.6H_2O$, 10 $g.L^{-1}$; $CaCl_2.2H_2O$, 5 $g.L^{-1}$), Na_2SO_4 50 $g.L^{-1}$, Vitamins (biotin, 2 $mg.L^{-1}$; folic acid, 2 $mg.L^{-1}$; pyridoxine–HCl, 10 $mg.L^{-1}$; riboflavin-HCl, 5 $mg.L^{-1}$; thiamine-HCl, 5 $mg.L^{-1}$; cyanocobalamine, 0.1 $mg.L^{-1}$; nicotinic acid, 5 $mg.L^{-1}$; p-aminobenzoic acid, 5 $mg.L^{-1}$; lipoic acid, 5 $mg.L^{-1}$; D-pantothenic acid hemicalcium salt, 5 $mg.L^{-1}$), Trace metals (Nitrilotriacetic acid, 2000 $mg.L^{-1}$; $Fe(SO_4)_2(NH_4)_2.6H_2O$ 800 $mg.L^{-1}$; H_3BO_3, 10 $mg.L^{-1}$; $ZnSO_4.7H_2O$, 200 $mg.L^{-1}$; $CuCl_2$, 20 $mg.L^{-1}$; $MnSO_4$, 1000 $mg.L^{-1}$; $Na_2MoO_4.2H_2O$, 20 $mg.L^{-1}$; $AlCl_3$, 10 $mg.L^{-1}$; $CoCl_2 \cdot 6H_2O$, 200 $mg.L^{-1}$; $NiCl_2$, 20 $mg.L^{-1}$; $Na_2SeO_4 \cdot 5H_2O$, 18 $mg.L^{-1}$; $Na_2WO_4 \cdot 2H_2O$, 22 $mg.L^{-1}$). Potassium dihydrogen phosphate (KH_2PO_4 1M) and dipotassium hydrogen phosphate (K_2HPO_4 1M) were used as buffering solutions. The medium was prepared by adding 20 $mL.L^{-1}$ of salts solutions, 1 $mL.L^{-1}$ of Na_2SO_4 solution, 10 $mL.L^{-1}$ of vitamins solutions, 10 $mL.L^{-1}$ of trace metals solution, 86 $mL.L^{-1}$ of KH_2PO_4 and 14 $mL.L^{-1}$ of K_2HPO_4. The pH of the medium under N_2 atmosphere was 5.98 ± 0.05.

2.5.2 Growth medium for the CSTR at 35 °C (TBI)

A minimal medium was used initially and composed of four different stock solutions. Solution A: NH_4Cl (20 $g.L^{-1}$); solution B: $MgCl_2.6H_2O$ (2 $g.L^{-1}$), $CaCl_2.2H_2O$ (1 $g.L^{-1}$); solution C: $FeCl_2.4H_2O$ (200 $mg.L^{-1)}$; H_3BO_3 (10 $mg.L^{-1}$); $ZnCl_2.7H_2O$ (10 $mg.L^{-1}$); $CuCl_2.2H_2O$ (8 $mg.L^{-1}$); $MnCl_2.4H_2O$ (20 $mg.L^{-1}$); $H_{24}Mo_7N_6O_{24}$, (7 $mg.L^{-1}$); $CoCl_2 \cdot 6H_2O$ (60 $mg.L^{-1}$); $NiCl_2$ (20 $mg.L^{-1}$); solution D: Na_2S (4 $g.L^{-1}$). The Four solution were mixed together in the appropriate volume of water to prevent precipitates between the different solutions: 50 $mL.L^{-1}$ of solutions A and B, 20 $mL.L^{-1}$ of solution C. This first mixture was flushed 10 min with nitrogen in the feeding bottle closed, then 25 $mL.L^{-1}$ of solution D were injected in the bottle with a syringe to ensure anaerobic addition of sulphide and prevent its oxidation and volatilization. Finally, a nitrogen pocket was connected to the bottle to compensate the loss of volume along the experiment and prevent O_2 inlet.

2.6 Analytical methods

2.6.1 Analytical methods in TBI, for the CSTR at 35 °C monitoring

2.6.1.1 COD dosage

Total COD was measured with kits of medium range (0-1500 $mg_{COD}.L^{-1}$) (HI-93754B-25, Hanna instruments) according to the manufacturer instruction manual, adapted from EPA 410.4 approved method. Appropriate dilutions of the samples were carried out prior to measurements. Soluble COD was measured in same type of tubes, after separation of the soluble fraction by centrifugation and filrtration at 0.2 µm. By subtracting the soluble COD measured to the total COD, suspended COD was estimated.

2.6.1.2 VFA analysis with gas chromatograph

Acetate, propionate, isobutyrate, butyrate, isovalerate, valerate and hexanoate were analysed with a gas chromatograph (430-GC, VARIAN). The carrier gas was N_2 at 25 $mL.min^{-1}$, in a column of polyethylene glycol (CP-WAX 58 FFAP CB, Agilent) of 15 m and external diameter of 0.53 mm. The calibration is carried out with a synthetic mix of the VFA analysed from 0.05 to 1 $g.L^{-1}$. 2-ethylbutyrate in orthophosphoric acid (5 %) was used as internal standard at 1 $g.L^{-1}$. Verification standard at 1 $g.L^{-1}$ were analysed every day. Injection is carried out at 250 °C, then a temperature program is carried out: 2 min at 90 °C, increase of 20 $°C.min^{-1}$ until 130 °C, 12 min at 130 °C and finally increase of 50 $°C.\ min^{-1}$ until 210 °C. 210 °C is maintained 2 min. FID detection was carried out at 240 °C.

2.6.1.3 Ionic chromatography

Anions (F^-, Cl^-, NO_2^-, Br^-, NO_3^-, SO_4^{2-}, PO_4^{3-}) and cations (Li^+, Na^+, NH_4^+, K^+, Mg^{2+}, Ca^{2+}) concentrations were determined with an ionic chromatograph (Dionex ICS 2000, Thermo

Scientific). Cation column was IonPac CS16 (2x250mm), eluent was methanesulfonic acid 30 mM at 0.36 mL.min^{-1} and 40 °C. Anions column was IonPac™ AS19 (2x250mm), eluent was KOH 20 mM, at 0.25 mL.min^{-1} and 30 °C.

2.6.1.4 VSS and TSS measurements

In order to know the quantity of dry matter in the reactor, a known volume (30-50 mL) of culture was centrifuged for 15 minutes at 13200 rpm. The pellet was taken up in a few mL of distilled water and then placed in an aluminium dish of known mass (m_d) at 105°C for 24 hours. At the end of 24 hours, the dish is weighed (m_{105}), placed for 2 hours at 500°C then weighed again (m_{500}). It is then possible to calculate the total suspended solid (TSS), the mineral suspended solid (MSS) as well as the volatile suspended solids (VSS):

$$TSS = (m_{105} - m_c)/V \quad \text{(T)}$$

$$MSS = (m_{500} - m_c)/V \quad \text{(U)}$$

$$VSS = TSS - MSS \quad \text{(V)}$$

2.7 Analytical methods in DTU, for successive batches, activity tests, and CSTR at 25 °C monitoring

Gas composition in H_2, CO_2, CH_4, N_2, O_2 was analysed using a gas chromatograph (GC 8610C, SRI Instruments, USA) while liquid was analysed for volatile fatty acids and alcohols concentrations determination (formic acid, acetic acid, butyric acid, valeric acid, hexanoic acid, isobutyric acid, isovaleric acid, ethanol, butanol) using a High-Performance Liquid Chromatograph (HPLC Shimadzu, USA). Detailed methods have been described in previous paper (Grimalt-Alemany et al., 2019). Microbial biomass was monitored with OD measurements at 600 nm using a spectrophotometer (DR2800, Hach Lange). Correlations between OD_{600} and dry weigh (DW), and between OD_{600} and volatile weight (VW) after 24h at 100 °C and 2h at 500 °C respectively, have been done with 50 mL samples of a CSTR culture inoculated with the same MMC at 25 °C under H_2/CO_2.

2.8 Microbial analysis

2.8.1 Methods in TBI for CSTR at 35 °C cultures

Two sample tubes of 2 mL were regularly stored at -20 °C for later DNA extraction and sequencing.

Total DNA extraction kit (MPbio, Fast DNA spin kit for soil) according to manufacturer instructions. Extracted DNA were submitted to the GetBiopuces Platform (TBI, INSA Toulouse). Amplification of V4 and V5 regions of 16 rRNA was carried out with 515F-Y 5' GTGYCAGCMGCCGCGGTAA and 926R 5' CCGYCAATTYMTTTRAGTTT primers (Walters et al., 2015). Library preparation was done with Ion Torrent S5 instrument. Data were processed with DADA2 pipeline, taxa assignment was done under rANOMALY package with the algorithm IDTAXA and database SILVA 138 16S and GTDB bac120_arc122 (Theil and

Rifa, 2021). Data visualization was processed with rANOMALY package.

2.8.2 Methods in DTU for successive batches and CSTR at 25 °C cultures

Samples for genomic DNA extraction and 16S rRNA sequencing were collected from the activated inoculum, from the successive batch enrichments at the end of the third transfer at 25 and 35 °C, and from the CSTR on day 41, 62 and 68. DNeasy PowerSoil™ DNA Isolation Kit (Qiagen, Denmark) was used for the DNA extraction of the activated inoculum. DNeasy Blood & Tissue™ Kit (Qiagen, Denmark) was used for the DNA extraction of all other samples. DNA extracted were submitted to Macrogen Europe. Amplification of V4 and V5 regions of 16S rRNA was performed with 515F-Y 5'-GTGYCAGCMGCCGCGGTAA and 926R 5' CCGYCAATTYMTTTRAGTTT primers (Walters et al., 2015). Library preparation was done according to Illumina NGS workflow with Illumina Miseq instrument (Vigliar et al., 2015). Data were processed with Qiime2 (Hall and Beiko, 2018) and Sklearn pipelines, and the taxa assignment was performed with database SILVA132. Data visualization was processed with rANOMALY package.

CHAPTER 3: Microbial competition between homoacetogens and hydrogenotrophic methanogens, a case study through biological methanation and modeling.

Associated manuscripts:

Rafrafi, Y., Laguillaumie, L. & Dumas, C. ***Biological Methanation of H2 and CO2 with Mixed Cultures: Current Advances, Hurdles and Challenges.*** *Waste Biomass Valor 12, 5259–5282 (2021). https://doi.org/10.1007/s12649-020-01283-z*

Laguillaumie, L., Rafrafi Y., Moya-Leclair E., Delagnes D., Dubos S., Spérandio M., Paul E., Dumas C. ***Stability of Ex Situ Biological Methanation of H2/CO2 with a Mixed Microbial Culture in a Pilot Scale Bubble Column Reactor.*** *Bioresour technol 354, 127180 (2022). https://doi.org/10.1016/j.biortech.2022.127180*

1 Summary and objectives

In this chapter, data from a pilot scale process of *ex situ* biological methanation at 55 °C have been analysed, regarding perturbation periods during which acetate and other VFAs were accumulated. The dynamics of the system facing parameters variations, such as gas partial pressures and nutrient supply were studied. This preliminary work aimed at understand what promoted HAC and other VFA producers in the methanation reactor. This allowed to prospect on key process parameters influencing the competition between HM and HAC. Then, a modeling work based on a kinetic parameters' literature review was joined to complement this chapter, and evaluate in what extend the MMC could produce acetate rather than methane. This modeling work explores different types of reactor managements for gas fermentation: with the gas and the liquid phase being closed (batch mode) or opened (continuous). A thermodynamic analysis is also addressed to evaluate the consistency of the dynamic model in the different configurations.

2 Case study: VFA accumulation during ex situ methanation at 55 °C

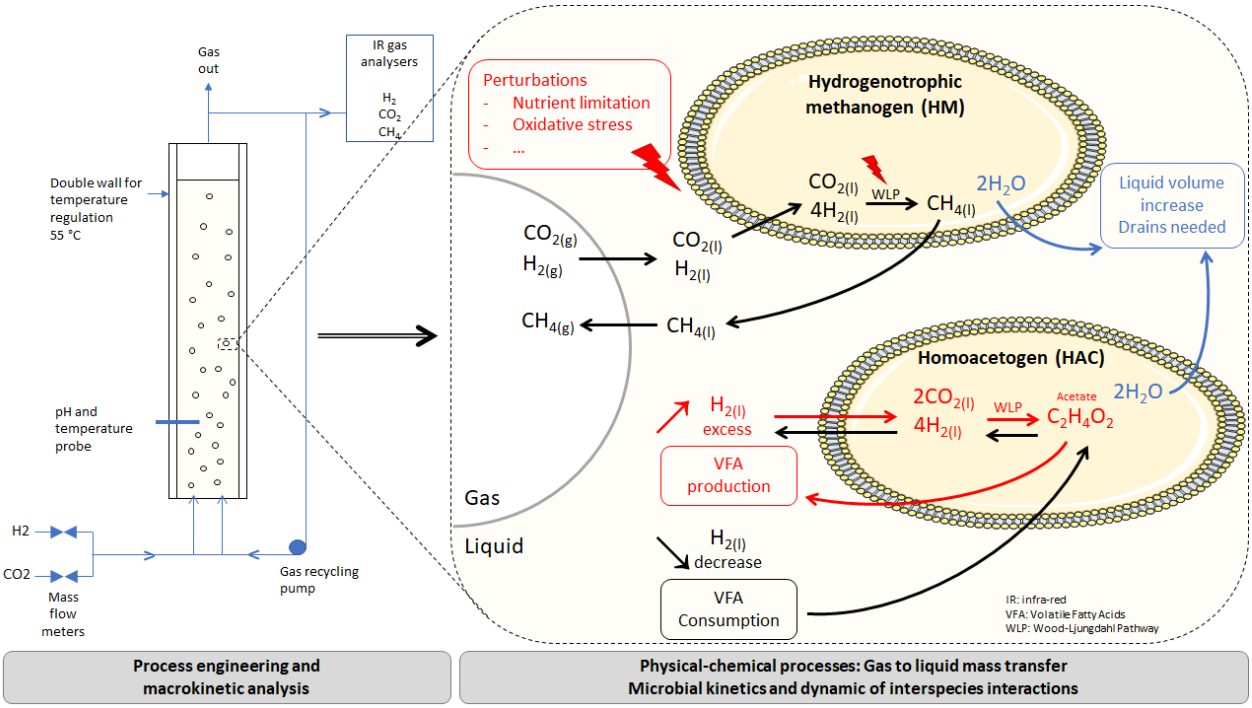

Figure 13: Representation of the biological methanation reactor and biochemical mechanisms studied (Laguillaumie et al., 2022).

2.1 Introduction

A pilot scale bubble column reactor was experimented for biological *ex situ* methanation at 55 °C prior to the PhD project. In this process, the liquid phase was conducted in pseudo-batch mode, meaning that only few volumes of liquid were sometimes extracted for volume regulation because methanation reaction produced water (Figure 13), or added for nutrient supply. These extractions and supplementations were necessary considering the duration of the operations that lasted over 400 d. However, the term pseudo-batch mode is used here, as the retention time was more than 100 d^{-1} during the two first periods presented in this chapter. Conversely, the gas phase was conducted in continuous mode, with a recirculation loop to improve the gas conversion yields. The gas inflow was composed of H_2/CO_2. The flow and the H_2/CO_2 ratio were modified during the process to test both the capacity, the adaptability and the stability of the methanation process (Figure 14 and Figure 16). VFA accumulations were observed during

this campaign (Figure 15), so the data were analysed in the framework of the PhD project. In this chapter, the two first periods of operation are discussed, regarding methane and VFA production, in order to understand the reason why VFA accumulated (Laguillaumie et al., 2022). VFA, and in particular acetate accumulation, was previously pointed as instability indicators in anaerobic digestion processes (Jacobi et al., 2009). More recently, it was also frequently observed in methanation processes, especially in *in situ* ones, and associated with H_2 additions in the reactors (Braga Nan et al., 2020; Agneessens et al., 2018, 2017). The analysis of process parameters is often undertaken, and is useful to understand the key parameters that affect these accumulations and instabilities of the processes. However, a deeper insight in the understanding of the microbial competitions within the MMCs is rarely addressed, although some studies brought some key findings about the effect of the temperature on the kinetic parameters of the different microbial communities (Fu et al., 2019; Grimalt-Alemany et al., 2019; Weijma et al., 2002).

Here, the objective was to analyse the data to confirm the key parameters previously pointed out, but also to study the microbial competition from a microbial kinetic point of view, within a modeling work, to enable to identify other parameters that could affect the competition between homoacetogens (HAC) and hydrogenotrophic methanogens (HM).

2.2 Results and discussion

Figure 14 represents the methane flow rates measured as a function of the H_2 and CO_2 inflows. The ranges of H_2 and CO_2 inflow rates varied from 1 to 8 $NL.L^{-1}.d^{-1}$ and from 0.13 to 1.9 $NL.L^{-1}.d^{-1}$ respectively, during both periods 1 and 2. During period 1, after 10 d of start-up period, the methane production increased proportionally with gas inflow rates (A), represented in green, with a yield of 0.22 $NL_{CH4}.NL_{H2}^{-1}$ and 1.02 $NL_{CH4}.NL_{CO2}^{-1}$ which is close to the stoichiometric yields of 0.25 and 1 respectively. When gas inflow was increased, represented in blue, CH_4 production increased proportionally. This indicates that the system was able to handle the flow rates variations while keeping methane selectivity and maximal substrate conversion rates. This also indicates that the maximal transfer capacity of the system was not reached in the range of inflows tested, and the system was limited by the gas supply. Conversely, during period 2,

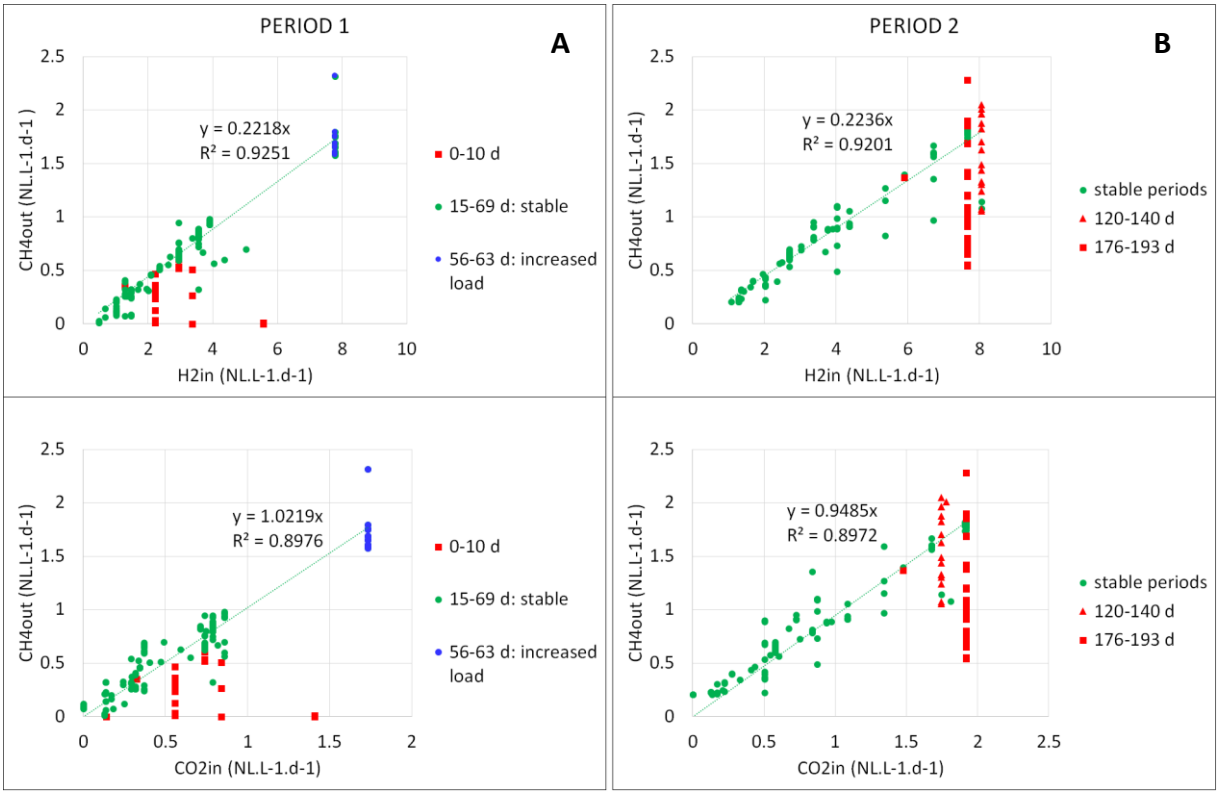

Figure 14: Methane production as a function of H_2 (up) or CO_2 (down) inflow during period 1 (left) and period 2 (right) of the ex situ methanation experiment (Laguillaumie et al., 2022).

the increase of inflow rates to the same range of values than during period 1, twice led to instability in the methane production, represented by red squares and triangles, between 127-140 d and again between 176-193 d (B).

Figure 15 represents VFA concentrations during periods 1 and 2. The two gas load increase phases during period 2 are represented by vertical lines. During these two phases of period 2, VFA, and in particular acetate accumulated in the liquid phase, while no accumulations were observed during period 1 at same gas inflows. Figure 16 represents H_2/CO_2 inlet ratio, and P_{H2} measured in the reactor. During gas increase phases, again delimited by vertical lines, P_{H2} reached 0.6-0.7 bars, indicating high amounts of substrate were not consumed, which is in accordance with methane production decrease observed. After sulphide supplementation directly injected in the reactor on days 136 and 192, maximal methane production was recovered and VFA concentrations decreased.

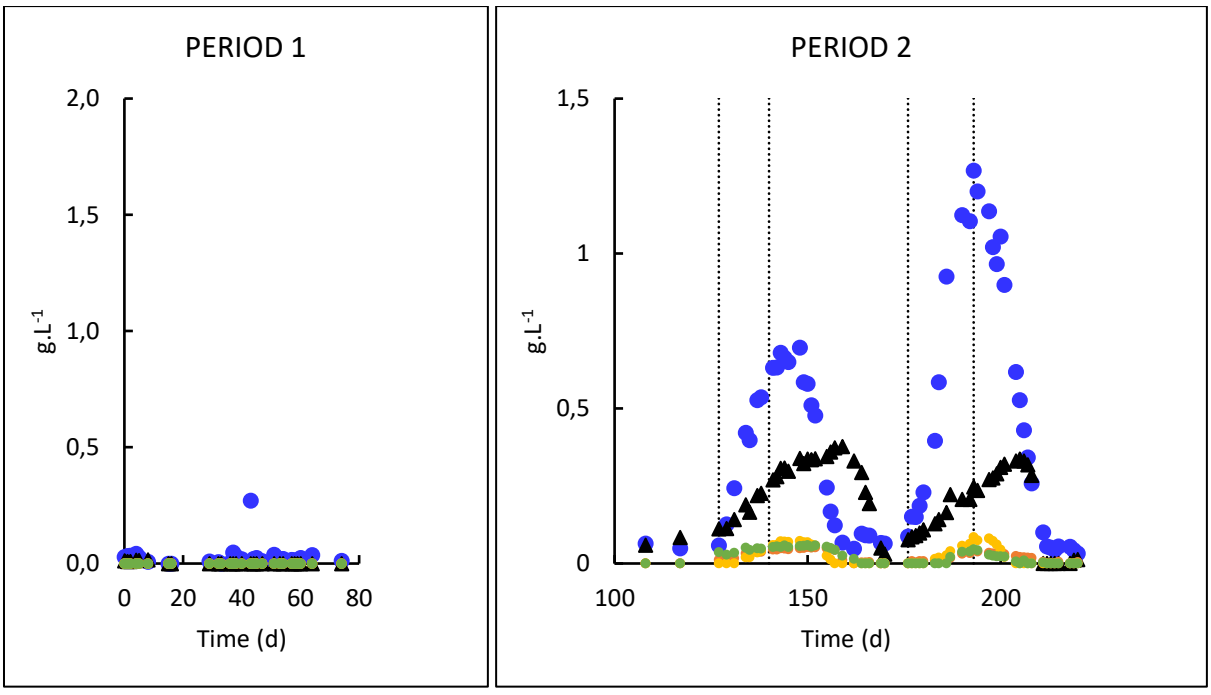

Figure 15: VFA concentration in the reactor during periods 1 and 2. Acetate (blue circles), propionate (black triangles), butyrate (yellow circles), isobutyrate (orange circles), methylbutyrate and isovalerate (green circles). Red vertical lines delimit the two phases during which methane production was not proportional to H_2/CO_2 inflow. Red arrows represent sulphide (Na_2S) injection in the reactor (Laguillaumie et al., 2022).

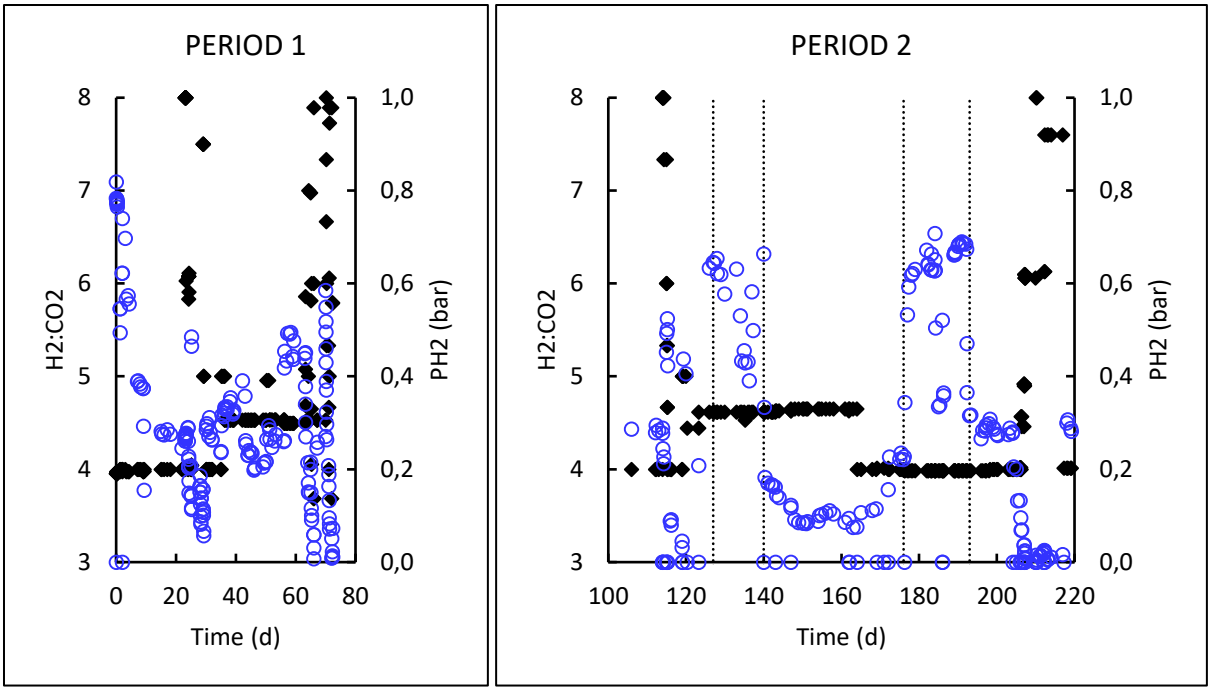

Figure 16: H_2/CO_2 ratio of the gas inflow (dark diamonds), and P_{H2} in bars (blue circles) of the gas inflow during periods 1 and 2 of the biological methanation process.

These results allowed to highlight the dynamic behaviour of the MMC in a biological methanation reactor. In particular, instability periods of the process were observed, and attributed to a sulphide limitation. After supplementing the culture broth with sulphide, process stability was recovered, demonstrating the reversibility of the system. Acetate accumulation was attributed to HAC, which turned to be favourable after H_2 availability increased in the system due to methanogens limitation. HAC dependence to H_2 partial pressure was previously demonstrated (Agneessens et al., 2018; Fuentes et al., 2021; Karekar et al., 2022), and it was observed and confirmed in this study.

Still, acetate productivities remained low, and represented only 1 % of the available COD, with high amounts of H_2 remaining unconverted. Hence, HAC were not able to handle all the H_2 available and dominate over HM. In the context of this experiment, actions were undertaken to recover methanogenesis and stop the VFA production, which makes difficult the interpretation of the competition as a steady state was not reached. However, this dynamic observation highlighted that HAC are opportunists becoming active as soon as the conditions are favourable,

i.e. H_2 availability increases. This is linked to thermodynamic feasibility of the reactions. Indeed, HAC as most anaerobic reactions, operates close to thermodynamic equilibrium. Acetogenic bacteria hence developed a very flexible metabolism, capable of consuming a wide range of substrates, and survive in very diverse environments, which explains acetogens are quite ubiquitous in nature. Acetogenic bacteria versatility has been documented, in natural environments they mostly grow heterotrophically, and switch to autotrophy in H_2 concentrated environments (Drake et al., 2008; Karekar et al., 2022). In other terms, they are capable of following thermodynamic feasibility of reactions to harvest energy in diverse environments. In the biological methanation reactor, they likely maintained themselves on lysis products, contributing to the robustness of the process over long periods. As they grew on lysis products, their growth rates and concentrations remained low. Hence, they were difficult to identify through 16S rRNA sequencing (Laguillaumie et al., 2022).

3 Modeling gas fermentation and the competition between hydrogenotrophic methanogens and homoacetogens

A modeling work has been carried out to simulate different culture modes of gas fermentation with suspended MMC. First, the biological methanation system is simulated, with a closed liquid phase, and an opened gas phase (Figure 17). This had for objective to explain and understand the acetate accumulations observed in the reactor. Then, two other configurations have been simulated, with the liquid and the gas phases being closed (batch) or opened (continuous) (Figure 20). These process configurations are described and discussed, regarding the microbial competition between HM and HAC, and from a process point of view to evaluate what configuration best suits for a given application. Kinetic and thermodynamic analysis are also addressed.

3.1 Modeling of the biological methanation reactor: Batch mode of the liquid phase, continuous mode of the gas phase (closed on liquid and opened on gas).

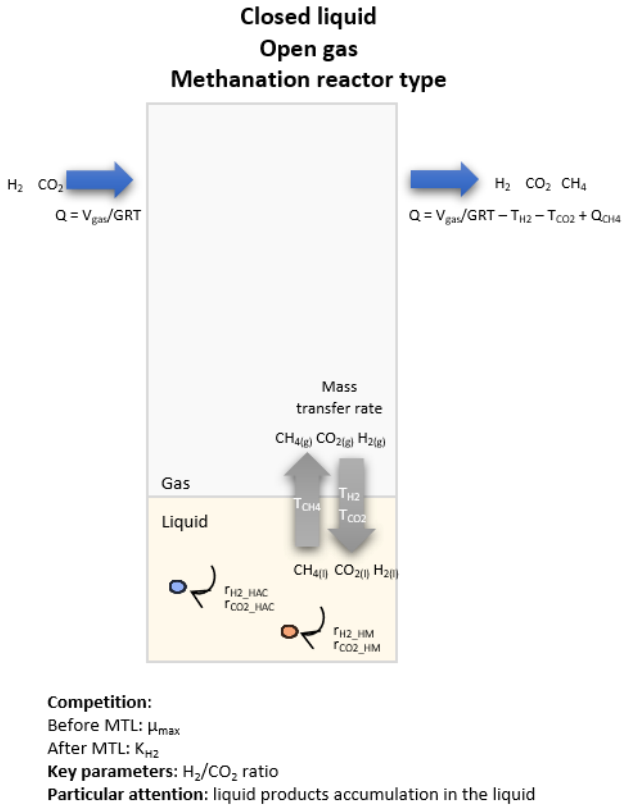

Figure 17: Biological methanation configuration tested within the model, with the liquid phase being closed, and the gas oopen. MTL: mass transfer limitation.

In this section, the biological methanation reactor studied and presented in the previous sections was implemented in the model with the objective of simulating the instability observed in methanogenic activity. This will bring understanding about the MMC behaviour, the transient VFA accumulations, and will allow to hypothesize some process management of biological methanation.

	μ_{max} d^{-1}	$Y_{X/H2}$ $gCOD_X.gCOD_{H2}^{-1}$	k_m $gCOD_{H2}.gCOD_X^{-1}.d^{-1}$	Ks $mol.L^{-1}$
HM	1.35	0.045	30	H_2: 0.000001

Table 13: kinetic parameters used to simulate the biological methanation reactor with only hydrogenotrophic methanogens being active.

The biological methanation reactor was simulated with a liquid volume of 20 L, and a gas volume of 3 L. The liquid phase is closed, and the gas is opened with an inflow of 100 $L.d^{-1}$, corresponding to an intermediate value of the inflows range tested during periods 1 and 2 (Figure 14). Temperature is set to 55 °C and pH fixed to 7. Kinetic parameters are chosen in accordance with the effect of temperature on HM and HAC found in literature (Table 13).

In the previous section, it was shown that the methanation reactor was limited by the gas supply, and not by the maximal transfer capacity of the reactor. Indeed, if this would be the case, residual concentrations of both H_2 and CO_2 would be found in the outlet gas. However, during period 1, H_2 and CO_2 conversion yields were 89 % and 100 % respectively, indicating that CO_2 supply was limiting the system. $k_La(O_2)$ of the reactor at 55 °C was measured around 720 d^{-1}. Hence, for the simulations, k_La were set to 1000, 700 and 600 d^{-1} for H_2, CO_2 and CH_4 respectively, in respect with Higbie penetration theory (Roustan, 2003). First simulations were carried out with HM as sole microorganisms to study biological methanation features. Then, sensitivity to K_{H2} in the range identified in literature (10^{-4} – 10^{-6} $mol.L^{-1}$) was tested. K_{H2} was not a sensitive parameter in the range tested (not shown), and K_{H2} was set to 10^{-6} $mol.L^{-1}$.
During the first period of biological methanation described, H_2/CO_2 ratio of the gas supplied variated from 4 to 5.8. CO_2 limitation was thus expected. However, H_2 or CO_2 limitation have different effects on the system, and this has been analysed with the model. Indeed, H_2/CO_2 ratio appeared to be a sensitive parameter depending on the growth yield of HM. However, to our best knowledge, only few studies discussed its effect on the process (Wahid et al., 2019). The molar ratio for Sabatier reaction is 4, and this ratio is often used in biological methanation processes. But this ratio doesn't consider the microorganisms growth yield. Indeed, the stoichiometry established here (Chapter 2, section 1.5.1), considering a growth yield of 0.045

$gCOD_X.gCOD_{H2}^{-1}$, leads to an actual H_2/CO_2 molar ratio of 3.83. Simulations at 3.6, 3.83 and 4 were carried out to evaluate the advantages or drawbacks of working at the exact molar ratio required for HM growth, or under H_2 or CO_2 limitation.

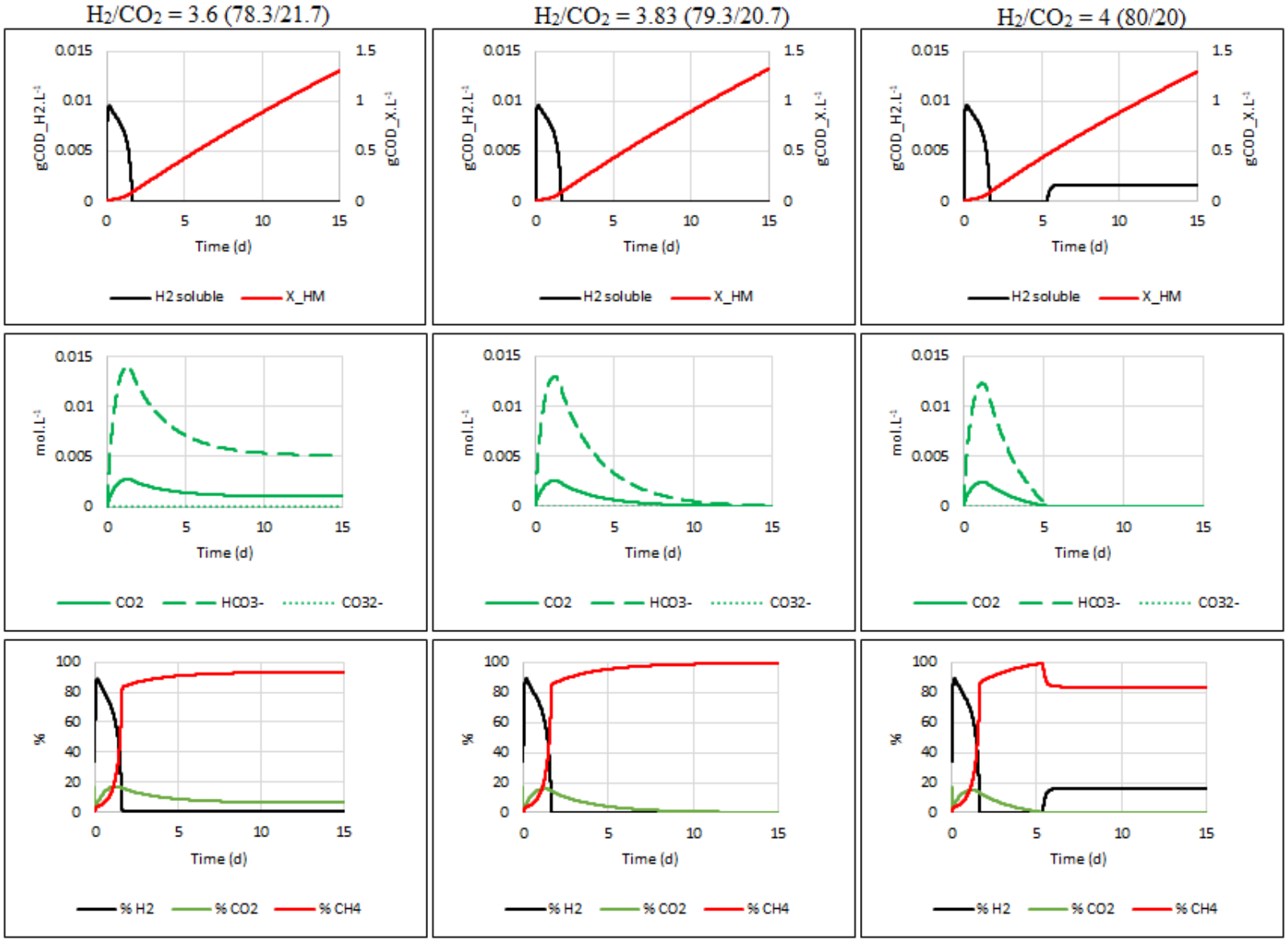

Figure 18: Results of the simulations of biological methanation of H_2/CO_2, for different H_2/CO_2 ratio. Growth yield: 0.045 $gCOD_X.gCOD_{H2}$; μ_{max}: 1.35 d^{-1}; Gas inflow: 100 $L.d^{-1}$; k_La: 1000, 700 and 600 $d^{-1}$for H_2, CO_2 and CH_4 respectively; Temperature: 55 °C; pH: fixed to 7.

Results are presented in Figure 18. The exact molar ratio of 3.83 allows a high purity of the methane produced, due to a minimisation of residual H_2 and CO_2. It thus increases the process efficiency in terms of gas valorisation. However, a ratio of 4 or 3.6 leads to a dilution of the produced methane due to the excess of one of the substrates. This has to be considered when implementing a biological methanation process, because if the H_2/CO_2 ratio is not in accordance with the stoichiometry of the biological reaction, the CH_4 concentration in the output gas is potentially limited independently of any other optimization lever. With a ratio of 4, H_2 is limiting during transitory state because of its lower solubility, but CO_2 is finally limiting during stationary state due to a lack of carbon in the system to supply growth. Conversely, a ratio of 3.6 leads to a residual H_2 concentration in the gas output. This seems trivial, but in practice, there are obstacles to correctly define the optimal H_2/CO_2 ratio. First, it is shown here that a difference of 0.17 on the input ratio (between 3.83 and 4) represents a variation in H_2 and CO_2 concentrations of only 0.7 % in the inlet gas, but leads up to 16 % of H_2 in the output gas, which significantly affects the methane purity and its direct downstream utilization. For example in France, although there is a desire to increase the authorized threshold, only 6 % of H_2 are accepted in the biogas to be injected in the natural gas grid currently (GRT gaz, 2019). Another obstacle is linked to biology, because the stoichiometric ratio is directly linked to microorganism's growth yield. Hence, a good knowledge of microorganisms in presence is crucial, and this could be difficult, especially working with MMCs. Also, side reactions, even with low rates, have to be understood and considered. Typically, heterotrophic growth on lysis products described in the biological methanation reactors will affect the H_2/CO_2 ratio as these reactions produce H_2 and/or CO_2.

In term of process management, H_2/CO_2 ratio could be of great importance, not only for the reasons previously discussed, but also because being in excess of H_2 or of CO_2 can lead to very different behaviours and process features. For example, it could be interesting to be in excess

of CO_2 and limited by H_2 supply to maintain a constant P_{CO2} in the reactor that will naturally regulate the pH of the process and ensure its stability. This is likely what explains the conclusions of Wahid et al. (2019). Indeed, the authors demonstrated that a molar H_2/CO_2 ratio of 4 led to better process stability in their *in situ* methanation process, while at a ratio above 4 the pH increased, and residual H_2 in the reactor also led to VFA accumulations.

3.2 Conclusion on biological methanation reactor modeling

Data from 200 d of operation in a biological methanation reactor have been analysed in regard of transient instability periods. During these specific periods, VFA, among which acetate, accumulated in the liquid phase running in pseudo-batch mode. These instability periods were attributed to a nutrient deficiency limiting growth of HM, leading to an increase of P_{H2} in the reactor, consequently this allowed HAC to grow. Nutrient limitation was attributed to sulphide, as the methanogenic activity recovered twice after sulphide supplementation in the reactor. This provided a new point of attention regarding the competition between HM and HAC, as HAC were apparently less sensitive to sulphide limitation. There can be different reasons for this difference. First, sulphide, or other reduced sulphur sources, are essential for HM (Jarrell and Kalmokoff, 1988; McInerney and Bryant, 1981). Additionally, sulphide is a reducing agent and contributes to maintain low oxidoreduction potential (ORP) in the reactor. HAC requirements in sulphur could be lower, and of different forms. Also, it is likely that considering the very diverse environments where HACs are found, they could be less sensitive to higher ORP than HMs.

However, acetate accumulation was difficult to characterize in the methanation reactor, due to low kinetics compared to HM. Hence, growth of HAC was not quantifiable, and HAC could not be clearly identified with the 16S rRNA microbial analysis. Simulation of HAC at this stage was not possible, but the methanation reactor was simulated in ideal conditions. The importance

of H_2/CO_2 ratio was pointed out to optimize the quality of methane produced.

In view of these observations, the thesis project aimed at understand the dynamic behaviour between HAC and HM in a MMC growing on H_2/CO_2, with the objective of promoting HAC and implement acetogenic bioreactors fed with H_2/CO_2 by controlling the microbial competition. The review of kinetic parameters of both communities presented in chapter 1 was used in the model. A theoretical work was carried out to formulate the features of gas fermentation under H_2/CO_2 regarding the competition between HAC and HM in a MMC. In the next section, different reactor configurations are explored with the model, to identify key parameters in the process control to promote HAC over HM.

4 Modeling study of the competition between HM and HAC in different process configurations: with closed gas and closed liquid (batch mode), and with opened gas and opened liquid (continuous mode).

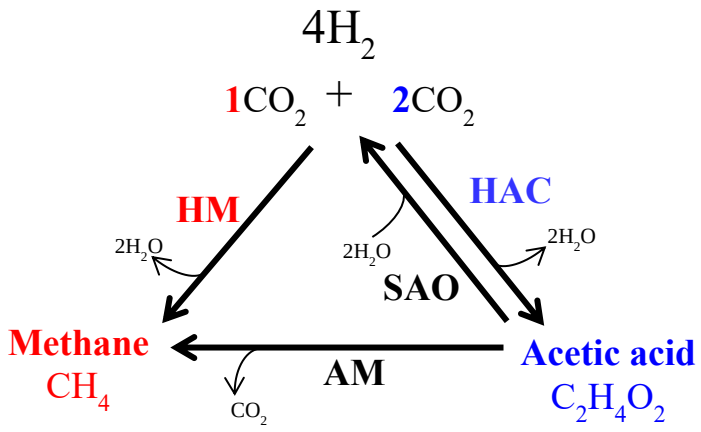

Figure 19: Main biological reactions considered in the system and discussed in this study.

HM	$4H_2 + CO_2 \rightarrow CH_4 + 2H_2O$	$\Delta rG°' = -131$ kJ.reaction^{-1}
HAC	$4H_2 + 2CO_2 \rightarrow C_2H_4O_2 + 2H_2O$	$\Delta rG°' = -82$ kJ.reaction^{-1}
AM	$C_2H_4O_2 \rightarrow CH_4 + CO_2$	$\Delta rG°' = -49$ kJ.reaction^{-1}
SAO	$C_2H_4O_2 + 2H_2O \rightarrow 4H_2 + 2CO_2$	$\Delta rG°' = +82$ kJ.reaction^{-1}

In this section, the possibility of promoting HAC rather than HM is explored with the model in different culture modes. The mechanisms of the competition from a kinetic and also a thermodynamic point of view is analysed. In the simulations presented, HAC growth is introduced. F_T and ΔrG are calculated in dynamic during the simulations, but not integrated in the kinetic equations at this stage of the study. The objective of this work is to identify how to favour HAC rather than HM, from environmental conditions potentially advantaging HAC.

	μ_{max} d^{-1}	$Y_{X/H2}$ $gCOD_X.gCOD_{H2}^{-1}$	k_m $gCOD_{H2}.gCOD_X^{-1}.d^{-1}$	Ks_{H2} $mol.L^{-1}$
HAC	1 – 8	0.033 – 0.081	30.3 – 98.77	0.00000231 – 0.00052
HM	0.8 – 5	0.021 – 0.064	38.1 – 78.13	0.0000011 – 0.000056

Table 14: Ranges of kinetic parameters for hydrogenotrophic methanogens and homoacetogens collected in literature between 20 and 35 °C.

The following hypothesis are formulated: HM and HAC are suspended biomasses; the culture broth is homogeneous regarding soluble concentrations. According to literature (Figure 5), working under thermophilic conditions should favour HM growth considering their high specific growth rates above 45 °C. To promote HAC, it is more interesting to operate in a range of temperature from 20 to 35 °C. Then, in the simulations, the upper growth rates of both population in this range of temperature were chosen, so the growth was maximized. Additionally, HM also have lower K_{H2} which makes them difficult to outcompete when substrate limitation occurs (*i.e.* mass transfer limitation, or gas supply limitation). For these reasons, kinetic parameters of both communities were collected in the literature, and ranges of specific growth rates, half-saturation constants, and growth yields were established (Table 14) for the simulations, from studies operating between 20 and 35 °C. According to Table 14, the major parameter to consider for orienting the competition should be the specific growth rate, as in certain conditions HAC have higher ones. It is also possible that in certain conditions HAC have lower K_{H2} than HM, especially at temperatures below 20 °C (Conrad et al., 1989). However, only few kinetic parameters were reported below 20 °C, so this case will not be integrated in this study. Hence, even when HAC have higher μ_{max}, substrate limitation should be handled as well to allow HAC to access to the substrate.

These parameters were tested with the model in two different configurations. The first type is called a batch mode, with the liquid and the gas phases being closed. In the second configuration, the liquid and the gas are opened (Figure 20).

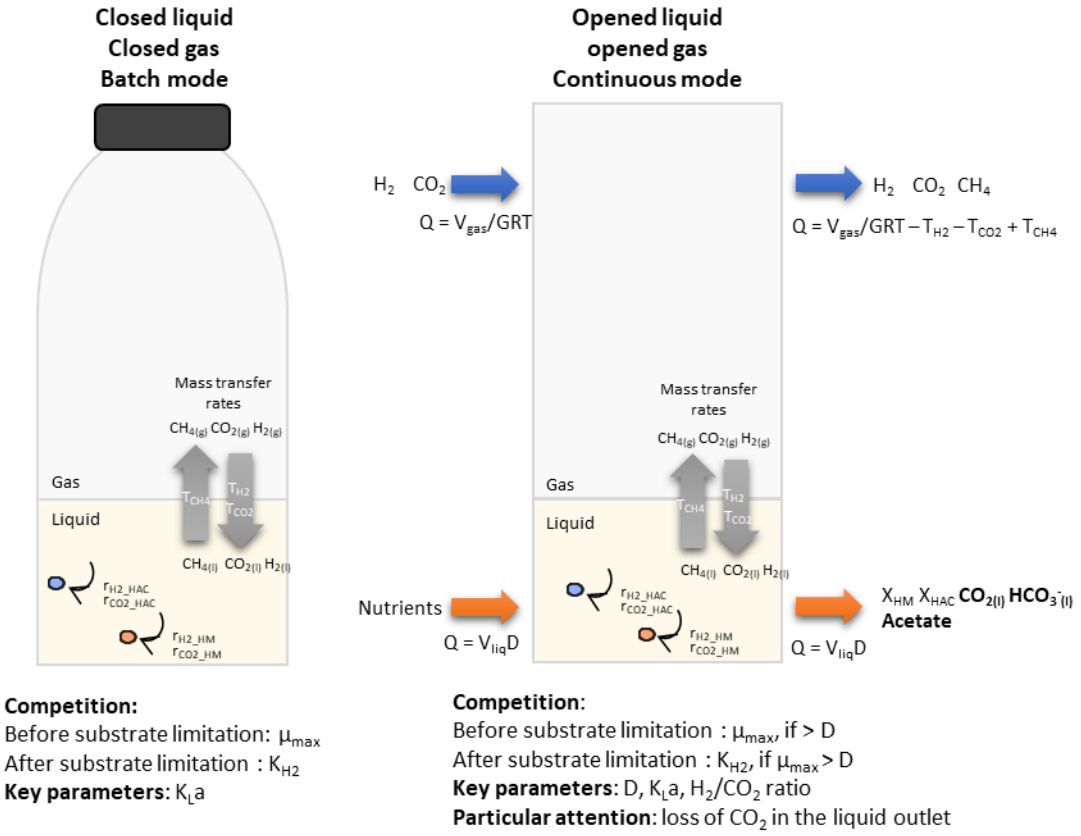

Figure 20: Scheme of the batch and the continuous modes tested with the model. GRT: gas retention time; T: mass transfer rate; D: dilution rate.

4.1.1 Batch mode: closed liquid and gas phases

In batch mode, a bottle of 2L with 0.5 L of liquid was simulated. HM and HAC initial biomass concentrations were set to 0.001 gCOD.L^{-1} and k_La of all gases to 10 d^{-1}. Figure 21 shows the results with maximisation of both growths according to Table 14, to understand and describe the features of the competition with one population having a better μ_{max} (HAC), and the other having a better K_{H2} (HM).

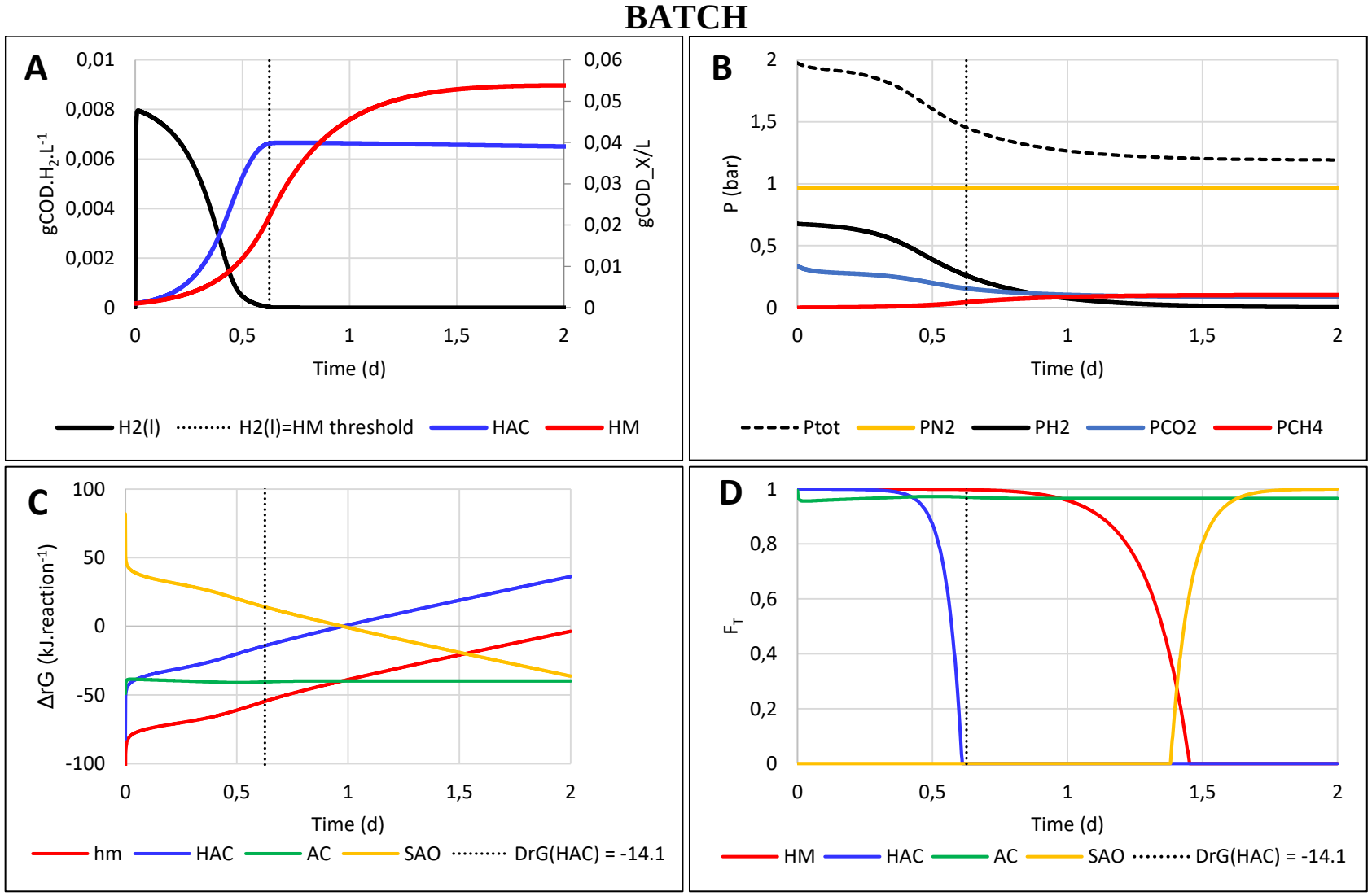

Figure 21: Simulation of microbial competition during H_2/CO_2 fermentation in batch mode. A: Hydrogen and biomasses concentrations in the liquid phase; B: Total pressure and partial pressures of the different gases. Liquid volume: 0.5 L; Gas volume: 1.5 L; k_La: 10d^{-1}; initial HM and HAC concentrations: 0.001 $gCOD.L^{-1}$; K_{H2} ($mol.L^{-1}$): 0.000001 for HM and 0.00052 for HAC; km ($gCOD_{H2}.gCOD_X^{-1}.d^{-1}$): 78.13 and 98.77 for HM and HAC respectively; growth yields ($gCOD_X.gCOD_{H2}^{-1}$): 0.064 and 0.081 for HM and HAC respectively. C: ΔrG and D: F_T were calculated as described in chapter2 section 1.7

The biomasses profile (Figure 21A) can be divided into two phases. During the first phase, soluble H_2 concentration is much higher than H_2 thresholds of HM and HAC. Both communities grow at their μ_{max}, which is the parameter that governs the competition (r-competition). So in this configuration, HAC dominate, but HM can also grow and remain in the reactor, leading to a cohabitation of both microbial communities. During the second phase delimited by vertical dot lines, soluble H_2 is limiting ($r_{H2} = T_{H2}$). Microorganisms enter in a phase of competition for trace amounts of H_2, in which HM take the advantage due to their better affinity to the substrate (K-competition). With these kinetic parameters, a k_La increase from 10 to 50 d^{-1} allows to produce twice more HAC than HM. However, further increase of the k_La doesn't promote anymore HAC. This is explained by the fact that increasing k_La delays the time when mass transfer limitation is reached. Hence, above a certain k_La value, the final H_2 consumption rate remains below the maximal mass transfer rate for the entire experiment, and the competition remains governed by μ_{max}.

Figure 21C and D show the calculations of ΔrG and F_T of HM, HAC, AM and SAO along the simulation. It is interesting to note that the mass transfer limitation is closely related to thermodynamic limitation for HAC. Indeed, when the system enters in mass transfer limitation (vertical lines), the ΔrG(HAC) reaches -14 kJ/reaction, which is close to the value of ΔrGc found in literature for this community (-14.85 $kJ.reaction^{-1}$) (Grimalt-Alemany et al., 2020). Additionally, from 0.7 d, it shows that HM are also thermodynamically limited until the end. Hence, the limitation term of Monod, defined with K_{H2} is closely related to thermodynamic constraints. This demonstrates that empirical parameters such as K_{H2}, could be replaced by thermodynamic limitation terms. This also show that when substrate is not limiting, the system is mostly governed by kinetics, provided that products concentrations are not above the thermodynamic threshold. When the system is mass transfer limited, then the main limitation is thermodynamic. Although SAO and AM growths were not activated in the model, F_T calculations

show that AM reaction is feasible all along the batch. A slight thermodynamic of AM during the batch is due to P_{CO2} first, and then P_{CH4} at the end of the batch. SAO reaction is not feasible until acetate is produced and P_{H2} et P_{CO2} fall below 0.08 bar.

Kinetic parameters on H_2 substrate seem accurate, as the simulations could be thermodynamically consistent by only considering H_2 Monod limitation term. However, kinetic parameters for other substrates have not been well measured and described in literature. Considering the difficulty to measure Ks, the use of thermodynamic limitation terms could be interesting to describe anaerobic systems under other types of limitations, such as CO_2 limitation. Indeed, F_T not only consider substrate availability, but also product concentrations inhibition, temperature, and pH. Therefore, F_T should be more suitable to describe systems in dynamic state, or in new environmental conditions for which kinetic parameters are not available.

According to these simulations, it should be possible to favour HAC in batch mode, as long as the mass transfer rate (T_{H2}) is higher than H_2 consumption rates (r_{H2}). Hence, in batch mode, a key process parameter is the ratio between r_{H2} and T_{H2}. In order to decrease this ratio, two main options are the increase of the k_La of the reactor, and the decrease of the initial biomass concentration by diluting the MMC. Of course, a compromise must be found between the biomass dilution, and the amount of enriched MMC needed by the end of the experiment. The initial concentration of HM is also important and should be minimized, for example be choosing a MMC coming from anaerobic environment where methanogenic activity is low, like in psychrophilic environments. Considering this, batch mode appears as an interesting cultivation strategy for MMC specialization and enrichment, to provide inoculum. However, it seems not advisable for acetate production processes, as the substrate limitation will be an unavoidable obstacle.

In batch mode, biomass accumulates and its concentration increases. This implies that r_{H2} reaches

mass transfer limitation sooner or later, as long as substrate is available. This explains why liquid closed mode is preferred for biological methanation, with a continuous gas supply. This way, higher biomass concentrations are reached, which increases methane production rate. Additionally, in the case of methanation, methane is continuously extracted in the gas phase, which makes it possible to operate over long periods without product accumulation issues.

In the case of acetate production though, the product accumulates in the liquid, which makes continuous mode on the liquid phase more interesting for this application to avoid product concentration inhibition effects. Considering lab constraints to implement continuous reactors, it can still be envisaged to carry out successive batches, diluting the biomasses at each new inoculation step and therefore maintaining low rates and preventing mass transfer limitation. This could be an interesting way to specialize and enrich a MMC with batch cultures. Figure 22 shows a simulation of such process, based on the same parameters used in the previous simulations in batch mode. The inoculation of successive batches with 15 % of the previous one was simulated, with transfer during the first phase of the gas fermentation (before substrate limitation is reached). This way, HM are maintained at pseudo-constant and low concentration, while HAC concentration increases along successive batches. This strategy could be a method of producing a specialized MMC, and operate with higher k_La would allow to reach higher HAC concentrations by the end of the experiment.

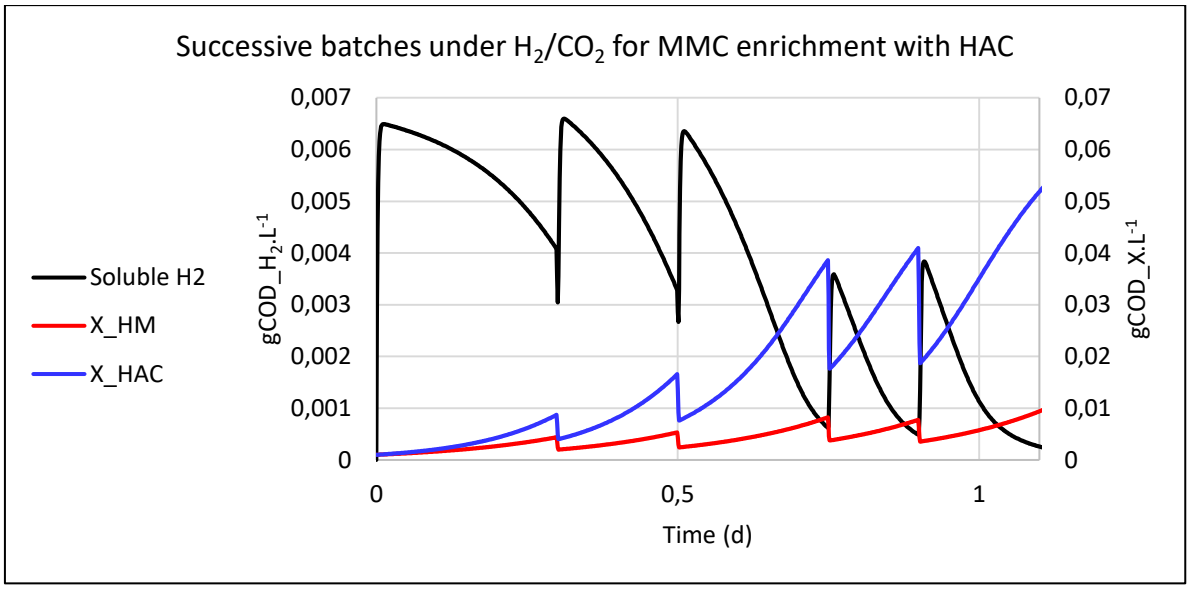

Figure 22: Simulation of the competition between homoacetogens (HAC) and hydrogenotrophic methanogens (HM) during successive batches under H_2/CO_2. Hydrogen (black), HM (red) and HAC (blue) concentrations in the liquid phase are represented. Liquid volume: 0.5 L; Gas volume: 1.5 L; k_La: 10d^{-1}; initial biomass concentration: 0.001 gCOD.L^{-1} for both populations; K_{H2} (mol.L^{-1}) : 0.000001 for HM and 0.00052 for HAC; km (gCOD$_{H2}$.gCOD$_X^{-1}$.d^{-1}) 78.13 for HM and 98.77 for HAC.

4.1.2 Continuous mode: open liquid and gas phases

Switch to a continuous management of the liquid phase should be more interesting for acetate production from H_2/CO_2. First, it allows to regulate the acetate concentration and its inhibitory effect of HAC. Also, continuous mode brings a new constraint, the dilution rate D, that imposes a minimal specific growth rate for the microorganisms to maintain themselves in the reactor. Hence, as it is assumed that under low temperature conditions HAC have higher specific growth rates than HM, this could be advantageous for HAC. Indeed, if environmental conditions a properly chosen, it should be a critical D value above which HM are washed out the process, while HAC remain alone.

In continuous mode, k_La doesn't influence the outcome of the competition, but only determines the maximal capacity of the system. Once mass transfer limitation is reached, the dissolved concentrations of H_2 and CO_2 will be low, and the competition will be governed by K_{H2}. Indeed, the continuous supply of substrate should necessarily drive the system to reach mass transfer limitation, provided that there is no other limitation or inhibition in the liquid phase. Finally, implementing continuous process with gaseous substrates leads to a loss of some of the not limiting substrates in the liquid outlet (Figure 20). This phenomenon is emphasized for CO_2 if it is not the limiting substrate, as it has a high solubility (Figure 23B). The loss of CO_2 will depend on D, but also on pH that regulates the amount of bicarbonates in the liquid, and temperature as gas solubilities decrease with increasing temperatures. The H_2/CO_2 ratio is also of great importance in continuous processes.

The model was used to simulate continuous mode, by opening the liquid compartment of the batch mode model. As the μ_{max} of HAC and HM were set to 8 and 5 d^{-1} respectively, setting D over 5 d^{-1} led to HM wash out. Hence, D has been set to 3 d^{-1} to observe the dynamic behaviour of the competition, again according two phases before and after reaching mass transfer limitation, and

with a H_2/CO_2 ratio of 2 or 4 (Figure 23). F_T was integrated in the growth rates to ensure thermodynamic consistency of the dynamics, especially under CO_2 limitation. First, conversely to the stoichiometric H_2/CO_2 ratio of HM, the one of HAC doesn't depend on the microorganism's growth yields and remains at 2 in any case. This simplifies the application of an optimal ratio, as it only depends on process parameters D, pH and T, regarding non-limiting substrate loss in the outlet, as discussed before. Figure 23A shows that with and excess of CO_2 (H_2/CO_2 67:33), or in other terms, under H_2 mass transfer limitation, the competition is in favour of HM at steady state as they have lower K_{H2}. However, before mass transfer limitation is reached, HAC grow faster, according to the same mechanism as described in batch mode, as they have higher specific growth rates. This explains why in numerous biological methanation studies, acetate accumulation is observed at the beginning of the operations before steady state. Here, D is below HM and HAC specific growth rates, so HM outcompete HAC once mass transfer limitation is reached. However, with the same D, but under CO_2 mass transfer limitation (H_2/CO_2 80:20), the competition is no more governed by K_{H2} but by K_{CO2}. Due to a lack of data on K_{CO2} of both communities, same K_{CO2} of 8.10^{-6} $mol.L^{-1}$ was arbitrary attributed to each population. Hence, HAC outcompete HM due to their higher specific growth rate in this case. Although these simulations cannot be overinterpreted due to the uncertainty of K_{CO2}, it shows that continuous mode can be interesting to overcome H_2 mass transfer limitation, and operate under other type of limitation that could promote HAC rather than HM. Furthermore, as F_T was integrated in the growth rates, the simulations are thermodynamically consistent. These results show that the outcome of the competition could be different whether if the system is H_2 or CO_2 limited. These results also demonstrate that operate with the molar ratio of substrate determined with the stochiometric equation without considering the biomass production is not relevant. Indeed, in these simulations, a ratio of 4 (80:20) promoted HAC, while a ratio of 2 (67:33) promoted HM. Yet, the molar ratio of the respective chemical equations are 2 and 4.

CONTINUOUS

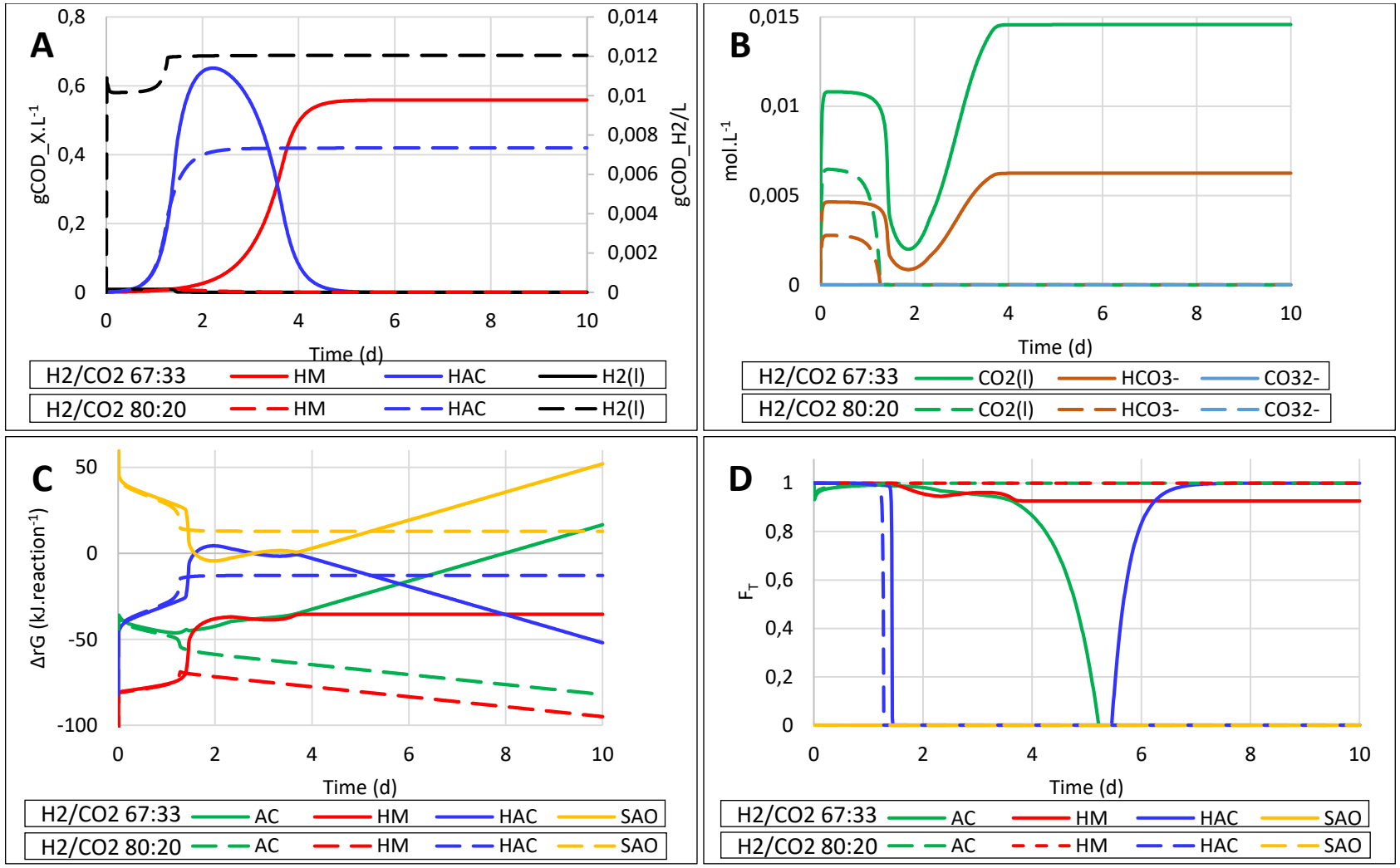

Figure 23: Simulation of the microbial competition during H_2/CO_2 fermentation with continuous liquid and gas phases. A: Hydrogen and biomasses concentrations in the liquid phase. B: CO_2, HCO_3^- and CO_3^{2-} concentrations in the liquid phase. kLa: 1680 d^{-1}; Liquid volume: 1.5 L; Gas volume: 1 L; Liquid dilution rate: 3 d^{-1}; initial biomass concentration: 0.001 gCOD.L^-; K_{H2} (mol.L^{-1}) : 0.000001 for HM and 0.00052 for HAC; km ($gCOD_{H2}.gCOD_X^{-1}.d^{-1}$); μ_{max}: 5 for HM and 8 for HAC. Growth yields: 0.064 and 0.081 $gCOD_X.gCOD_{H2}^{-1}$ for HM and HAC respectively.

These two different profiles according to H_2/CO_2 ratio, also led to different thermodynamic profiles (Figure 23C and D). Especially, under H_2 mass transfer limitation (H_2/CO_2 67:33), HM is thermodynamically feasible all along the process, and even if HAC becomes feasible from 5 d, the competition is under kinetic control, and the effect of K_S prevails. However, what is interesting is that under CO_2 mass transfer limitation (H_2/CO_2 80:20), ΔrG of HAC is of -13 kJ.reaction^{-1}, meaning that the reaction is under strong thermodynamic limitation. The model even predicts that it is unfeasible ($F_T = 0$), considering the energy conserved (ΔGc) set for the F_T calculation to -14.85 kJ.reaction^{-1}. However, there is uncertainties on the ΔGc of the reactions, due to ATP yields and ΔrG of ADP phosphorylation variations depending on the strains (Bengelsdorf et al., 2018; Jin and Bethke, 2007).

These simulations demonstrate that kinetic models are incomplete if not considering thermodynamic constraints, as previously stated (Grimalt-Alemany et al., 2020), especially under conditions in which kinetic parameters has not been accurately defined. Here, the thermodynamic limitation of HAC is due to the concentration of acetate (0.06 M), and a very low P_{CO2} in the case of CO_2 limitation. The fact that HAC requires two-fold more CO_2 than HM enhances even more the thermodynamic limitation of HAC compared to HM.

5 Conclusion

This first work aimed to establish a theoretical analysis of the competition between HM and HAC. The competition has been observed and analysed in a thermophilic *ex situ* biological methanation reactor to highlight the key parameters and operational conditions that promoted acetate accumulations in this reactor. However, the acetate production rate was low, the reactor was optimized for HM. However, HM deficiency could be identified as the main HAC promoting factor, as when sulphide was supplemented in the reactor, HM activity recovered and acetate production ceased. This confirmed that the main challenge for acetate production from CO_2 is the inactivation of methanogenic activity. From the literature, some specific environmental conditions were pointed out to favour HAC. Among them, the decrease of the reactor temperature, and the increase of P_{H2} were recurrent. Hence, the model was used in batch and continuous mode, with kinetic parameters identified for HM and HAC between 20 and 35 °C.

With the parameters considered, the overcome of substrate limitation appeared as the key challenge to promote HAC in batch mode. According to the simulations, implementing successive batches allow to specialize and enrich the MMC with HAC along the transfers. Continuous reactors also appeared as interesting tools for MMC specialization for HAC. But conversely to batch mode, in continuous mode the HM can be completely eliminated at steady state, provided that HAC have higher specific growth rate than HM, for example under low temperatures.

This work also highlighted that depending on the H_2/CO_2 ratio, H_2 or CO_2 can be limiting. However, in literature, it is often assumed that H_2 is limiting. Kinetic parameters are well described regarding H_2 limitation, and the model in batch mode showed that only considering kinetic parameters, the simulation was consistent with thermodynamics. However, the applicability of these parameters in continuous mode, and under CO_2 limitation is questionable,

as few of them have been determined in these conditions. Therefore, a thermodynamic analysis of the reaction's feasibility is an interesting way of evaluating the feasibility of the reactions and the consistency of kinetic simulations. It also helps for the understanding of the MMC behaviour. The calculation of F_T allows to bring some precision to describe the community's dynamics, and is robust tool as pH, temperature, substrates and products concentrations are considered. Considering the difficulty to measure K_S for example, but also μ_{max} due to mass transfer limitation, these simulations suggest that thermodynamic calculations could be used to describe the dynamics of MMC.

When gas inflows applied exceed the maximal mass transfer capacity of the system, in continuous mode, gas partial pressures remain stable at significant values, while the liquid phase is actually mass transfer limited. Working in such conditions should help to stabilise the system when the objective is to study it and not optimize a production process. In the latter case, it seems more advisable to apply gas loads very close to mass transfer capacities, so the gas is not wasted.

Also, this particularity of the system should allow to estimate the maximal mass transfer capacity of the system in real conditions. Indeed, k_La is generally measured in water, and for O_2 in air. Hence, the conditions are significantly different than the operating conditions, and the numerical corrections of k_La values bring uncertainties. Additionally, the biomass concentration could have an effect on gas diffusivity and solubility which is generally not considered.

After studying acetate accumulations in a biological methanation reactor, a theoretical modeling work was based on kinetic parameters from the literature. This introductive chapter allowed to give the principles of the competition according to different culture modes. Furthermore, it has been demonstrated that in theory, there should be some conditions and culture modes that promote HAC over HM under H_2/CO_2. However, this has to be confronted

to real conditions. Therefore, experimental studies were conducted during the thesis project, and they are presented in chapters 4 and 5. In chapter 4, successive batches were implemented, the effects of temperature between 25 and 35 °C, and of mass transfer limitation were analysed. Then, the microbial competition was studied in continuous reactors. Different pH and dilution rates were applied to test the system and analyse the behaviour of the microbial communities in different conditions. These results aim to complement each other to provide information on the competition between HM and HAC, and identify the main parameters to drive the process toward the production of acetate.

CHAPTER 4: Microbial competition control between hydrogenotrophic methanogens and homoacetogens for selective production of acetate under H_2/CO_2 in successive batches

Associated manuscript:

Laguillaumie L., Peyre-Lavigne M., Grimalt-Alemany A., Gavala H.N., Skiadas I.V., Paul E., Dumas C. ***Controlling the microbial competition between hydrogenotrophic methanogens and homoacetogens using mass transfer and thermodynamic constraints****. Journal of Cleaner Production, Volume 414 (2023). https://doi.org/10.1016/j.jclepro.2023.137549.*

1 Introduction

HAC is a promising route for biotechnology development of C1 compounds (CO, CO_2, methanol etc.) recovery into value added molecules. Studying the competition between HM and HAC could result in a method for inoculum development that presents advantages compared to the addition of inhibitors or heat treatments. As highlighted in chapter 3, maintaining low H_2 consumption rates compared to mass transfer rate of the reactor is crucial in the outcome of the competition between HM and HAC in batch mode. Indeed, mass transfer limitation will lead to a K-competition, benefiting to HM in most cases. The exception could be psychrophilic conditions, under which HAC could have better H_2 fixating capacities.

In this chapter, an experimental work aiming at confront the previous statements to real conditions is presented. In batch mode, there should be a way of promoting HAC in a MMC by implementing successive batches, provided that in the conditions of the tests, HAC have higher growth rates than HM. According to literature review, HAC and HM have similar specific growth rates in the range of 20 – 40 °C, but the disparity of the data found makes it difficult to predict the outcome of the competition. Hence, a first objective in this chapter is to evaluate if it is possible to promote HAC in a MMC by lowering the temperature.

The modeling work presented in chapter 3 showed that in batch mode a successive batches approach is interesting to maintain low H_2 consumption rates compared to H_2 mass transfer rates, contributing to enhance acetate production. However, batch mode should not allow to eliminate HM, as they are also able to fix the substrate. In these conditions, a cohabitation of HM and HAC is expected, and the cultivation management should be properly operated so the HM concentration remains low, and HAC concentration increases along the experiment. A second objective is to confront these statements based on modeling to real conditions. Hence, successive batches (SBs) were implemented in serum bottles. The effect of temperature

between 25 °C and 35 °C was investigated, as well as the SB cultivation method to control the mass transfer limitation. Indeed, SBs were transferred either during the first stage of fermentation before mass transfer limitation was reached, or during stationary phase after multiple gas injections for reaching mass transfer limitation. Activity tests and microbial analysis were carried out on the MMCs obtained by the end of four SBs to identify active metabolic functions, and dominant microbial taxa. Same culture medium was used for SBs and activity tests, sulphide was omitted in the culture medium, and replaced with sulphate. This had for objective to weaken HM, as it has been observed in the methanation reactor studied in chapter 3.

2 Results and discussion

2.1 Functional activities selected in SBs

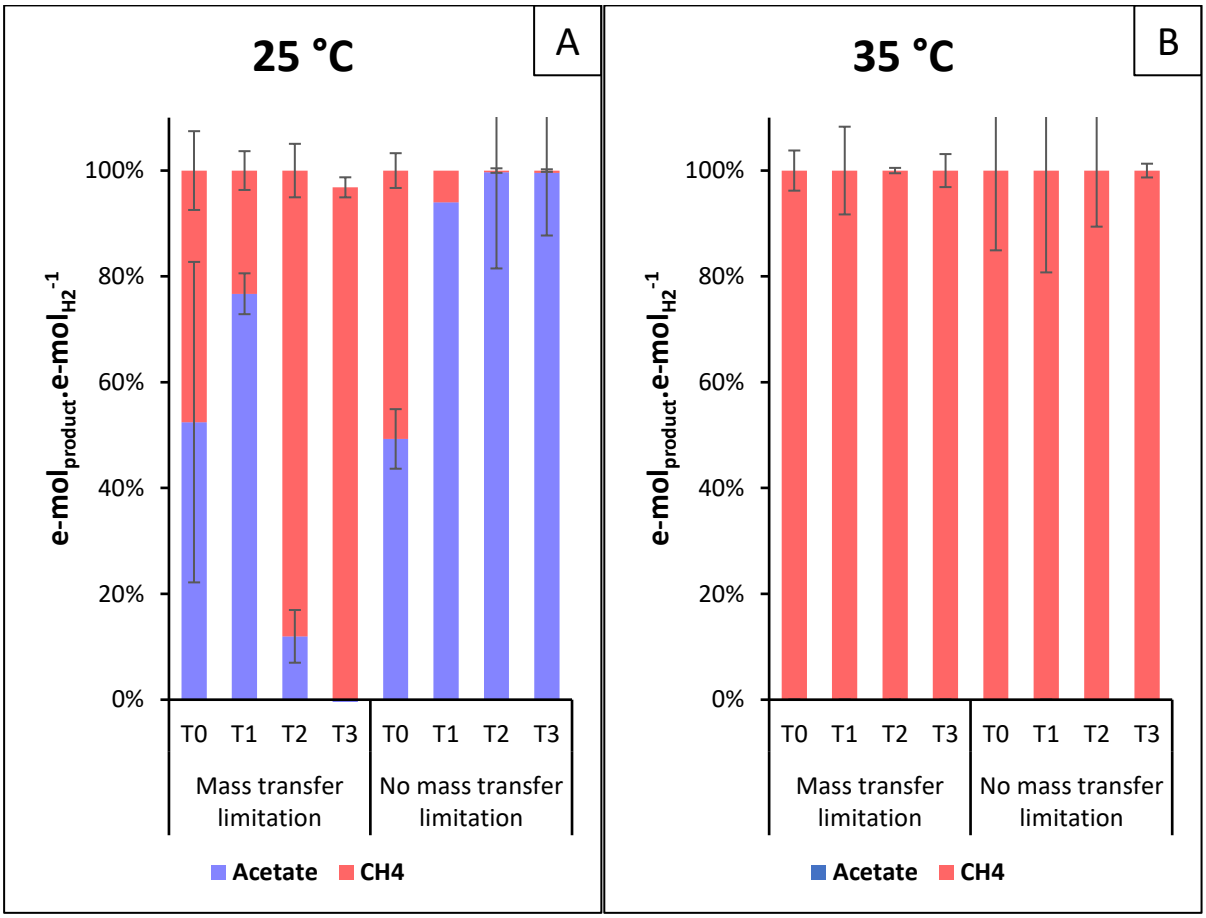

Figure 24: Electron balances in e-mol$_{product}$.e-mol$_{H2}^{-1}$considering acetate and methane produced over H_2 consumed during the four sets of SBs carried out at 25 °C and 35 °C, under mass transfer limitation or not (Laguillaumie et al., 2023).

Figure 24 shows the electron balances between acetate and methane produced over H_2 consumed along the different SBs carried out. Some of these balances are not satisfying, and this is attributed to measures uncertainty. Also, for the first batch of each SB set (T0), complex materials were present, originated from the inoculum used. Hence other metabolisms could be active in this batch, but were not considered in the balances, bringing some errors.

However, significant differences can be observed between the different SBs. First, acetate was never detected in the liquid phase of SBs conducted at 35 °C. In the other hand, at 25 °C, acetate could be detected, and the balance even moved toward acetate as sole product when mass

transfer limitation was overcome. On the other hand, in SBs supposed to be mass transfer limited, acetate was detected in the first batches, but the balance progressively moved toward methane as sole product by the end of the experiment. The fact that acetate was detected at the beginning of these SBs may be due to mass transfer limitation being delayed because of higher gas solubility, and also lower HM specific growth rates at 25 °C than at 35 °C.

These results demonstrate a strong effect of temperature on the microbial competition between HM and HAC. Additionally, the implementation of SBs without mass transfer limitation allowed to progressively eliminate methane production along the experiment. In order to characterize the MMCs obtained by the end of the SBs, and identify active metabolic functions, activity tests were carried out.

Activity tests on MMCs enriched in SBs at 35 °C under mass transfer limitation:

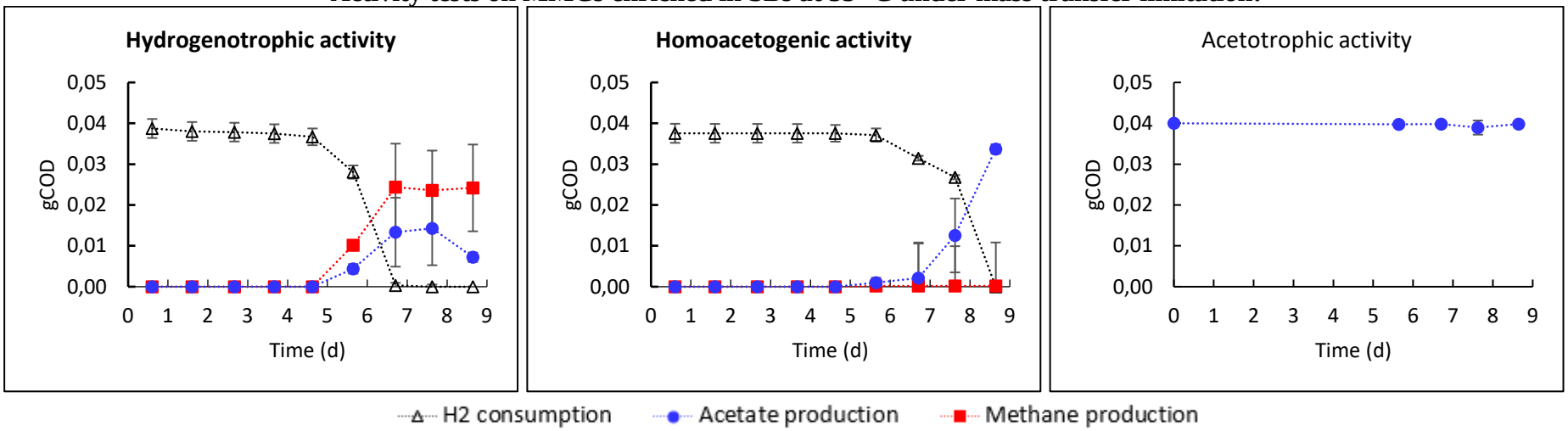

Figure 25: Results of the activity tests carried out with the MMCs enriched in SBs at 35 °C under mass transfer limitation (Laguillaumie et al., 2023).

A: Activity tests on MMCs enriched in SBs at 25 °C under mass transfer limitation:

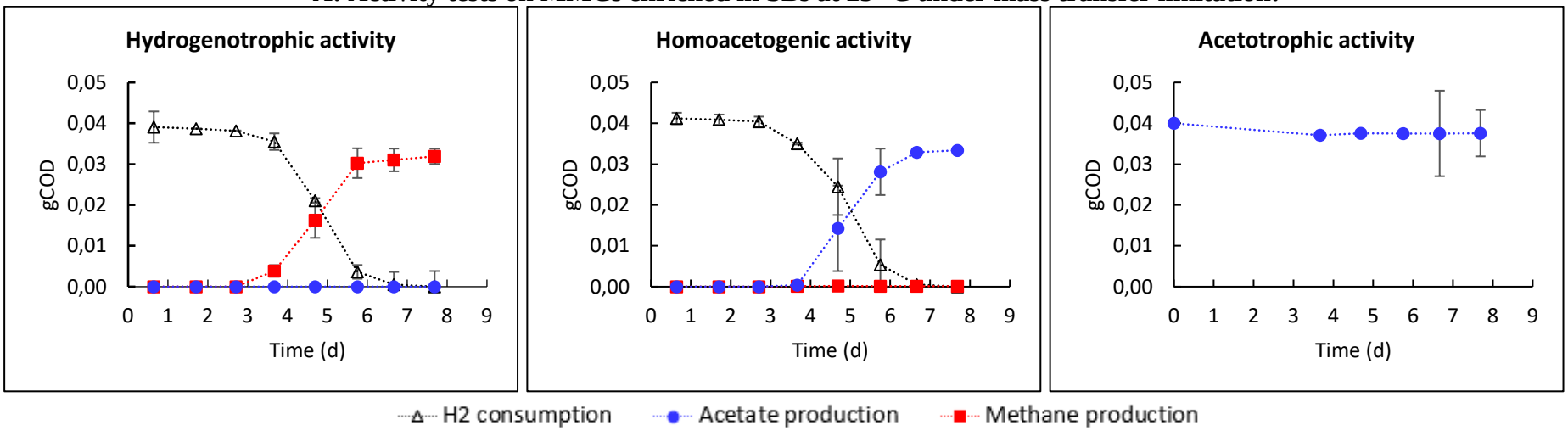

B: Activity tests on MMCs enriched in SBs at 25 °C avoiding mass transfer limitation:

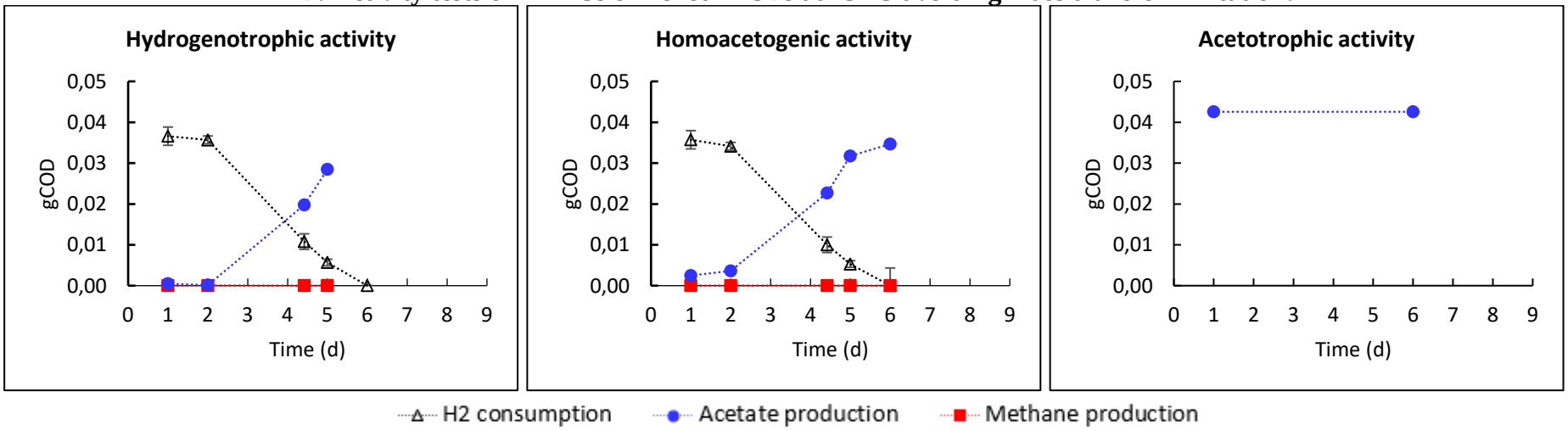

Figure 26: Results of the activity tests carried out with the MMCs enriched in SBs at 25 °C A: under mass transfer limitation; B: avoiding mass transfer limitation (Laguillaumie et al., 2023).

Figure 25 shows the results of activity tests carried out on the MMC enriched at 35 °C. Only the MMC obtained after mass transfer limited SBs' was tested, due to a lack of time. The results show that even if acetate was not detected during the SB period, HAC as well as HM were active in the activity tests. Hydrogenotrophic tests show that HAC and HM could grow, with methane begin the main product. At 35 °C, HM specific growth rate was likely higher than that of HAC, and also higher than at 25 °C. Additionally, H_2 solubility is lower at 35 °C than at 25 °C, so the mass transfer limitation was reached earlier, benefiting to HM. Activity tests were also carried out on the two MMCs obtained at 25 °C. According to Figure 26A, in MMC enriched at 25 °C under mass transfer limitation, HAC was active in the homoacetogenic tests, but couldn't grow in hydrogenotrophic tests in which HM outcompeted them. This indicates that HAC were still in the MMC even if acetate production was not detected anymore at the end of these SBs. However, with HM being active, acetate production is not observed. Conversely, in the MMC enriched in SBs at 25 °C, overcoming the mass transfer limitation, it was methane production that was not detected anymore at the end of the SBs. But in this case, activity tests revealed that methanogenesis function was lost in the MMC obtained. Indeed, only acetate production was detected in the hydrogenotrophic test.

These results demonstrate that methanogenic function could be irreversibly eliminated from the MMC by implementing a specific cultivation method. This method consisted in lowering temperature to 25 °C, and avoid mass transfer limitation by transferring from a batch to another as soon as some substrate consumption was observed. In fact, the short time of each batch must have been another constraint for HM. Indeed, at 25 °C, longer lag phases were observed for HM than for HAC during the SBs phase. Hence, this might have contributed to progressively loose them along the SBs, which explains why the activity was lost while the simulations predicted a cohabitation. The longer lag phase of HM than that of HAC can be due to a higher oxygen

sensitivity during the batch transfers.

Acetate concentration and total pressure (not shown) remained constant in all acetotrophic activity tests, indicating that the MMCs were not able to consume acetate in these conditions. The results of these activity tests show that AM and SAO were likely washed out from the MMCs along the SBs, and could not be reactivated afterwards when placed under favourable conditions. Am have generally lower specific growth rates than HM (Batstone et al., 2002, p. 1), so if HM were washed out, it is consistent that AM were too. Regarding SAO, the thermodynamic analysis of the theoretical batch culture presented in chapter 3 showed that this reaction was not favourable until acetate is produced, and H_2/CO_2 partial pressures are low. In the case of the SBs transferred rapidly to overcome mass transfer limitation, substrate partial pressures were still significant in the gas phase, so SAO could not be active. A discussion about thermodynamic analysis of the SBs is presented in section 2.3.

2.2 Microbial composition of the MMCs provided after SBs enrichments

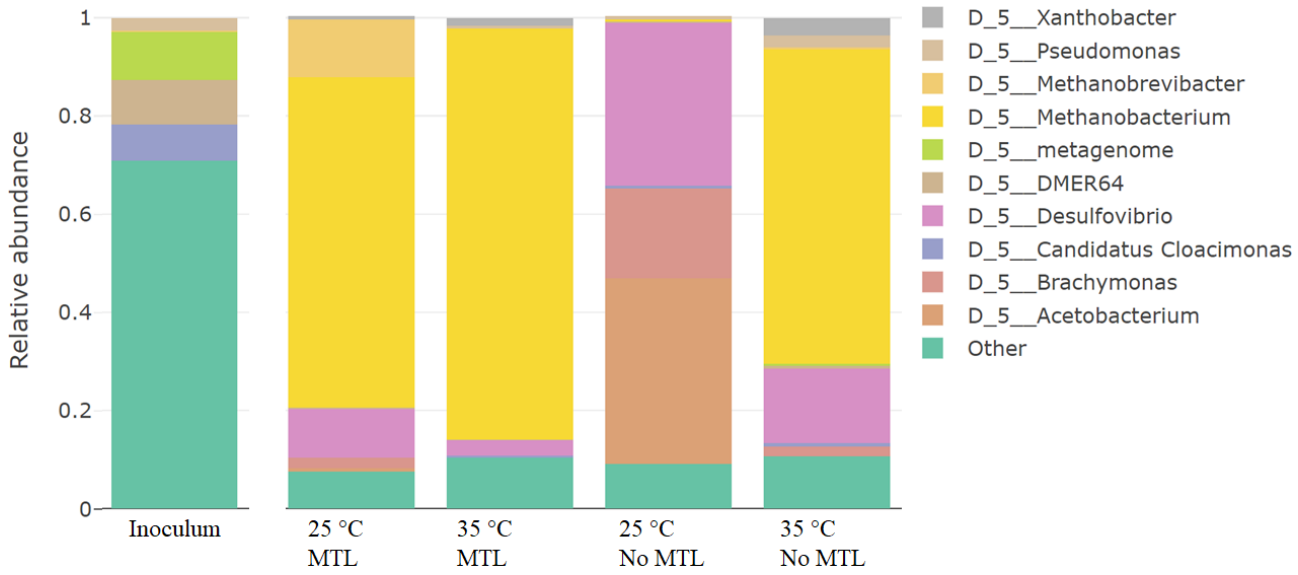

Figure 27: Relative abundance of taxa detected in the MMCs, at genus level, generated with rANOMALY package in R. MTL stands for mass transfer limitation.

Figure 27 shows the different genera found in the enriched MMCs after the different SBs carried out. HAC genus *Acetobacterium* was only selected at 25 °C and not at 35 °C, with highest abundance of 38 % in the MMC enriched avoiding mass transfer limitation. Additionally, genus *Methanobacterium* was selected in all enrichments except in this same MMC. However, *Methanobrevibacter* was found in all samples, with the highest abundance of 12 % in the enriched MMC at 25 °C under mass transfer limitation. This suggests that *Methanobrevibacter* was more adapted to 25 °C than *Methanobacterium*, and that temperature also affects the competition between different HMs. Finally, *Desulfovibrio* was found in all the samples, with particularly high abundance of 33 % in the SB at 25 °C without mass transfer limitation. The latter are sulphate reducing bacteria (SRB) capable of growing in chemolithoautotrophy on CO_2, but also in heterotrophy on acetate, using the WLP or the reductive glycine pathway. Sulphate is the electron acceptor of the metabolism, and the electrons can come from different monomers such as sugars,

amino acids, short chain fatty acids (including acetate), ethanol, and hydrogen. Consistently, they can be found in acetogenic and hydrogenic systems when sulphate is available (Sánchez-Andrea et al., 2020; Weijma et al., 2002; Cord-Ruwisch et al., 1988; Wood et al., 1986; Badziong et al., 1979). Since the mineral medium contained sulphates, these bacteria remained in competition with HAC at 25 °C when mass transfer limitation was overcome, demonstrating that conversely to HM, they had competitive specific growth rates with HAC in these conditions. SRB are capable of using H_2 to reduce sulphate of the mineral growth medium as an anaerobic respiration, they can also oxidize acetate as an anaerobic fermentation, according to the following stoichiometries:

$$4H_2 + SO_4^{2-} + H^+ \rightarrow HS^- + 4H_2O \qquad \text{SRB}$$

$$C_2H_4O_2 + SO_4^{2-} \rightarrow 2HCO_3^- + HS^- \qquad \text{SAO-SRB}$$

$$H_2S + H_2O \leftrightarrow HS^- + H_3O^+ \qquad \text{pka} = 7.04$$

The initial concentration of sulphate in the medium was 0.35 mM corresponding to a maximum of H_2 consumed by SRB of 1.4 mM, or 0.022 $gCOD_{H2}.L^{-1}$. As the reactions produce reduced sulphur in the forms of HS^-, this can explain that HM were enriched in most of the SBs despite the omission of sulphide addition in the mineral medium.

2.3 Thermodynamic analysis of the SBs

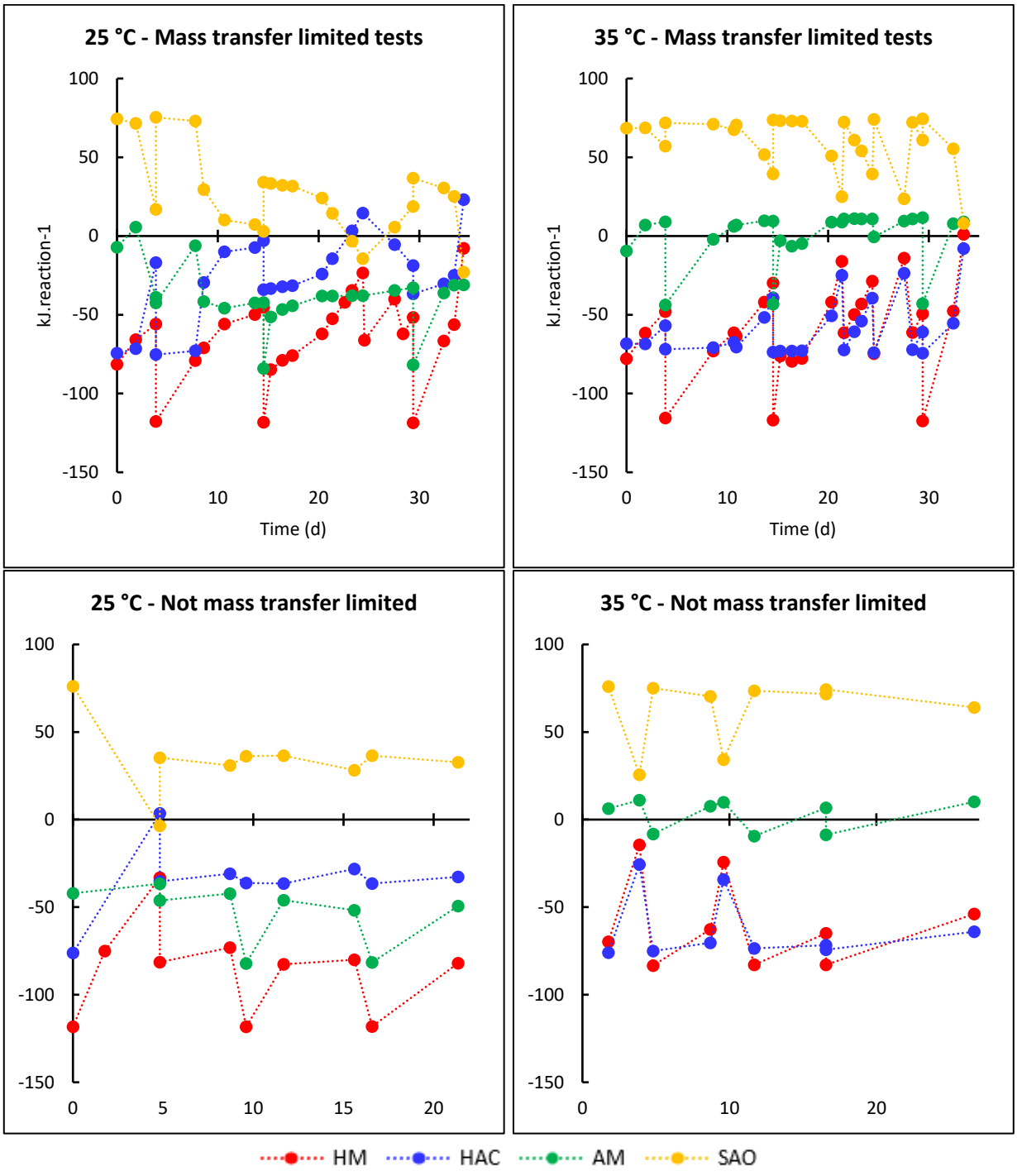

Figure 28: Calculation of the ΔrG during the experimental SBs.

In order to go further in the understanding of the competition between HM and HAC, ΔrG from the experimental data during the SBs were calculated (Figure 28). At 35 °C, the calculations show that the ΔrG of HM and HAC were negative enough for the reaction to proceed, and close. This indicates that at 35 °C the competition must be governed by kinetics. Hence, HM likely have better kinetic properties at 35 °C than at 25 °C, explaining that they outcompeted HAC in the SBs at 35 °C. However, HAC activity was detected in the activity tests of the corresponding MMCs, indicating that HAC were able to maintain themselves in the SBs, probably consuming traces of H_2.

At 25 °C, ΔrG of HM and HAC were different, the one of HAC being higher. This indicates that lowering the temperature does not benefit to HAC from a thermodynamic point of view. However, the effect of the cultivation method at 25 °C is visible. Indeed, in the not mass transfer limited SBs, ΔrG of HAC have been maintained low enough for the reaction to proceed, while in the first strategy with mass transfer limitation reached, and longer batch times, the thermodynamic limitation of HAC is reached at the end of each batch, and this contributed to progressively promote HM along this set of SBs.

These results show that mass transfer limitation is closely related to thermodynamic limitations. Hence, under mass transfer limitation, the competition is governed by thermodynamics, which promoted HM both at 25 °C and 35 °C. However, when mass transfer limitation is overcome, then the competition is governed by kinetics, and HAC could outcompete HM at 25 °C showing that lowering temperature had an effect on the relative kinetic performances of HM and HAC, in favour of HAC. SAO was never favourable according to thermodynamics, while an acetate consumption was observed at the end of batches at 25 °C. It is likely that this consumption was due to AM activity, as the reaction was thermodynamically feasible especially at 25 °C when both acetate and methane were observed.

2.4 HAC and HM kinetic features

In the MMC enriched under mass transfer limitation at 25°C, HM dominated (Figure 27), however, activity tests revealed that HAC could grow when HM was inhibited. Hence, the hydrogenotrophic activity test was used to characterize HM, and the homoacetogenic test to characterize HAC. Growth yields were calculated along the tests.

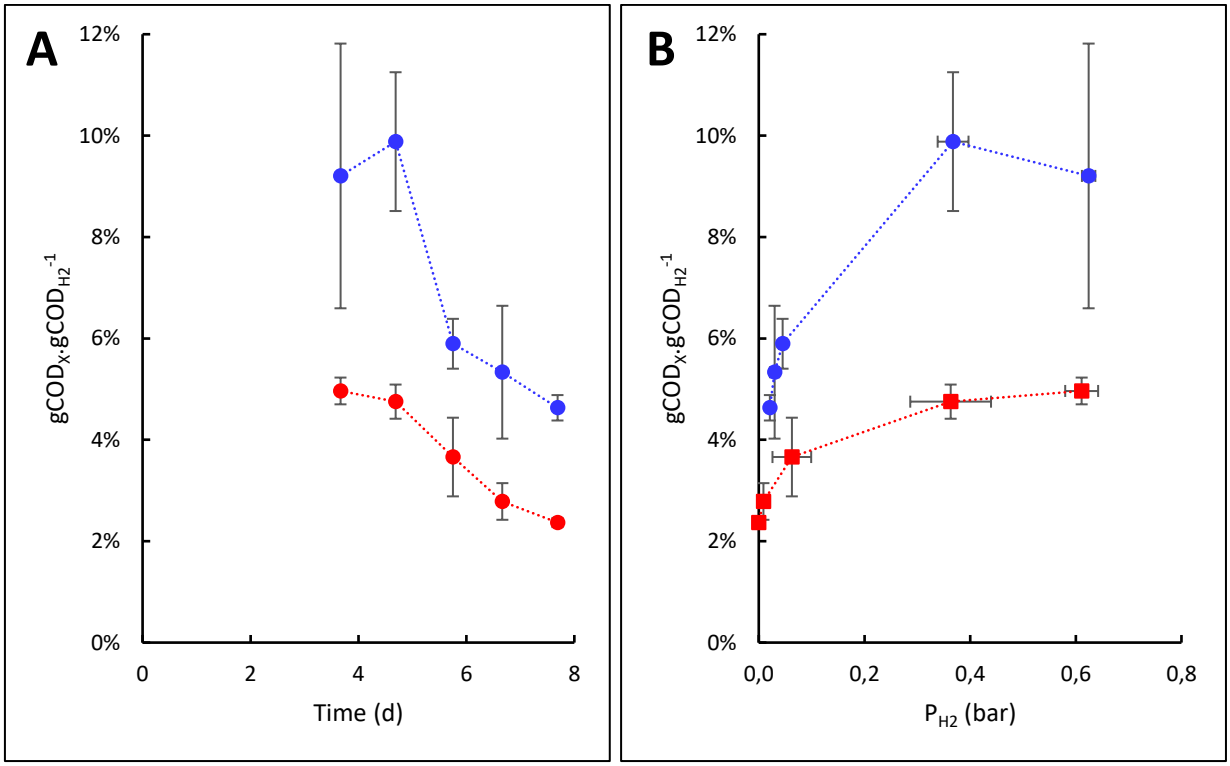

Figure 29: Growth yields calculated during the activity tests of MMC enriched in SBs at 25 °C under mass transfer limitation. In blue the data of the homoacetogenic tests in which only HAC was detected. In red the data from the hydrogenotrophic tests in which only HM was detected. A: growth yields as a function of time (HAC: n=3; HM: n=2). B: Growth yields as a function of P_{H2}.

According to Figure 29A, HAC had higher growth yields than HM. For both HM and HAC, the growth yield was not constant along the activity tests and decreased. This indicates that the production of biomass represented a higher part of H_2 fixed during the first stage of the batch. This is consistent with the profile of acetate production during this test (Figure 26A), as at 3.7 d H_2 consumption was detected, while acetate production was not detected yet. According to Figure 27B, it is possible that HM and HAC growth yields are P_{H2} dependent, and increase with P_{H2}. This

would imply a variable stoichiometry, assuming that under H_2 limiting conditions, microorganism's produce acetate, but the energy they harvest from it is not necessarily used for growth but also for maintenance. In the contrary, when the P_{H2} is higher, they are capable of higher growth yields. Though, the fact that acetate is later produced is not consistent with the fact that acetate production is linked to catabolism, meaning that it should be necessary for the cell to support growth. An explanation could be that the energetic capacities of HAC are very diverse, and some mechanisms, still not completely understood, improve energetic efficiency of the metabolism, such as electron bifurcating enzymatic systems (Figure 4). This could explain that stoichiometry used here were not applicable in every conditions, especially under energetic limitations (Regueira et al., 2018).

Interestingly, it was possible to identify a minimal P_{H2} below which HAC could not grow anymore. In the case of HM, this P_{H2} threshold was not quantifiable. However, for HAC, an average residual P_{H2} of 0.021 ± 0.004 bar was identified in the vials, corresponding to a residual H_2 concentration of 1.65.E-05 $mol.L^{-1}$ in the liquid phase at 25 °C. This confirms that HAC had higher H_2 threshold than HM, so lowering temperature to 25 °C was not enough to reverse the substrate affinity order of both communities. This P_{H2} threshold must be linked to thermodynamics of the reactions, especially the conserved energy ΔGc. The calculated ΔrG of HAC at the end of the homoacetogenic tests was of 2.8 $kJ.reaction^{-1}$. This value is lower than the ΔGc of 15 $kJ.reaction^{-1}$ found in literature. Methanogenic and homoacetogenic tests of this MMC have been simulated in the model (Figure 30 and Figure 31).

Both simulations led to a km estimation of 12 $gCOD_{H2}.gCOD_X^{-1}.d^{-1}$, suggesting that the activity tests were mass transfer limited. Hence, it is only possible to say that both HM and HAC had km above this value. Hence, this set of data were not suitable for the characterization of maximal specific performances of the HM and HAC.

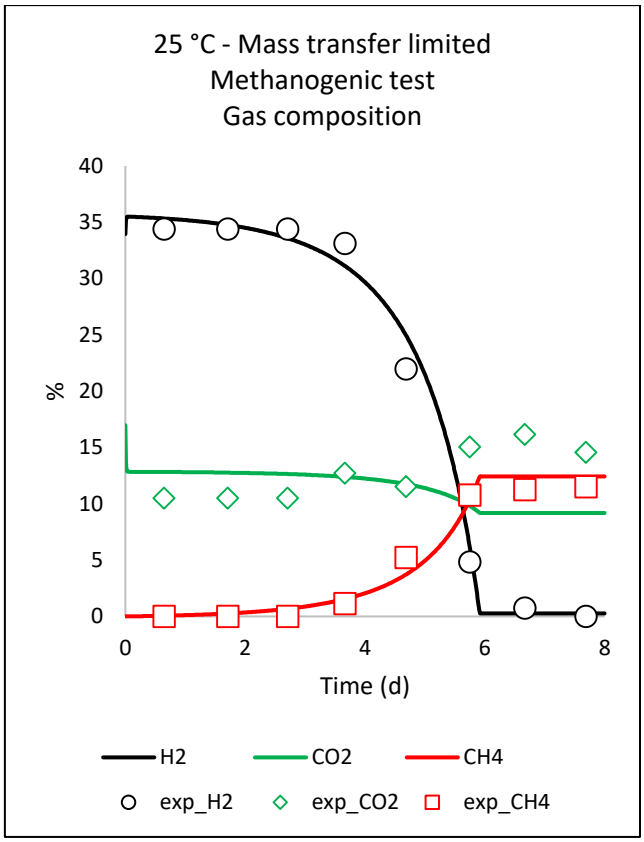

Figure 30: Simulation with the AQUASIM model of the methanogenic test on the MMC enriched at 25 °C in mass transfer limited SBs. Dots represent experimental data. Full lines represent the model simulation with km = 12 $gCOD_{H2}.gCOD_X^{-1}.d^{-1}$; $Y_{X/H2}$ = 0.090 $gCOD_X.gCOD_{H2}^{-1}$; K_{H2} = 0.00052; Xi = 0.001 $gCOD.L^{-1}$; k_La = 100, 70, 60 d^{-1} for H_2, CO_2 and CH_4 respectively; T = 25 °C; pH fixed to 6, as experimental pH was 6 ± 0.1.

Nevertheless, the kinetic model representation of the methanogenic test was satisfying (Figure 30). On the other hand, the representation of the homoacetogenic test with the kinetic model didn't describe the P_{H2} threshold observed at the end of the batch (Figure 31). The addition of the F_T in the HAC growth rate led to the inhibition of the reaction earlier than in experimental conditions. Hence, the ΔGc of HAC was set to 2.8 kJ.reaction, which was the value calculated in section 2.1. This time, the acetate production profile could be better represented. However, the gas profile was still not correctly represented at the end of the batch, and this must be due to the sensitivity of the gas phase composition to slight changes in H_2/CO_2 ratio, growth yields, pH and temperature as discussed in chapter 3.

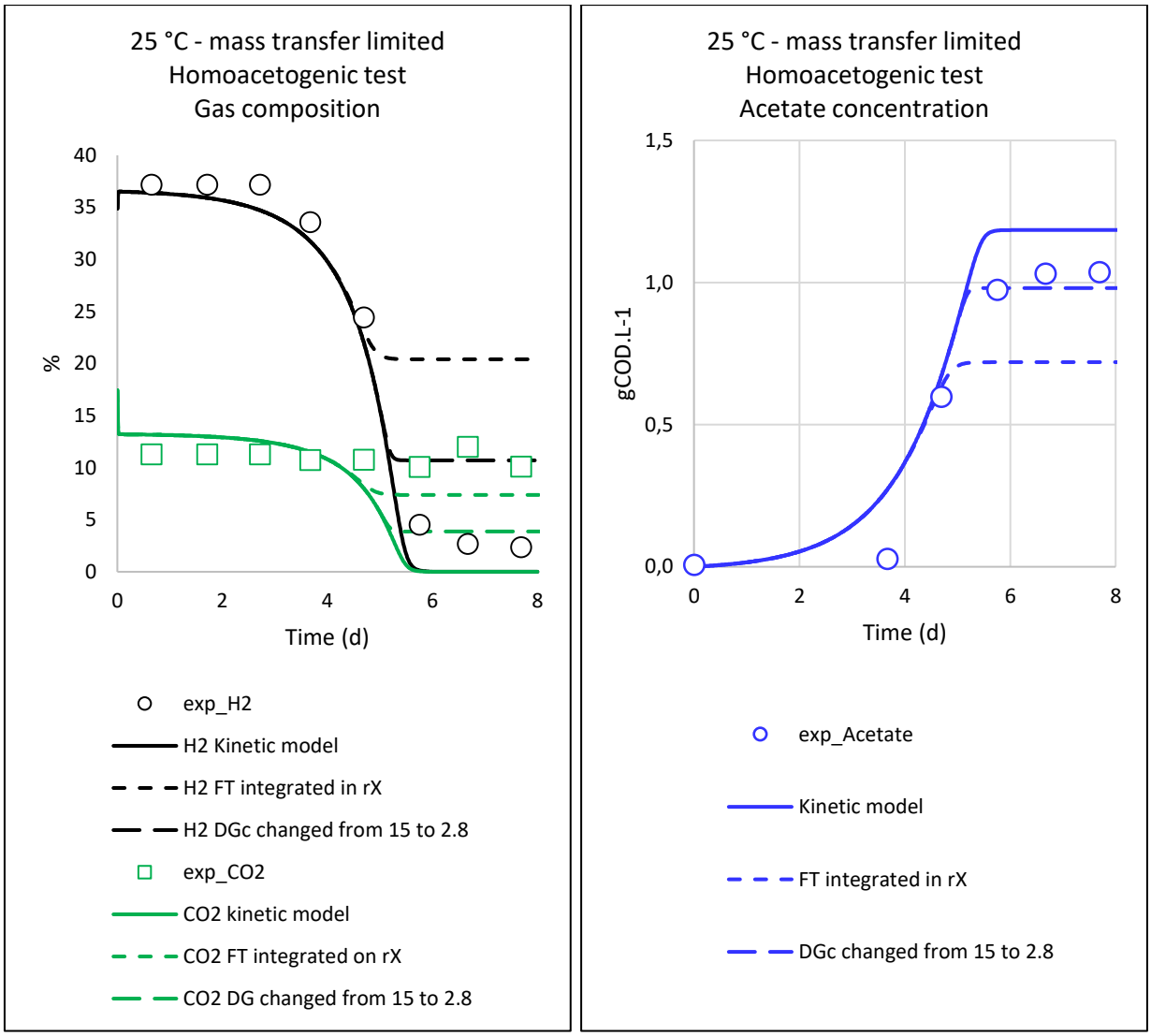

Figure 31: Simulation with the AQUASIM model of the homoacetogenic test on the MMC enriched at 25 °C in mass transfer limited SBs. Dots represent experimental data. Lines represent the model simulation with km = 12 $gCOD_{H2}.gCOD_X^{-1}.d^{-1}$; $Y_{X/H2}$ = 0.081 $gCOD_X.gCOD_{H2}^{-1}$; K_{H2} = 0.0000011; Xi = 0.001 $gCOD.L^{-1}$; k_La = 100, 70, 60 d^{-1} for H_2, CO_2 and CH_4 respectively; T = 25 °C; pH fixed to 6, as experimental pH was 6 ± 0.1.

Here, the temperature and pH were relatively constant during the batches, so the difficulty of representing the data is more likely due to the growth yield definition. Implementing a variable stoichiometry depending on P_{H2} should be envisaged in the future works.

Activity	SB cultivation strategy	Substrate	T °C	Maximal volumetric H_2 uptake rate $gCOD_{H2}.L^{-1}.d^{-1}$	Maximal specific H_2 uptake rate $gCOD_{H2}.gDW^{-1}.d^{-1}$	$Y_{X/H2}$ $gVSS.gCOD_{H2}^{-1}$	$Y_{X/H2}$ $gCOD_X.gCOD_{H2}^{-1}$	Majority genus associated
HM	Mass transfer limited	$N_2/H_2/CO_2$ (50:33.5:16.5)	25	0.55	4.9	0.045	0.064	*Methanobacterium Methanobrevibacter*
	Not mass transfer limited	$N_2/H_2/CO_2$ (50:33.5:16.5)	25	ND	ND	ND	ND	ND
	Mass transfer limited	$N_2/H_2/CO_2$ (50:33.5:16.5)	35	0.89	9.1	0.051	0.072	*Methanobacterium*
	Grimalt-Alemany et al., 2020	$CO/H_2/CO_2$ (20:65:15)	37	NA	0.8	0.090	0.127	*Methanospirillum*
		$CO/H_2/CO_2$ (20:65:15)	60	NA	4.1	0.064	0.091	*Methanothermobacter*
HAC	Mass transfer limited	$N_2/H_2/CO_2$ (50:33.5:16.5)	25	0.60	4.8	0.056	0.079	*Acetobacterium*
	Not mass transfer limited	$N_2/H_2/CO_2$ (50:33.5:16.5)	25	0.34	3.2	0.059	0.084	*Acetobacterium*
		$N_2/H_2/CO_2$ (50:33.5:16.5)	25	0.34	3.2	0.063	0.089	*Acetobacterium*
	Mass transfer limited	$N_2/H_2/CO_2$ (50:33.5:16.5)	35	0.88	7.7	0.063	0.089	*Clostridium sensu stricto 12*
	Grimalt-Alemany et al., 2020	$CO/H_2/CO_2$ (20:65:15)	37	NA	0.8	0.068	0.096	*Acetobacterium*
		$CO/H_2/CO_2$ (20:65:15)	60	ND	ND	ND	ND	ND

Table 15: kinetic parameters calculated for each activity test performed on the MMC enriched in SBs. HM parameters were calculated from the hydrogenotrophic tests and HAC from the homoacetogenic tests. 1.4159 $gCOD_X.gVSS^{-1}$ is assumed. ND: not detected; NA: not available.

Finally, Table 15 is a summary of the main kinetic parameters of HAC and HM calculated from the hydrogenotrophic and the homoacetogenic activity tests in this study, gathered with previously obtained results with similar approach at 37 °C and 55 °C on syngas (Grimalt-Alemany et al., 2019). For each condition of this study, volumetric H_2 consumption rates were similar for HM and HAC, suggesting that the tests were mass transfer limited, and this has been confirmed with the simulations of Figure 30 and Figure 31. Hence, maximal specific kinetic parameters such as μ_{max} could not be estimated from these data.

Higher HM growth yields were reported at 37 °C on syngas than at 35 °C on H_2/CO_2 in this study. This confirms that growth on syngas allows better growth performances of microorganisms, and this is due to CO being a better electron donor than H_2. However, this tendency is not observed for HACs, as all the growth yields measured at mesophilic conditions are of the same magnitude in both studies. Hence, it is possible that HAC have evolved with better energetic conservation mechanisms than HM to handle energetic limitations. This would be consistent with the fact that HM doesn't suffer from energetic limitations as the reaction thermodynamics are much better than that of HAC. Considering maximal specific uptake rates though, values obtained here at 35 °C are higher than the one obtained at 37 °C on syngas. However, this is attributed to a better mass transfer capacity of the activity tests in this study because stirring rate was higher.

Enriched HMs genera were not the same under syngas or H_2/CO_2, thus it is possible that *Methanobacterium* could not handle CO at the concentrations tested, and that *Methanospirillum* was preferentially selected on syngas. Regarding HACs, *Acetobacterium* was selected in all the conditions except the one at 35 °C with transfer during stationary phase. In this MMC, HM were highly dominating, and only traces of *Clostridium sensu stricto 12* was detected.

3 Conclusion and outlook

In this chapter, the microbial competition between HM and HAC was investigated in real conditions in order to confront the statements from the modeling work presented in chapter 3. Indeed, the simulations showed that it should be possible to find conditions of temperature and substrate availability that promote HAC growth and maintain HM at low concentration in the MMC. SBs were implemented, at 25 °C and 35 °C, and with two different cultivation strategies. The first one waiting for mass transfer limitation after multiple gas injections and consumption phases, and the second not waiting for mass transfer limitation by transferring faster as soon as activity was detected after a single gas injection phase.

The experimental results were successful. First, the effect of temperature was observed, as acetate was never detected in the SBs at 35 °C. Then, at 25 °C and avoiding mass transfer limitation, homoacetogenesis remained as the sole metabolic function identified in the activity tests. Hence, this cultivation method even allowed to eliminate HM in the MMC. This was due to too low kinetic parameters values of HM, and their potentially higher oxygen sensitivity during the transfers, leading to their loss along the SBs set. In perspective of this study, it will be interesting to evaluate the reproducibility of this cultivation method with different starting anaerobic MMCs to prove its robustness and applicability to provide HAC specialized MMCs.

The system was further analysed, first in terms of microbial communities analysis and kinetics. The temperature effect between 25 °C and 35 °C was also observed on the microbial selection, as well as the gas nature when compared to enrichments on syngas. *Methanobacterium* HM outcompeted HAC at 35 °C, while *Acetobacterium* HAC coexisted with *Methanobacterium* and *Methanobrevibacter* HMs at 25 °C. A diversity in the HMs selected was observed, while HAC was mostly belonging to *Acetobacterium* genus in all enriched MMCs. Furthermore, growth

yields of HM decrease with the increase of temperature in the range of 25 – 60 °C, and are higher on syngas than on H_2/CO_2. Conversely, HAC growth yields were similar in all of these conditions, highlighting the better metabolic efficiency strategies developed by HAC to face energetic limitations. Regarding growth yields, a variability of its value was observed along the activity tests, and this was enhanced in the case of HAC. In future works, a variable stoichiometry could be considered for the representation of such systems, as it has been previously proposed in organic wastes valorization models (Regueira et al., 2018). The development of more detailed models in terms of bioenergetic could be required and help for the understanding of the mechanisms ruling HAC growth.

AM and SAO were not observed in the activity tests. At 35 °C, this was mostly because of thermodynamic limitation of the reaction, and because acetate was not produced along the SBs enrichments. However, at 25 °C, AM was feasible but still not detected. According to literature, AM have lower specific growth rates than HM, explaining that they were not capable of maintaining themselves in the SBs, especially because their substrate, acetate, was produced along the batches, and so decreasing their potential time for growth. However, the SRB *Desulfovibrio* was detected at significant relative abundance in the MMC, because of the addition of sulphate instead of sulphide in the mineral medium. The promotion of SRB provided reduced sulphur in significant amounts as sulphate is the electron acceptor of these bacteria. Hence, HM were not sulphur limited during the tests. The consideration of SRB in the framework of the microbial competition will of interest for further optimizations of the MMC specialization cultivation method developed here.

Regarding thermodynamics of the system, HM were never thermodynamically inhibited in the conditions tested. Additionally, mass transfer limitation was closely related to thermodynamic

limitation, confirming that under mass transfer limitation, the competition is governed by thermodynamic and HM outcompete HAC. Hence, the kinetic model was satisfying for the simulation of HM growth, while HAC growth representation required the integration of F_T. However, a different ΔG_c of 2.8 kJ.reaction^{-1} than the one found in literature (15 kJ.reaction^{-1}) was estimated to correctly describe the acetate production profile. However, this value has to be better determined in future studies. Indeed, the gas phase behaviour was not correctly described, especially at the end of the batch, probably because of the fix stoichiometry used, and the sensitivity of the gas composition to H_2/CO_2 ratio. This makes difficult the interpretation of the exactitude of the ΔG_c estimated.

It has been demonstrated in this chapter that SBs are successful cultivation methods for the enrichment of MMC with HAC under H_2/CO_2. Lowering the temperature and overcoming mass transfer limitation were the key parameters for successfully enrich MMCs with HAC. Activity tests and microbial analysis allowed to identify the metabolic functions enriched and the dominant taxa associated. Thermodynamic and modeling tools were used to better describe and understand the system.

In chapter 5, continuous cultures of MMCs were implemented, to evaluate the potential of such reactor management for the selection of HAC. Considering the results obtained in chapter 4, HAC selection in continuous mode should be possible at 25 °C, as HAC had higher specific growth rates than HM in successive batches at this temperature. However, the thermodynamic limitation, *i.e* mass transfer limitation, will have to be overcome.

CHAPTER 5: Competition between homoacetogens and hydrogenotrophic methanogens in a continuous process, opened on the gas and the liquid phases. Effect of pH, dilution rate and nutrient limitations.

1 Introduction

In this chapter, the competition between HAC and HM is studied in continuous stirred tank reactors (CSTRs), with open liquid and open anaerobic gas phase. The two phases are managed independently, with their proper retention time in the system. The biomass is suspended and the liquid phase is considered perfectly mixed. Continuous processes can be used for different objectives. First, they enable to study a biological system with different features than in batch mode, they also can be used for microbial selection, and finally they also are production processes. A critical discussion regarding these different aspects in the case of H_2/CO_2 fermentation for the production of acetate with MMC will be addressed.

As discussed in chapter 3, continuous processes should be interesting for MMC specialization with HAC, under conditions for which they have higher specific growth rates. In addition to the substrate limitation, and the eventual thermodynamic limitations, opening the liquid phase imposes the microorganisms' growth rates. Hence, there is a minimal specific growth rate required for the microorganisms to be able to maintain themselves in the reactor. At steady state, the system should be substrate limited, either by the gas inflow, or by the mass transfer rate, provided that there is no other limitation or inhibition in the system. However, thermodynamic limitations may occur, especially for HAC because ΔrG is closer to thermodynamic equilibrium, and the product of the reaction accumulates in the liquid phase. Continuous mode allows the regulation of the product concentration, and could be advantageous to overcome thermodynamic limitations compared to batch processes.

In chapter 4, the study of the competition in batch mode highlighted the effect of the temperature on the specific growth rates of HM and HAC. Indeed, at 35 °C, HM had higher specific growth rate, as well as lower K_{H2}, making them outcompeting HAC whatever the mass transfer limitation

state. However, decreasing the temperature to 25 °C resulted in HAC having higher growth rates than HM and could outcompete methanogens, except under mass transfer limitation, suggesting that HM still had lower K_{H2} than HAC at 25 °C. The SBs carried out have similarities with continuous processes. Indeed, there is a semi-continuous substrate supply, and also a retention time (batch time) applied to the MMC after each transfer from a batch to the next one.

To go further, it is proposed in this last chapter to investigate the competition in continuous reactors, opened on the gas and on the liquid. Hence, a first objective is to verify the results obtained in batch mode. Especially: at 35 °C, HM should outcompete HAC and remain alone at steady-state, and it should be no D allowing to keep HAC and wash out HM. At 25 °C though, HAC should outcompete HM and remain at steady-state, provided that D is properly chosen between the maximal specific growth rate of HM and the one of HAC. The effect of pH is also addressed, by conducting CSTRs at neutral pH or pH 5. Working at pH 5 could be advantageous in terms of operations, because it is close to acetate pka. However, the productivities could be lower due to inhibition effects and thermodynamic limitations. Also, the reduction of acetate into ethanol should be promoted at pH 5.

Different experimental campaigns are presented. First, at 35 °C in the system developed in TBI (Chapter 2, section 2.3.1). Although these results were not expected, high acetate concentrations were reached in the reactor at 35 °C, so different assays have been carried out at this temperature. The pH was regulated at 5 or 6.5-7, and dilution rates between 0.2 and 1 d^{-1} were tested depending on the assays. High gas inflows were applied to ensure maximal mass transfer capacities of the system, and stabilize gas partial pressures all along the experiments. The high mass transfer capacity (k_La = 74 h^{-1}) compared to batch experiment allowed to increase the period before mass transfer limitation is reached. This should increase the biomass concentration in the reactors, and facilitate the calculations. However, different obstacles were encountered. First, the gas balances

were complicated due to the high gas inflow compared to the gas consumption rates. Secondly, changing from batch to continuous mode led to nutrient limitations that may have changed the competition rules. Nutrient investigations were conducted to identify the requirements for the system.

Finally, a test at 25 °C was conducted, in a different reactor (Chapter 2, section 2.3.2), with lower gas inflows in order to better quantify gas consumption rates. pH and dilution rate were changed in dynamic during this test to evaluate the reaction of the system to these changes, and the effect on the different biological activities. In this process, the culture medium was supplemented with nutrients identified as essentials. Also, sulphate was added as sulphur source in this assay, to evaluate the effect of sulphide omission in continuous processes, and see if SRB were selected or not.

2 Results and discussion

2.1 CSTR at 35 °C

2.1.1 Development of the continuous study system

A bioreactor was developed at TBI to specifically study the microbial competition in continuous mode, with gas and liquid phases opened. Hence, a 2 L glass tank was used and instrumented (Figure 10). Different conditions were considered important for the development of the system to be able to study the microbial competition. First, maintaining high and constant gas partial pressures over a long period of time to ensure high and stable substrate availability. This required to ensure a high gas/liquid mass transfer coefficient (k_La = 74 h^{-1}), and apply high gas inflows so the gas partial pressures were stable along the experiment. A first assay (CSTR1) was carried out to evaluate if the system was suitable to the study of the microbial competition in continuous mode, and if the mass transfer limitation was reached late enough to be able to study the system with or without mass transfer limitation.

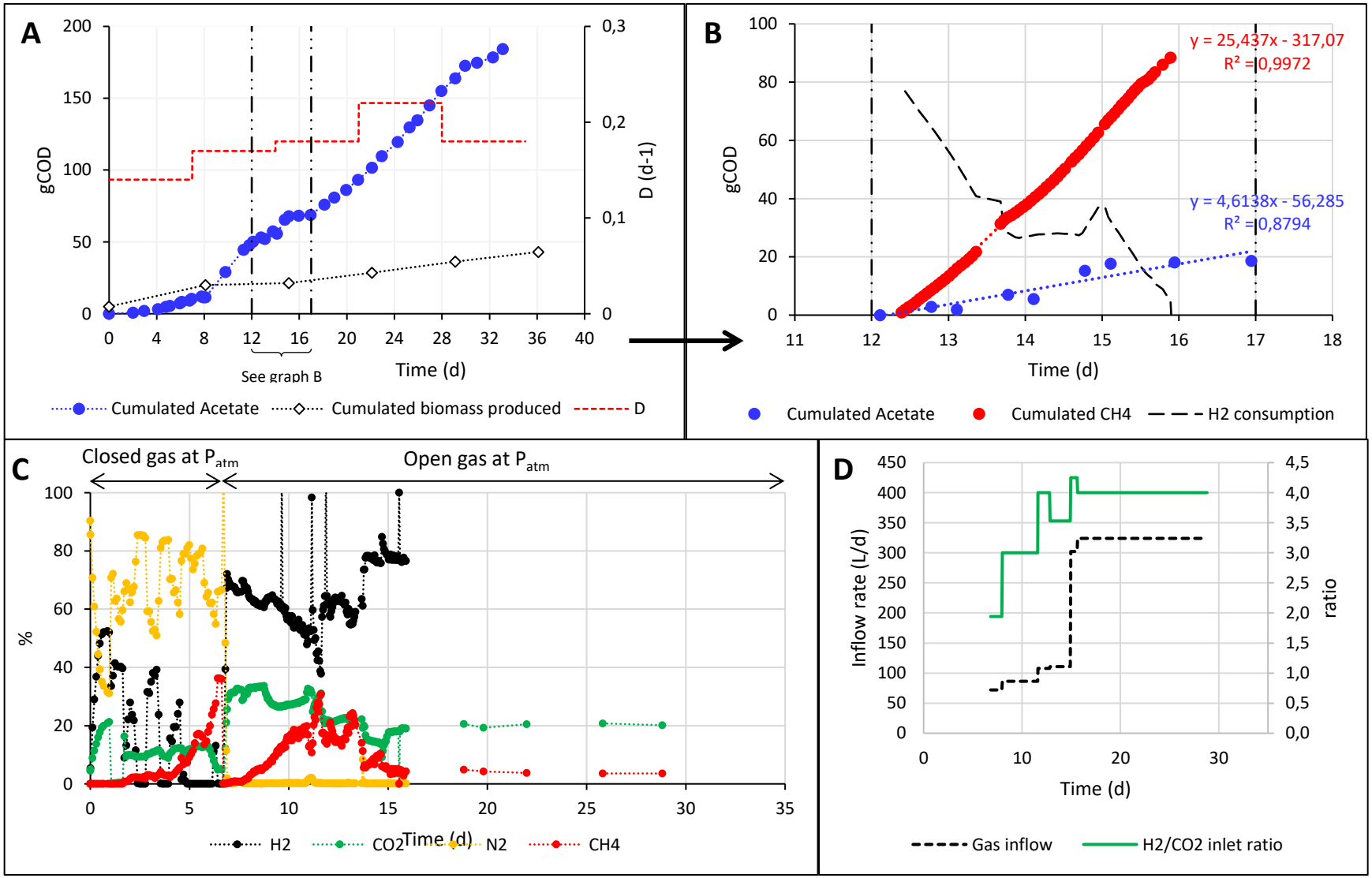

Figure 32: Results of CSTR1 at pH 7 and 35 °C, for the development of the reactor. A: Cumulated acetate and VSS productions in gCOD and average dilution rate. Vertical lines delimit a period between 12 and 17 d when all the data from the gas and the liquid phases could be measured. B: cumulated acetate and methane productions, H_2 consumption, in gCOD between 12 and 17 d when data from the gas phase were available. C: gas composition, N_2, CO_2, CH_4 and H_2 were analysed. D: Gas inflow rate and H_2/CO_2 ratio of the inlet gas.

2.1.1.1 Acetate and methane production

CSTR1 was carried out at pH 7 with a targeted HRT of 7 d. During this assay, high acetate concentrations were reached in the liquid, and methane was detected at significant concentrations in the gas phase (Figure 32C). Figure 32B shows methane and acetate produced in cumulated gCOD over time between 12 and 17 d. Due to the numerous optimizations and instrumentations carried out during this assay, it was only possible to measure all the data needed for mass balances during this short period. Acetate production was of an average of 4.6 $gCOD.d^{-1}$, and methane was produced. In order to promote HAC by applying high gas availability, and to stabilise the gas phase composition and partial pressures, high gas inflow was set. But this led to uncertainties in the measurements of the gases consumed and produced, as it is much lower than the overall gas flow. Between 12.4 and 13.4 d, acetate and methane production represented 73 % of the COD balance. Even considering 5 – 10 % of biomass yield, this balance is not satisfying and suggests that all the gas related calculations were not accurate. It is also possible that other products accumulated in the liquid, but were not analysed in this study.

However, acetate concentrations in the liquid, and methane concentration in the gas were considered accurate. Hence, it is possible to quantify acetate production, and qualitatively know if methane was produced or not. During this first assay, that mainly aimed to the development of the system, simultaneous production of acetate and methane was observed during 35 d, suggesting cohabitation of HM and HAC, that remained stable from 15 to 35 d. This result significates that the bioreactor developed was a suitable study system of the microbial competition between HAC and HM in continuous mode. The microbial analysis confirmed that at the end of CSTR1, the MMC have been enriched with 21 % of *Acetobacterium wieringae* (HAC) and 18 % of *Methanobacterium formicicum* (HM) (Figure 33). This information, together with the gas composition profile, suggest that mass transfer limitation was not reached,

allowing to avoid the K-competition for low substrate concentrations. The system stabilised at a pseudo-steady state during which acetate concentration was 16.2 ± 2.3 $g.L^{-1}$ between 12 and 34 d and CH_4 amount of around 4.7 ± 0.9 % in the gas phase from 15 to 28 d.

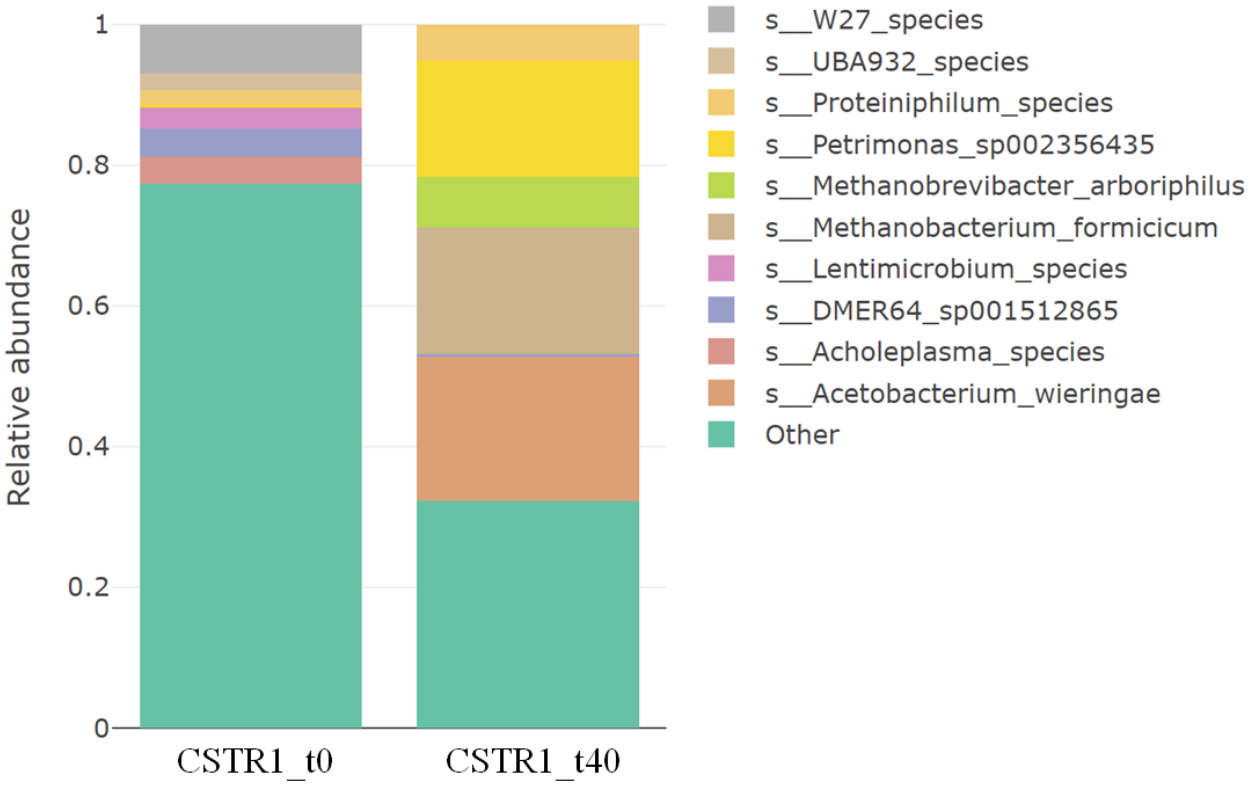

Figure 33: Relative abundance at species level of the MMC in CSTR1 at t0 and after 40 d of operation.

During this assay, a cohabitation between HM and HAC occurred, and the system remained relatively stable for more than 20 d. The limitations of the process during this pseudo-steady state will be investigated, so further analysis and discussions will be addressed in this chapter.

2.1.1.2 Discussion about pH regulation and dilution rate variation

During the first assay, the actual HRT varied between 4.6 and 7.1 depending on the amount of NaOH added. NaOH addition was mainly correlated to acetate production in the system. To stabilise the pH all along the experiment, NaOH addition compensated the protons release due to acetic acid production and dissociation. Depending on the pH, the dissociation was more or less important. The lower the pH, the less dissociation and the need for NaOH addition. As the drain of the reactor was done with a surface canula in order to maintain a constant liquid volume, the liquid outflow variated. As a consequence, the dilution rate of the liquid phase increased with the acetate increasing concentration, and oscillated around an average value during the pseudo-steady state (Figure 32A).

Acetic acid production rate:

$$r_{AcH} = \left(1 - Y_{\frac{X_{HAC}}{H_2}}\right) \times k_{m_{HAC}} \times \frac{C_{H2}}{C_{H2} + K_{H2_{HAC}}} \times X_{HAC} (\times F_T) \ \ (mol_{AcH}.L^{-1}.d^{-1})$$

Proton release:

$$r_{H^+released} = Ka_{AcH} \times C_{AcH} \times V_{liq} \ (mol_{H^+}.d^{-1})$$

NaOH inflow:

$$Q_{NaOH} = \frac{r_{H^+released}}{C_{NaOH}} \ (L_{NaOH}.d^{-1})$$

Finally:

$$D = \frac{(Q_{in_{liq}} + Q_{NaOH})}{V_{liq}} \ (d^{-1})$$

Where Q_{in_liq} is the nutrient solution inflow.

To avoid too many changes in the D variation, it is possible to use a concentrated alkaline solution, for example. However, the accuracy of the addition system must be considered so the

minimal volume of base added (a drop), doesn't cause pH fluctuations. Another possibility is to concentrate the nutrient solution and decrease the liquid inflow. However, this particularity of the system is not necessarily a drawback.

From the point of view of the microbial competition, the D increase with acetate concentration could be interesting to promote HAC. Indeed, HAC will fix the D to a high value according to their acetate productivities. Additionally, the increase of the dilution rate will also decrease the acetate concentration in the reactor, limiting the thermodynamic limitation and toxicity inhibition effects on HAC, increasing even more their productivities. A compromise between acetate productivity, NaOH concentration, and acetate concentration in the liquid outflow must be found, to allow high acetate productivity, but also provide a sufficiently high concentration of acetate for the downstream process. In this study, the pH was regulated because it was one of the main parameters studied. The objective was to evaluate the effect of pH value on productivities and microorganism selection in MMCs. However, in order to develop a production process in future works, pH regulation will have to be discussed and specifically studied regarding the productivities, but also the process management strategies and costs. It is possible that a pH regulation would not be necessary, or that it could be regulated very close to the acetic acid pka (for example between 5 – 5.5) to ensure satisfying productivities.

In the next sections, new assays are described. Each of them has been carried out with different pH regulation and D set points. pH 7 led to the cohabitation of HM and HAC. Additionally, pH 8 led to complicated process management due to high amount of NaOH addition (unsuccessful assay, not shown). For these reasons, assays at pH of 6.5 and 5 have been tested, with D ranging from 0.2 to 1 d^{-1}. A phosphate buffer (0.1 M) was added to the medium for the test at pH 6.5 to limit alkaline solution addition and D variation.

2.1.2 Effect of pH and dilution rate on the continuous process of H_2/CO_2 conversion with MMC

An experimental campaign was started to evaluate the effect of pH and D, in different assay. A first analysis axis is the competition between HM and HAC at the beginning of the assay, in transitory and pseudo-steady states. Then a second axis of analysis is the viability of the process and its stabilisation, with the understanding of the pseudo-steady-states reached. Microbial composition of the MMC over time will be discussed according to the functional activity observed in the reactor.

Experiment name	CSTR1	CSTR2	CSTR3	CSTR4
pH	**7**	**6.5**	**5**	**5**
Targeted HRT (d)	7	3	1	5
Real HRT (d)	4.6 – 7.1	2.6 – 11	1.0	3.9 – 5.8
D (d^{-1})	**0.14 – 0.22**	**0.09 – 0.38**	**0.98**	**0.17 – 0.25**
Duration (d)	35	14	6	124
Gas flow ($L.d^{-1}$)	72 – 324	126 – 170	110	151
H_2/CO_2 input ratio	1.9 – 4	2	1.8	1.9
Acetate maximal productivity ($molC.L^{-1}.d^{-1}$)	0.227 (15 d)	0.652 (3 d)	0.074 (0.25 d)	0.083 (12 d) 0.218 after vitamins addition
Acetate stabilised productivity ($molC.L^{-1}.d^{-1}$)	0.139	0.296	0.021	0.020
Acetate maximal concentration ($mol.L^{-1}$)	0.33	0.37	0.01	0.15
Methane production	All along the experiment	Not detected	Not detected	Until 20 d
Methanogenic archaea	40 d: 18 % *Methanobacterium formicicum* 7 % *Methanobrevibacter arboriphilus*	Not detected	Not detected	25 d: 37 % *Methanobacterium Bryantii* Not detected after 25 d
Potential homoacetogenic bacteria	40 d: 21 % *Acetobacterium wieringae*	6 d: 22 % *Acinetobacter bereziniae* 16 % *Oscillibacter ruminantium* 15 % *BRH-c20a sp.*	4 d: 31 % *Clostridium sensu stricto 12* 15 % *Acinetobacter bereziniae*	20 d: 31 % *Clostridium autoethanogenum.* 11 % *Clostridium sensu stricto 12* 112 d: 68 % *Clostridium autoethanogenum*
Biomass stabilised concentration (gVSS/L)	1.88	0.16 ± 0.02	0.08 ± 0.02	25 – 55 d: 0.06 ± 0.02 87 – 117 d: 0.26 ± 0.06
Biomass ratio gCOD/gVSS	/	/	1.50	1.47
Specific acetate productivity ($molC.gVSS^{-1}.d^{-1}$)	0.074	1.850	0.263	0.286

Table 16: Operational conditions of the different CSTR tests performed at 35 °C, and summary of major results.

2.1.2.1 Competition between HM and HAC in continuous mode, effect of pH and D

Table 16 is a summary of the results obtained in the four CSTRs operated, regarding the microbial competition. CSTR1 is the first assay discussed in the previous section. Then, three other CSTRs (CSTR2 to CSTR4) have been tested, with different pH and D.

Acetate was produced in all CSTRs, until the end of each experiment. However, methane production was only observed in CSTR1 until the end, and CSTR4 until 25 d. These two tests correspond to the lowest D tested, around 0.2 d^{-1}. During CSTR3 and CSTR4 at pH 5, acetate productivity was similar, of 0.02 $molC.L^{-1}.d^{-1}$. However, at neutral pH, during CSTR1 and CSTR2, acetate productivities were much higher: 0.139 and 0.296 $molC.L^{-1}.d^{-1}$ respectively. The higher productivity in CSTR2 is likely due to the exclusive acetate production, while in CSTR1 methane was produced.

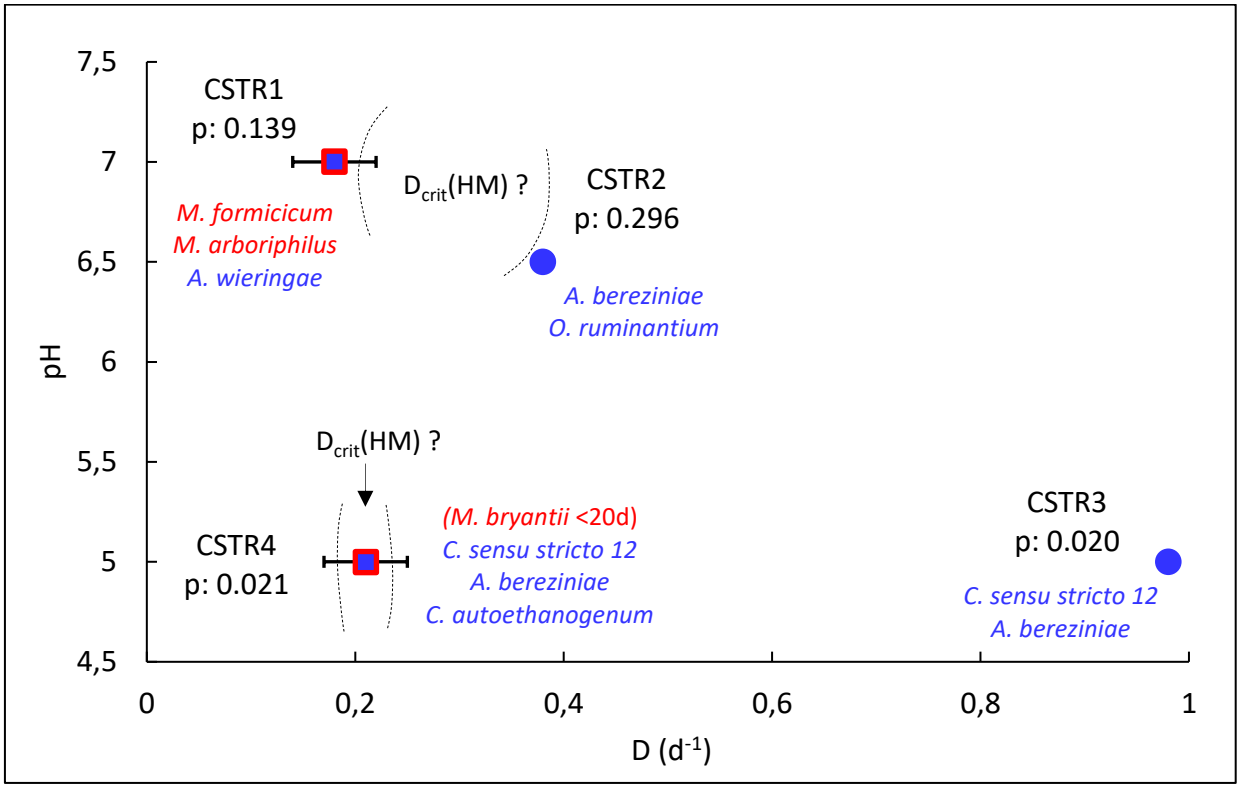

Figure 34: Summary of the different conditions of pH and D tested in CSTR at 35 °C and determination of potential critical D zones for HM wash out (dot curves delimitations). Blue and red squares represent cohabitation of HM and HAC observed during the corresponding assay, blue circles represent dominance of HAC in corresponding assays. P: acetate stabilised productivities ($molC.L^{-1}.d^{-1}$)

Figure 34 is a representation of the different CSTRs according to pH and D of each of them. First, methane production, and HM were only detected in CSTR1 and CSTR4, suggesting that the D had an important effect on the selection of HM, both at pH 5 and neutral. However, HAC were selected until the highest D tested of 1 d^{-1} (CSTR3). This allows to estimate critical D (D_{crit}) above which HM could be washed out. At neutral pH, D_{crit} of HM should be around 0.30 ± 0.08 d^{-1}. Indeed, at 0.2 d^{-1} methane was produced until the end, while at 0.38 d^{-1} methane was never detected. At pH 5 though, the critical D might be lower, very close to the tested value of 0.2 d^{-1}, as HM and methane production was observed at the beginning of the experiment, but did not maintain themselves in the reactor after 25 d. This pH effect could be due to high maintenance cost at low pH, especially for HMs, but also to a difference in microorganisms selected according to pH (Valgepea et al., 2017).

Comparing CSTR1 and CSTR4, in addition to the great difference in acetate productivity, a strong effect of pH on microbial communities enriched was observed, both for HM and HAC. At pH 7, a cohabitation of HM species *Methanobacterium formicicum* and *Methanobrevibacter arboriphilus* was revealed, while at pH 5, the HM *Methanobacterium bryantii* was the only archaea detected (Figure 27 Figure 35 Figure 36 Figure 41). Considering HAC, at pH 7 *Acetobacterium wieringae* was the majority species detected, while at pH 5 it was a cohabitation of *Clostridium autoethanogenum* and *Clostridium sensu stricto 12.* Additionally, the D also had an effect on the HAC selection. Indeed, at pH 5 *C. autoethanogenum* was selected only at low D, indicating that this species is likely not able to grow at D of 1 d^{-1}. But as the acetate productivities in CSTR3 and CSTR4 were similar, it can be concluded that a functional redundancy exists within HAC, and that the MMC composition is dynamically adapting to process parameters and constraints.

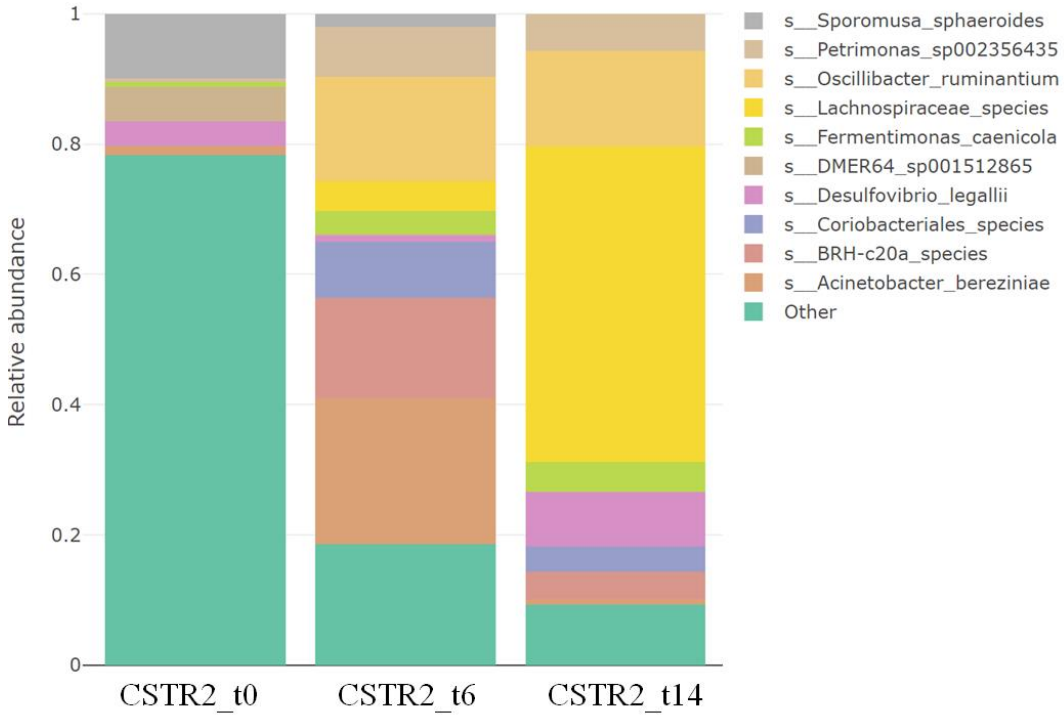

Figure 35: Relative abundance at species level of the MMC in CSTR2 at t0 and after 6 and 14 d of operation.

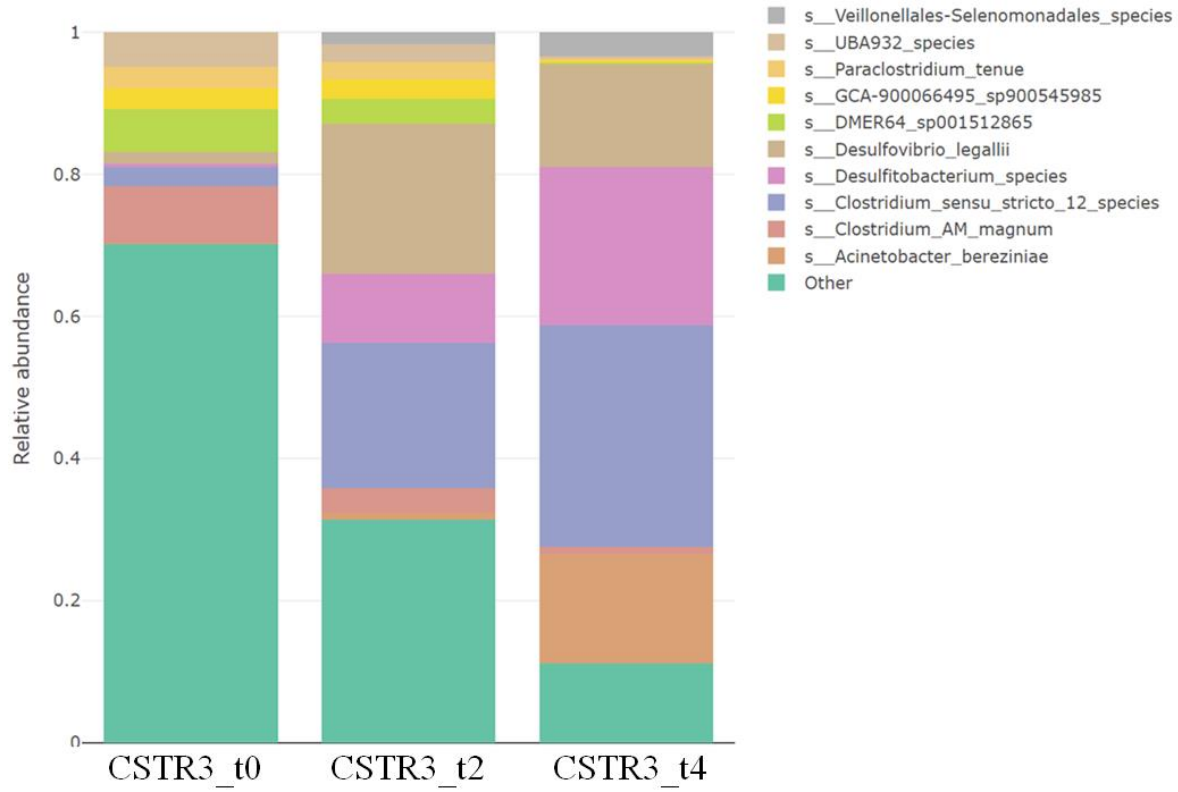

Figure 36: Relative abundance at species level of the MMC in CSTR3 at t0 and after 2 and 4 d of operation.

2.1.3 Investigations and understanding of the limitations of the system

2.1.3.1 Mass transfer limitation reached at neutral pH

During all CSTR assays, gas partial pressures were maintained at 0.67 bar and 0.33 bar for H_2 and CO_2 respectively. However, this doesn't mean that the system was never mass transfer limited, but that the gas inflows applied were sufficiently high to make invisible the mass transfer rate and stabilise the gas partial pressures in the gas phase. This was one of the particularities wanted for the study of the system, to ensure stable operations and keep thermodynamic favourable conditions for HAC.

Considering the k_La measured in this reactor (74 h^{-1}), the maximal H_2 mass transfer rate at P_{H2} of 0.6 bar should reach 1.2 $mol_{H2}.L^{-1}.d^{-1}$, corresponding to a maximal acetate productivity of 0.3 $mol_{Ac}.L^{-1}.d^{-1}$. This value was only reached during the stabilised period of CSTR2 between 3 and 6 d, indicating that CSTR2 reached mass transfer limitation after 3 d.

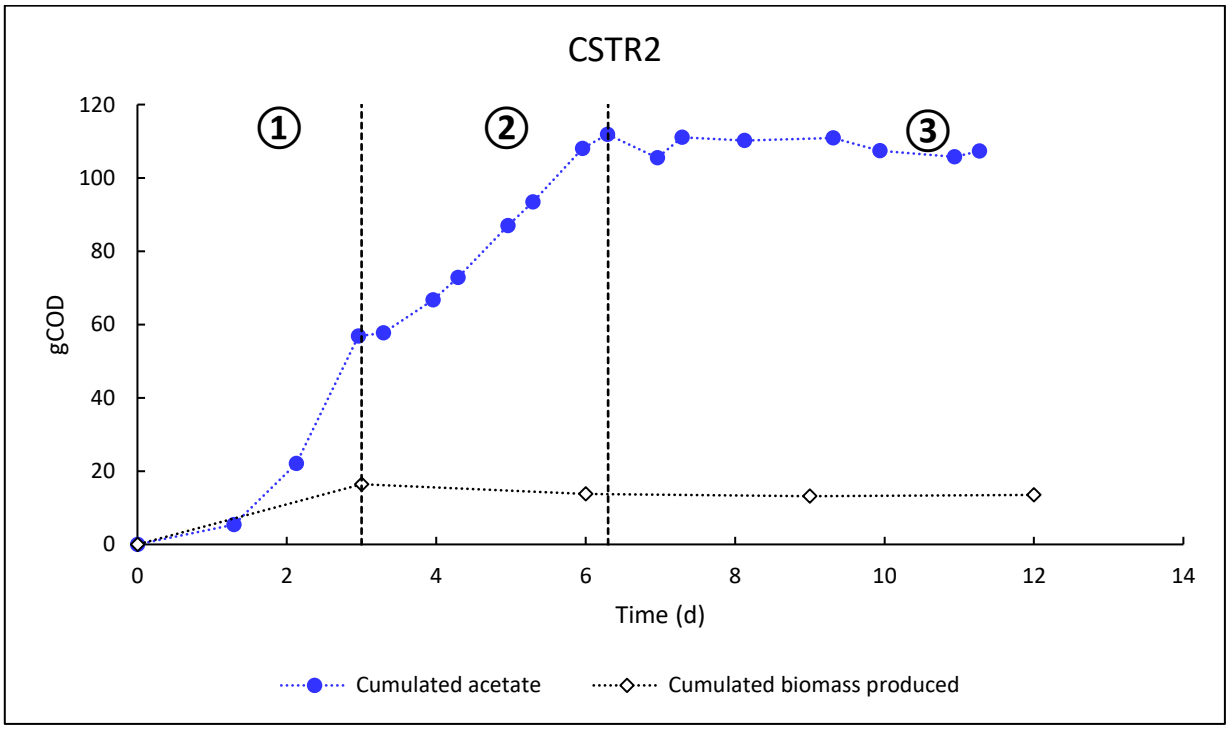

Figure 37: Cumulated biomass and acetate produced over time, in gCOD, during CSTR2 at 35 °C, pH 6.5 and D = 0.09 – 0.38 d^{-1}. Phase 1: before mass transfer limitation; Phase 2: mass transfer limitation; Phase 3: nutrient limitation.

On Figure 37, the cumulated acetate and biomass production during CSTR2 is represented. Three different phases can be observed. During the first one, substrate was in excess. The HAC grew at μ_{max}, with a significant biomass production observed during this period. Then, during phase 2, mass transfer limitation was reached, leading to a linear production of acetate governed by the H_2 mass transfer rate. During this phase, no net biomass production could be observed. The substrate limitation might have forced the microorganisms to stop their growth, and only produce energy for their maintenance, in the form of ATP, through acetate production. Finally, during phase 3 after 6.3 days, the acetate production stopped brutally. However, methanogenic activity was not observed either, meaning that HAC didn't stop because of HM outcompeted them, which was the expected result after mass transfer limitation, as demonstrated with the modeling work in chapter 1.

During CSTR 3 and 4 at pH 5, mass transfer limitation was not reached. But again, three phases could be observed, a first one of growth and high acetate production rates, a second short phase of stabilisation, and a third phase of activity drop (Figure 38). However, during CSTR4, activity was not null during phase 3, but stabilised at a low value from 30 d. These periods of stabilisation, but not mass transfer limited, are defined as pseudo-steady states. Further investigations of what was limiting during these periods are described in next sections

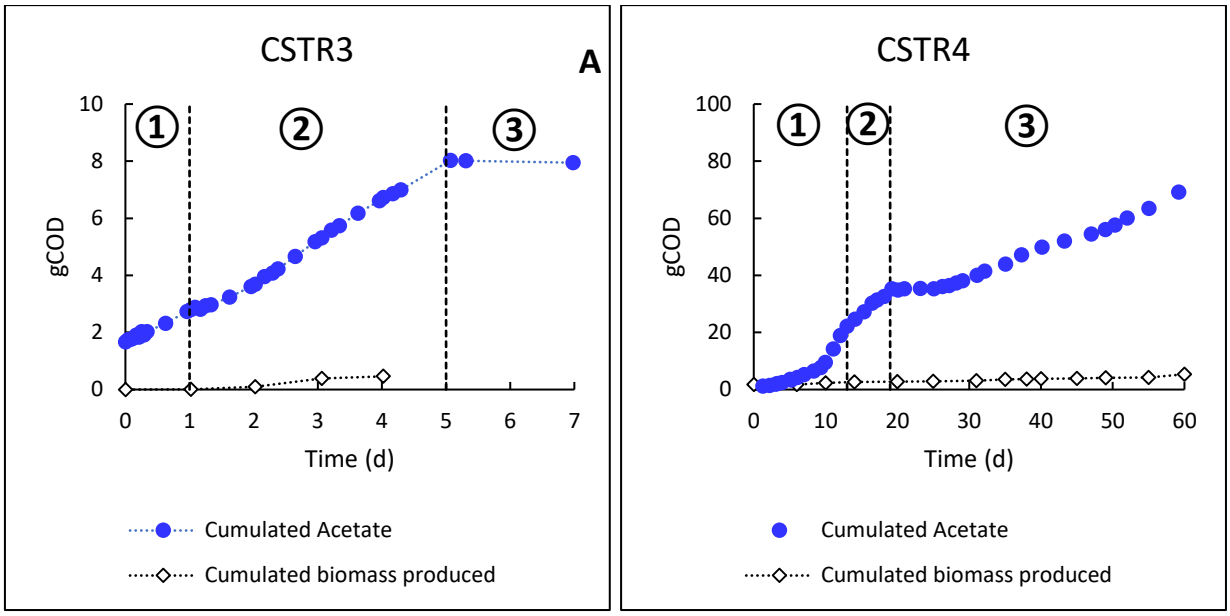

Figure 38: Cumulated acetate and VSS produced over time, in gCOD, during the CSTR assays at 35 °C. A ratio of 1.4159 $gCOD_X/gCOD_{VSS}$ was assumed (biomass composition: $C_5H_7NO_2$).

2.1.3.2 The system is limited by thermodynamics at pH 5

The model was used to simulate the assay CSTR4, with respect of the dilution rate variations, the pH regulation to 5, the k_La measured in the reactor, and the gas inflows applied during the experiments. Parameters k_m (specific uptake rate) and X_i (initial biomass concentration) were estimated with fitting to phase 1. This way, phase 1 was correctly represented. The simulation stabilised at a F_T value of 0.26, indicating a strong thermodynamic limitation, and explaining why mass transfer limitation was not reached during this assay (Figure 39). The thermodynamic limitation is linked to acetate accumulation in the liquid phase, inducing an indirect product inhibition caused by an increase of the ΔrG of HAC. Hence, the integration of the thermodynamic factor F_T allowed to describe the beginning of the test, and shows that the mass transfer limitation would not have been reached in any case, as the thermodynamics of HAC reaction was limiting before, stabilising the acetate concentration to 8 $gCOD.L^{-1}$. This result demonstrates the importance of considering thermodynamics of the reactions to represent anaerobic systems, especially at low pH when VFA are produced. Furthermore, the use of the F_T is more accurate

and robust than empiric VFA inhibition terms, as it considers the pH, the substrates and products concentration, and can be used in dynamic systems, while inhibition constant have to be determined in the specific operating conditions to be used correctly.

The F_T calculation showed that HM reaction was thermodynamically feasible, yet, only few methane concentrations were observed until 15 d, and then HM activity disappeared. This confirms that methane production was avoided by the process parameters used, in particular pH and D. In these conditions, HAC selected might have higher growth rates than methanogens. Additionally, acetate was likely not consumed by acetate consumers, as SAO was not feasible according to the F_T calculation, and that no AM were detected with the microbial analysis. Experimentally, acetate concentration was not maintained to 8 $gCOD.L^{-1}$ as predicted with the model (Figure 39), but decreased and stabilised around 2.5 $gCOD.L^{-1}$. This behaviour is needs to be further investigated. In next section, investigations of nutrient limitations are presented. They have been done on CSTR4, to explain phases 3 observed in the different assays.

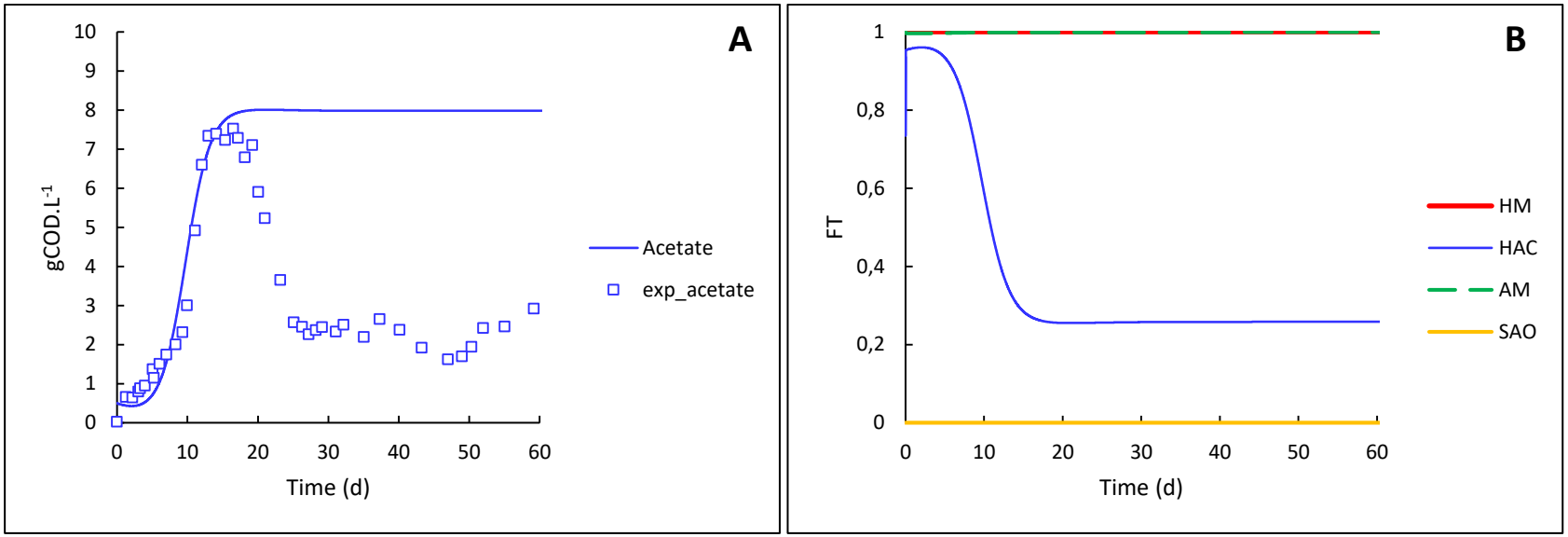

Figure 39: A: Acetate concentration in the reactor during CSTR4. Squares are experimental measurements, line is the simulation with the model integrating F_T in the growth rates. B: F_T dynamic calculations in the model for HM, AC, HAC, and SAO reactions.

	Microbial community	k_m ($gCOD_{H2}.gCOD_X.\ d^{-1}$)	X_i ($gCOD.L^{-1}$)
Model considering thermodynamic factor from (Jin and Bethke, 2007)	HAC	10.6	0.03
	HM	3.1	0.10

Table 17: Parameters set in the model in the different simulations presented to fit the assay CSTR4 at 35 °C.

2.1.3.3 Nutrient limitations investigation and culture medium optimization

Finally, to described phase 3, nutrient limitation was suspected. Indeed, after few days of stabilization at a maximal acetate concentration value, the activity dropped systematically. The mineral medium used in the CSTRs at 35 °C was the same as the one used for the reactor of biological methanation described in chapter 1, at the exception of phosphate buffer addition for the assay at pH 6.5. However, it is possible that HAC have different nutrient needs than HM, it is also possible that opening the liquid leads to the loss of some essential nutrients (present in the inoculum), while they could be recycled in the methanation reactor as the liquid was closed. Hence, culture medium supplementation tests were operated during CSTR4 which was extended to 120 d.

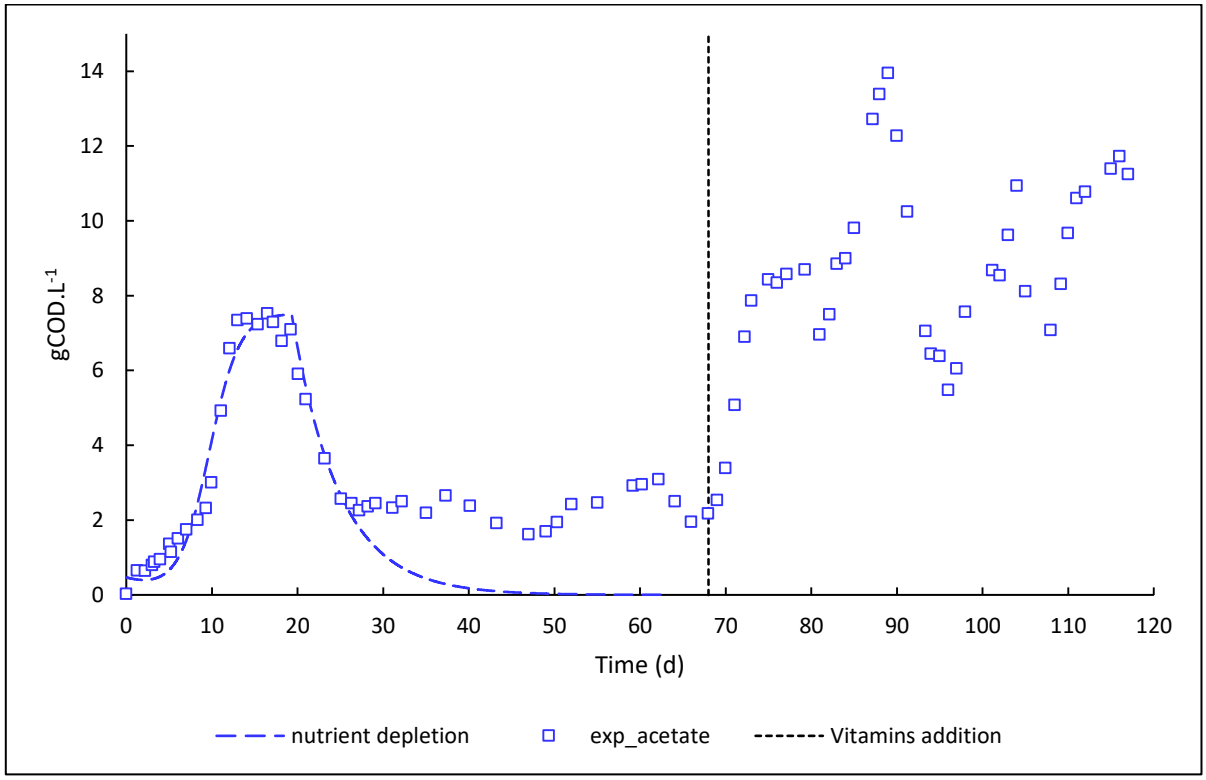

Figure 40: Extension of CSTR4 for limitations investigations, and simulation of an essential nutrient z only supplied in the inoculum and depleted.

	k_m ($gCOD_{H2}.gCOD_X.\ d^{-1}$)	X_i ($gCOD.L^{-1}$)	$Y_{X/z}$ ($mol_X.mol_z^{-1}$)	z_i ($mol.L^{-1}$)	Ratio $z_i/Y_{X/z}$
CSTR2	29.6	0.05	0.0001	0.0016	16
CSTR3	16.0	0.03	0.0001	0.0004	4
CSTR4	10.6	0.03	0.0001	0.0018	18

Table 18: parameters used for the simulation of HAC growth with an essential component z only supplied in the inoculum. $Y_{X/z}$ and z_i were estimated in CSTR2, CSTR3 and CSTR4.

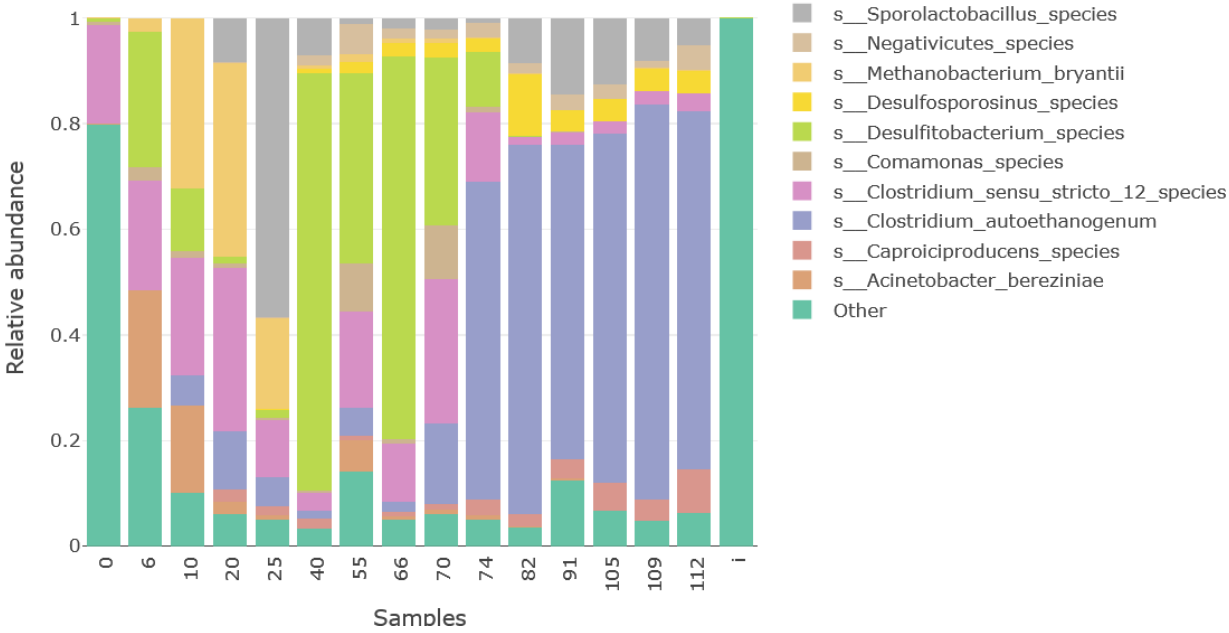

Figure 41: Relative abundance at the species level during CSTR4.

With the model, the simulation of an essential component z for HAC growth, only present in the inoculum, was simulated. The growth yield of this component was arbitrary set to 0.0001 mol_X/mol_z, and the initial concentration was fitted to the acetate concentration drop (Table 18). For CSTR2 and CSTR4, the initial concentration estimations were close, with a ratio $z_i/Y_{X/z}$ of 16 and 18 respectively. However, for CSTR3, this ratio was only 4, four times lower. This would suggest either that z was four times less available for the microorganisms during this test, or that the microorganisms selected needed four times more of z than in the other tests. However, there should be no reasons why z would be four times less available, as pH was the same as CSTR4. Additionally, this test was carried out between the two others, excluding the possibility of a variation in the inoculum composition. Hence, this is more likely attributed to

the different microorganisms enriched, that had different needs of this essential nutrient. In order to identify the limiting nutrient, different medium supplementations were done to observe the reaction of the system and if acetate productivity increased. These investigations were done from 40 to 120 d of CSTR4.

Table 19 and Table 20 summarize the macronutrients and micronutrients needed by microorganisms for growth. Some of them are essential, such as sources of C, H, O, N, P and S, but also some metals. Mg, Na, Ca and K should always be available in culture media, and are considered essential for the cell functioning. Additionally, anaerobic microorganisms encoding the WLP need more of Fe, Co, Mo, Ni, W, Se, and S than other microorganisms, because numerous enzymes and cofactors of the pathway contain such elements. Indeed, metals often are the catalysts in the enzymes. They are needed at very low concentration, but yet essentials (Madigan and Martinko, 2007; RIVIERE, 1975). Growth factors such as vitamins are also often added to culture media. These are organic compounds necessary in very small quantities but essential for growth like trace elements. These are vitamins, amino acids, purines, pyrimidines. Most of these molecules are synthesized by microorganisms. But some are said to be essential because they are not synthesized. In particular, B group vitamins as summarized in Table 21 are often supplemented in culture media. They enter into the composition of coenzymes. Vitamins are not necessarily essential for all microorganisms, first because each of them is involved in specific processes, but also because some microorganisms have the capacity to synthesise them. Some bacteria such as *Lactobacilli* require a supply of almost all the vitamins in their environment. Conversely, other microorganisms do not need any contribution of these growth factors. The most commonly essential vitamins are: thiamine (B1), biotin, pyridoxine (B6) and cobalamin (B12). Group of vitamins K and quinones are also involved in electron transport and synthesis of sphingolipids.

Macronutrients	**Cell components and functions**	**Assimilated forms**	**Residual concentration measurement during CSTR4 ($mol.L^{-1}$)**	**Concentration in the mineral medium ($mol.L^{-1}$)**
Carbon	50 % dry weight, cellular structure, energy metabolism	CO_2 (autotrophy), organic compounds (heterotrophy)	Solubility at 35 °C and P_{CO2} of 0.3 bar 7.53E-03	-
Nitrogen	12 % dry weight, nucleic acids, proteins	NH_3, NO_3^-, N_2, NH_4^+	NH_4^+ (1.67 – 5.56)E-03	1.87E-02
Phosphor	nucleic acids, phospholipids	Organic or inorganic phosphates	NA	$H_2PO_4^-$ 7.32E-04
Sulphur	Synthesis of amino-acids: Cys and Met vitamins: Thiamin (B1), biotin (B8), lipoic acid and Coenzyme A	SO_4^{2-} or HS^-	NA	S^{2-} 4.05E-04
Potassium	Enzymatic activity, including protein synthesis, nucleic acid, energy production (ATP)	K^+	5.12E-04 – 8.95E-02 depending of alkaline solution used for pH regulation	1.47E-03
Magnesium	Stabilizes ribosomes, cell membranes, nucleic acids, and also a cofactor for many enzymes	Mg^{2+}	NA	4.92E-04
Calcium	Stabilizes cell walls, and role in endospore heat resistance, growth regulation, microbial aggregates formation	Ca^{2+}	NA	3.40E-04
Sodium	Essential to particular environment organisms like sea water for their growth. Growth regulation and respiration/membrane exchange mechanisms.	Na^+	2.17E-03 – 1.52E-01 depending on alkaline solution used for pH regulation	1.67E-03

Table 19 : macronutrients and their roles for the cell and its growth (adapted from Madigan and Martinko, 2007).

Micronutrients	Cell components and functions	Concentration in the mineral medium (mol.L^{-1})
Iron (Fe)	Respiration: cytochrome; iron/sulphur electron transfer proteins; catalase; peroxidases; oxygenases; nitrogenases Anoxia: reduced form Fe^{2+} (ferrous) soluble Needed in larger amounts than other micronutrients. **In WLP: FMD/FWD, Fd, Ni-Fe and Fe hydrigenases, HDR**	Fe^{2+} 1.01E-05
Bore (B)	Auto-inducer (quorum sensing) of bacteria; polyketide antibiotics	H_3BO_3 1.62E-06 (pKa $B(OH)_3/B(OH)_4^-$ = 9.3)
Chrome (Cr)	Not required for microorganisms	-
Cobalt (Co)	Vitamin B12; transcarboxylase (propionic bacteria)	Co^{2+} 2.52E-06
Copper (Cu)	Respirations, cytochrome c oxidase; plastocyanin photosynthesis; superoxide dismutase	Cu^{2+} 4.69E-07
Manganese (Mn)	Enzyme activator, superoxide dismutase, and photosystem II (enzyme that dissociates water in phototrophs)	Mn^{2+} 1.01E-06
Molybdenum (Mo)	**Flavin enzymes**, nitrogenases, nitrate reductase, sulfite oxidase, DMSO-TMAO reductases, **formate dehydrogenases**, tRNA synthesis	$H_{24}Mo_7N_6O_{24}$ 6.01E-07
Nickel (Ni)	**In WLP: Hydrogenases, coenzyme F430 of methanogens, carbon monoxide dehydrogenase, CODH/Acs, methyl-H_4MPT** urease	Ni^{2+} 8.41E-07
Selenium (Se)	**Formate dehydrogenase, hydrogenases**, amino acid selenocysteine	-
Tungsten (W)	**Formate dehydrogenases**, oxotransferases of hyperthermophiles	-
Vanadium (V)	Vanadium nitrogenase, bromoperoxidase	-
Zinc (Zn)	**Carbonic anhydrase, alcohol dehydrogenase**, RNA and DNA polymerases, DNA binding proteins	Zn^{2+} 7.34E-07

Table 20: Micronutrients (or trace elements) required by microorganisms. Bold font highlights the specific needs of HAC, HM, and WLP expressers (adapted from Madigan and Martinko, 2007).

Vitamins	Coenzymes	Enzymatic reactions
Nicotinic acid	Pyridine nucleotides (precursor of NAD and NADP)	Dehydrogenation
Riboflavin (B2)	**Flavin nucleotides; FMN; FAD; flavoproteins involved in electrons transport**	**Dehydrogenations and electrons transport**
Thiamin (B1)	Carboxylase; transketolases	Alpha-decarboxylation
Pyridoxin (B6)	Pyridoxal phosphate	Amino acids metabolism (transamination, deamination, decarboxylation); Amino acid conversion to keto-acids
pantothenic acid	**Coenzyme A**	**Oxidation of ketonic acids, fatty acid metabolism; acetyl activation and other acyl derivatives**
P-aminobenzoic acid	Precursor of folic acid	
Folic acid	**Tetrahydrofolic acid**	**1C metabolism; methyl transfers**
Biotin	Enzyme with biotin type prosthetic group	CO_2 fixation and transfer of carbonyl groups; biosynthesis of fatty acids (Mostly in aerobic conditions)
Cobalamin (B12)	**Cobalamine coenzyme (ex: CoM of methanogenesis)**	**Molecular rearrangements; Reduction and transfer of 1C groups; deoxyribose synthesis**
Lipoic acid		Acyl transfer during decarboxylation of pyruvate and alpha-ketoglutarate

Table 21: B group vitamins (growth factors) and diverse enzyme activities involving them (Madigan and Martinko, 2007; RIVIERE, 1975). Bold font highlights potential essential vitamins for HM and HAC.

From this regard, the nutrients limitations have been investigated. First, a verification of the non-limitation of the ions analysed in the lab along the different assays was carried out. Ionic chromatography analysis confirmed that the system was not limited by ammonium, sodium, and potassium (Table 19). Additionally, a free reduced iron measurement was carried out on day 42 of the assay at pH 5 and D of 0.2 d^{-1}, when acetate concentration was limited. The measurement confirmed that 1.5 $mg.L^{-1}$ of Fe^{2+} was available in the medium, excluding iron limitation, or precipitation, as the media used in the fields generally contains around 0.6 – 1.1 $mg.L^{-1}$ of Fe^{2+} (Grimalt-Alemany et al., 2018; Groher and Weuster-Botz, 2016; Gao et al., 2013).

Nutrient limitation of components that were not analysed such as sulphur, other trace elements and vitamins were then investigated. First, additional phosphate, Na_2S and Trace elements solutions injections in the reactor were done daily from 40 to 60 days. Then, nine vitamins were added to the composition of the mineral medium from 68 d to the end. Finally, aluminium, selenium and tungsten were also added to the mineral medium from 101 d to the end.

Figure 40 shows that the pulses of phosphate, sulphide and trace elements didn't help to recover the acetate concentration predicted with the F_T limited model. This indicated that the elements already present in the mineral medium were not limiting. However, a significant enrichment of the MMC with *Desulfitobacterium sp.* was observed (Figure 41). Some species of the latter use hydrogen as electron donor with lower thresholds than HM and HAC. They also use sulphate as electron acceptor and are often found in syntrophic association with sulphate reducing bacteria (Spring and Rosenzweig, 2006; Villemur et al., 2006). Here, it is more likely that the sulphides, supplied in excess during this period, chemically oxidised to sulphates with oxygen traces that could enter the continuous system. These sulphates can therefore participate to maintaining *Desulfitobacterium sp.* in the reactor.

Then, a significant increase of acetate and biomass concentrations was observed after vitamins

addition to the mineral medium (Figure 40). The MMC composition switched from 72.5 % of *Desulfitobacterium sp.* to up to 60 % of *Clostridium autoethanogenum* within 6 days (Figure 41). *C. autoethanogenum* is a known species for the conversion of CO to ethanol, and it is used at industrial scale in pure culture. However, it is also capable of growth on H_2/CO_2 (Liew et al., 2016; Simpson et al., 2007).

	This study	**Heffernan et al., 2020**
Catalyst	Enriched MMC with an average of 67.8 % of *C. autoethanogenum* between 82 – 112 d	Pure culture *C. autoethanogenum* DSM 10061 strain—DSM 19630
Substrate	H_2/CO_2 (67:33)	H_2/CO_2/Ar (67:23:10)
Type of process	2 L chemostat	0.75 L chemostat
pH	5	5
Temperature (°C)	35 °C	37 °C
D (d^{-1})	0.21 ± 0.04	0.5
Acetate specific productivity (mmolC.gVSS.d^{-1})	176 considering 100 % of the VSS 260 considering 67.8 % of the VSS	226

Table 22: Comparison of the results obtained in this study with a published result in pure culture of C. autoethanogenum grow under mesophilic conditions and H_2/CO_2.

Table 22 shows the results obtained during CSTR4 after vitamins addition, and a result of the literature in similar conditions but with a pure culture of *C. autoethanogenum* and D of 0.5 d^{-1}. Acetate specific productivity when considering only *C. autoethanogenum* portion within the VSS, was of the same order of magnitude than previous results obtained in pure culture. Vitamins addition hence allowed to reach a common performance in these conditions. Further investigations will be useful to identify if all the nine vitamins added are essential, or if only some target ones are crucial. Culture media optimization for these applications will be of interest to implement such processes at larger scales, and ensure sustainability of the production.

After 80 d, the acetate concentration oscillated from values below the thermodynamic threshold

of 8 $gCOD.L^{-1}$, to values up to 14 $gCOD.L^{-1}$. This behaviour could be explained by perturbations in the dilution rate during this period. Also, it could be a toxicity effect of high acetate concentrations, and the need of few days next to recover the activity, leading to oscillations and not stabilization of the acetate concentration. The addition of Al, Se and W from 101 d didn't allow to reduce this effect.

2.1.4 Discussion about the composition of the inoculum for the different CSTR implemented

Samples for microbial analysis were taken from the inoculum stored at 4 °C which was used for the inoculation of CSTR2 and CSTR4. Then, the reactors were also sampled after the acclimation period with closed liquid (t0). Here, the purpose is to verify that the composition of the inoculum used was similar for each test performed, and then to evaluate the effect of the acclimation periods, during which only pH was different from an assay to another.

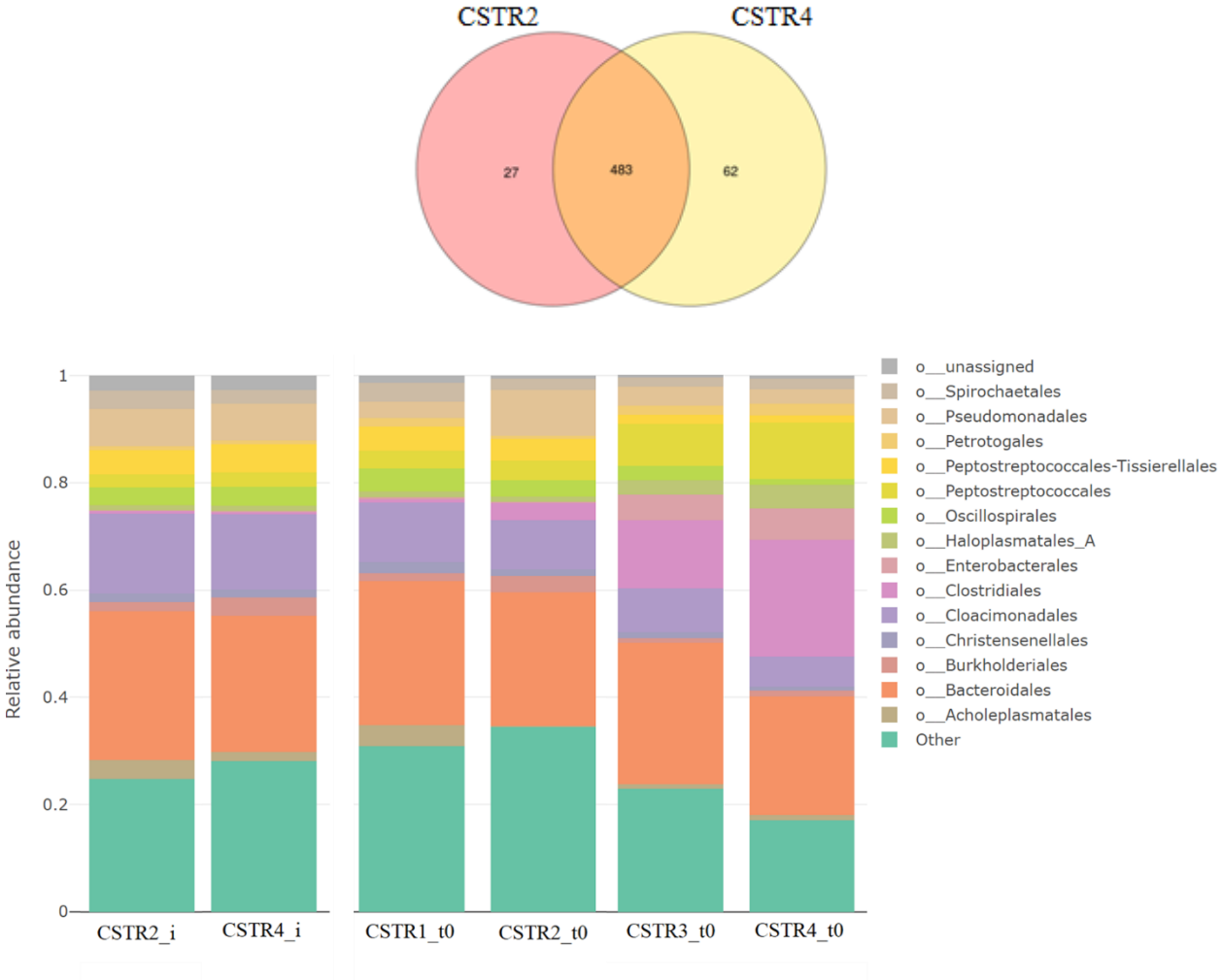

Figure 42: Venn diagram of the inoculum composition of CSTR2 and CSTR4. Relative abundance at the order level in the MMC in the inocula of CSTR2 and CSTR4, and t0 after acclimation periods of MMC in CSTR1 to CSTR4.

Figure 42 shows that during the campaign period, the inoculum stored at 4 °C had a stable and similar composition between the second and the last assays, with a majority of the orders

Bacteroidales and *Cloacimonadales*. The microbial composition was quite similar after the acclimation periods of CSTR1 and CSTR2 at neutral pH. However, at pH 5 (CSTR3 and CSTR4), the composition slightly changed with the increasing abundance of the order *Clostridiales*, and in a lesser extent the orders *Enterobacterales* and *Peptostreptococcales*. These results significate that during the acclimation period in closed liquid mode, only the pH affected the microbial composition of the consortium, but the contact with the substrate H_2/CO_2 as well as the temperature didn't have a visible effect. However, as the reactor was closed on the liquid, these results doesn't indicate if the microbial communities detected were active or not, and it is likely that the contact with H_2/CO_2 only activated the adapted microorganisms. Hence, when opening the liquid phase, the non-activated communities were washed out. Additionally, as the digested sludges mixed to constitute the inoculum were collected from mesophilic AD plants, the storage at 4°C allowed to conserve the microbial composition, and once injected in the reactor at 35 °C, the composition didn't change.

Although the composition of the consortium should be less determinant than the process parameters in the orientation of the activity and the selection, here it is demonstrated that the results of the consortium engineering strategies used in CSTRs can only be due to the process parameters tested: pH and dilution rate.

2.2 CSTR at 25 °C

Finally, as at 35 °C it was possible to maintain HAC and eliminate HM in certain conditions of pH and dilution rate, a last CSTR assay was carried out at 25 °C to investigate the effect of temperature in continuous mode, but also the dilution rate and the pH in dynamic, by changing the parameter during the same assay. The objective is to confirm previous observations, calculate mass balances and process performances, and compare the results obtained with the batch assays presented in chapter 2, and the other CSTRs at 35 °C.

This test was carried out in a different system with lower gas inflows, and changing the parameters during the assay to evaluate the dynamic responses of the system. The parameters that changed were the dilution rate from 0.33 to 0.5 d^{-1} at 30 d, the gas inflow rate doubled at 39 d and the pH from 6 to 5.5 at 48 d. The culture medium was supplemented with vitamins, and sulphide was replaced by sulphate. The latter choice was motivated by two reasons: first it implies that the ORP can be higher, and it is possible that HAC have better tolerance to higher ORP than HM (Grimalt-Alemany et al., 2021). Additionally, sulphide is essential for HM, not supplying it in the mineral medium could be a way to weaken them, provided that sulphate is not chemically or biologically reduced to sulphide, inducing a syntrophic interaction between SRB and HM.

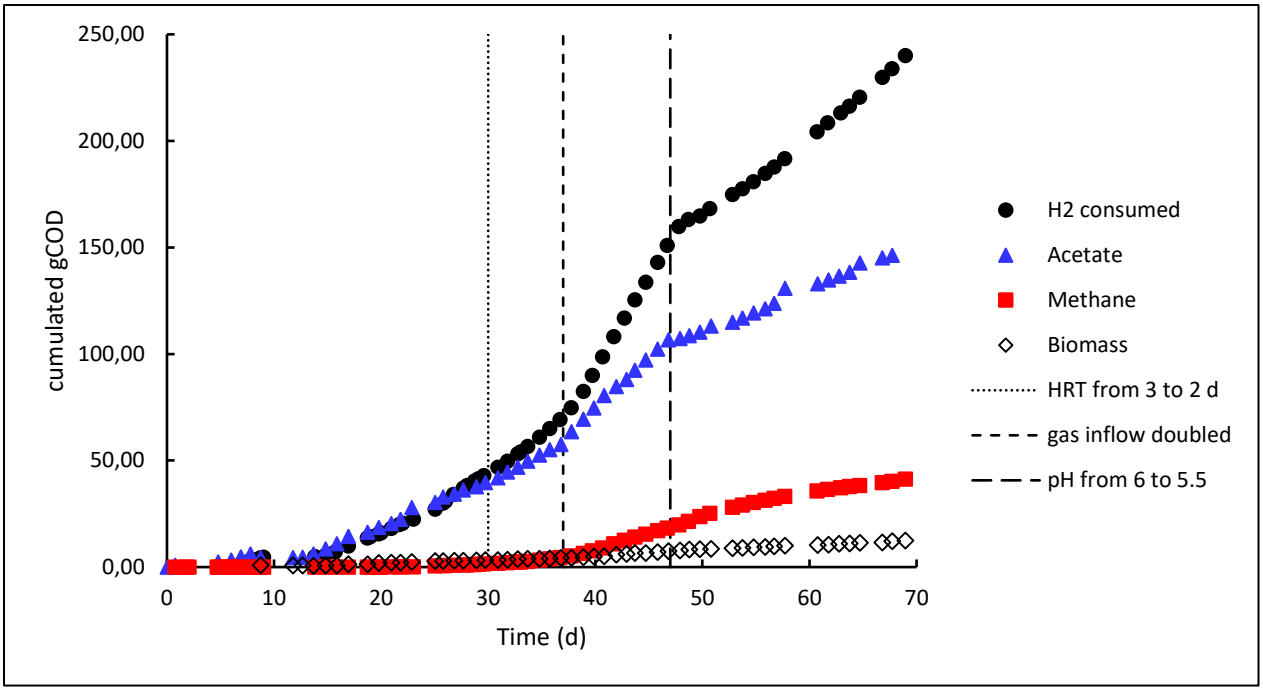

Figure 43: Cumulated acetate, methane and biomass produced, and H_2 consumed, in gCOD, along the CSTR assay at 25 °C. Vertical lines represent parameters changes during the process.

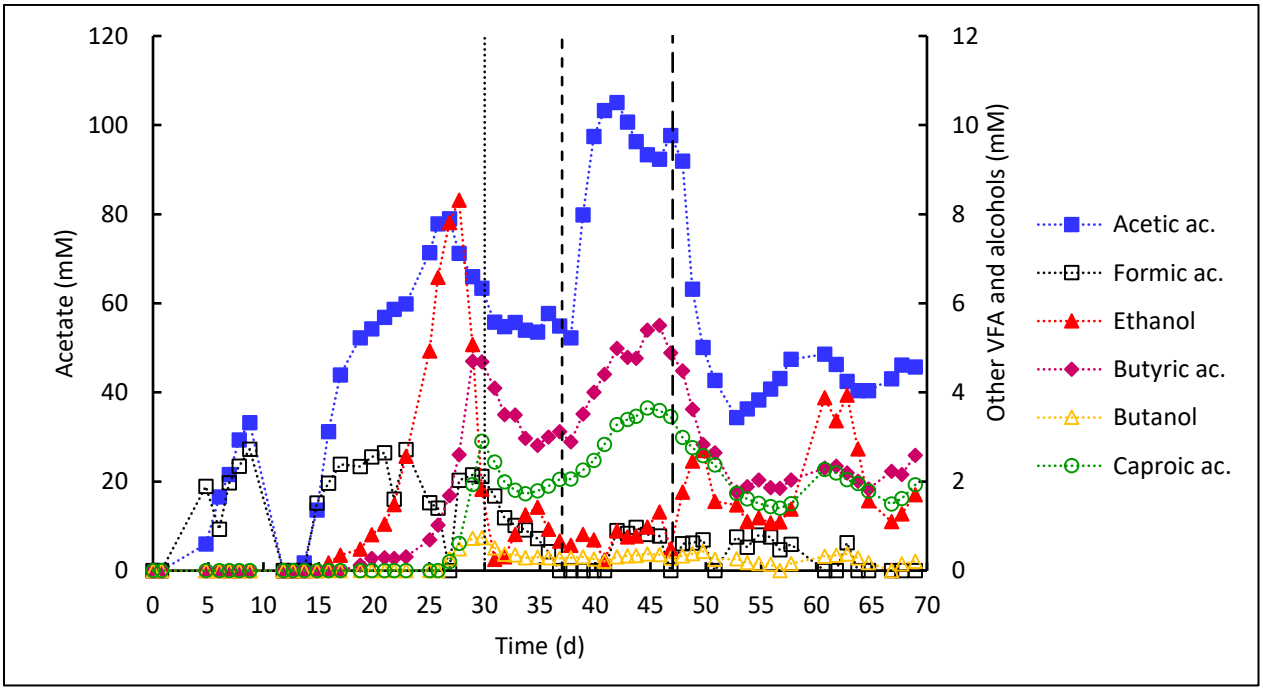

Figure 44: VFAs and alcohols concentrations during the CSTR assay at 25 °C. Acetic acid was the majority product (left axis), while the other products were found at lower concentrations (right axis).

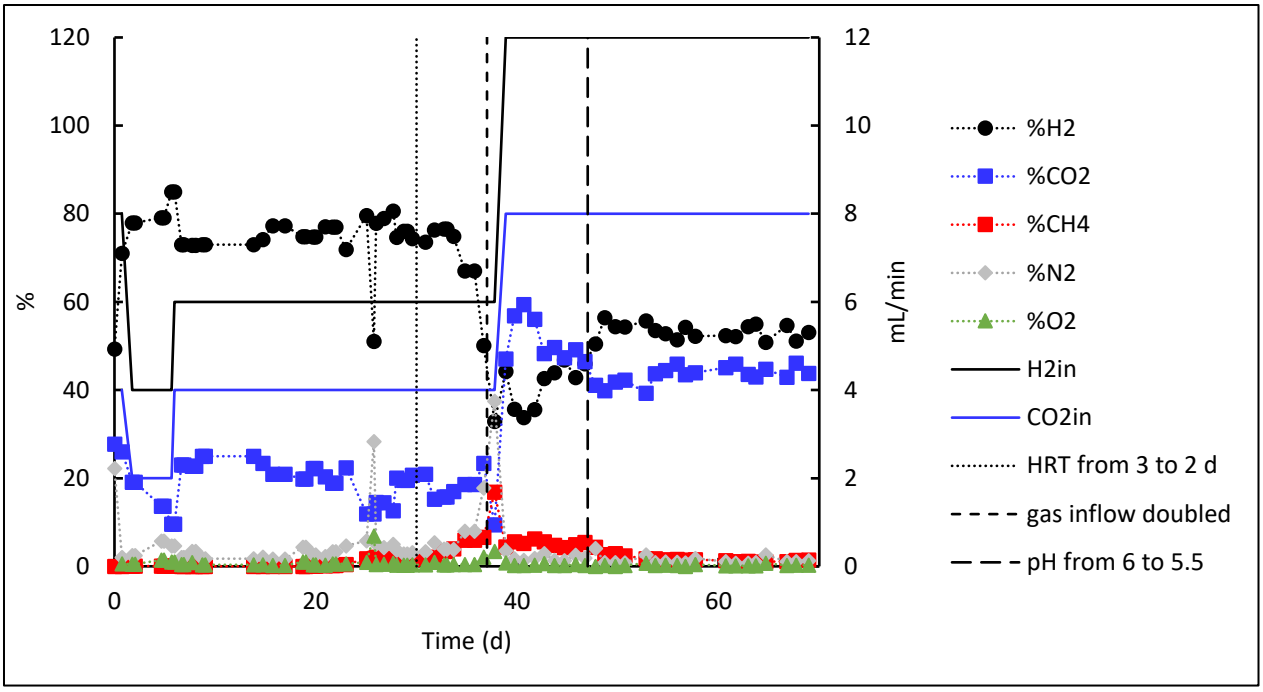

Figure 45: Gas composition (left axis) and H_2/CO_2 inflow rates (right axis) during the CSTR assay at 25 °C.

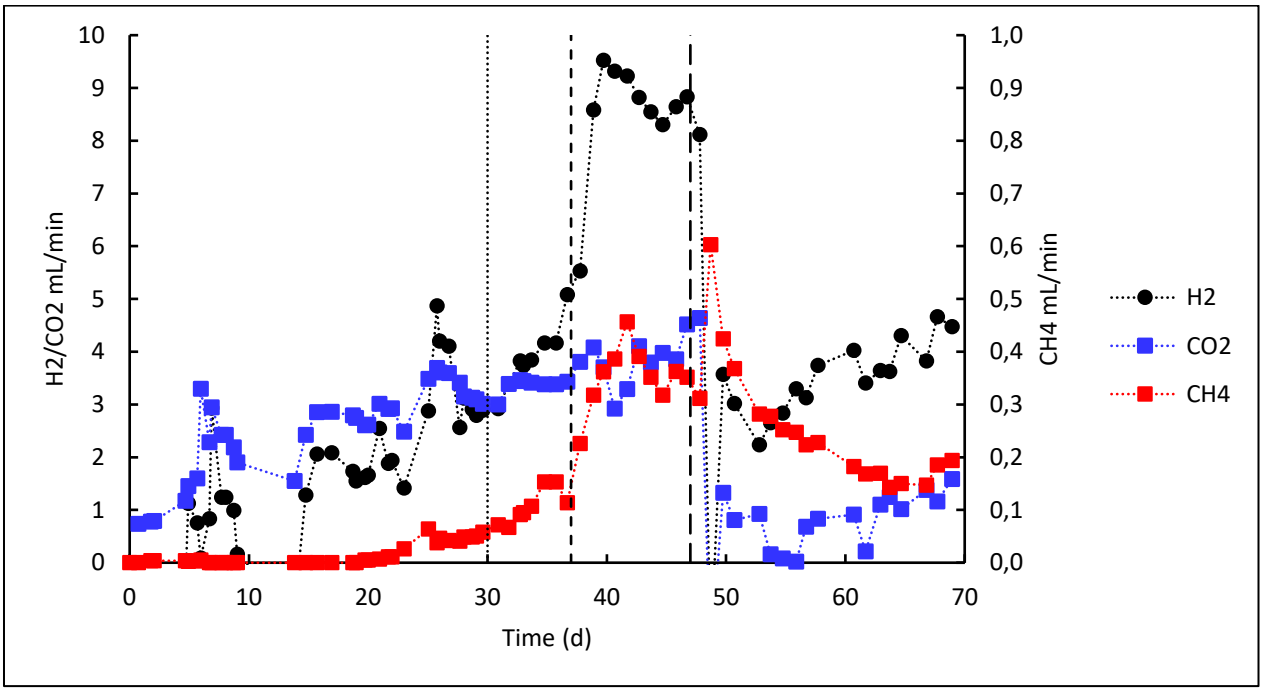

Figure 46: H_2 and CO_2 consumption rates (left axis), and methane production rate (right axis).

2.2.1 Results and discussion

Acetate was the majority product all along the CSTR experiment at 25 °C, accounting for 60 % of the total COD balance after 70 d. However, methane started to be produced after 20 d, and accounted for 17 % of the total COD balance. 12.5 gCOD of biomass were produced, corresponding to a growth yield of 5.2 % ($gCOD_X.gCOD_{H2}^{-1}$). Finally, side products accounted for around 10 % of the COD balance. Within these side products, an accumulation of ethanol was observed between 15 and 28 d (Figure 44). After 28 d, the ethanol concentration decreased brutally, simultaneously to the accumulation of butyrate and caproate. This behaviour indicates that biological chain elongation occurred in the reactor, consuming ethanol, and equivalent quantity of acetate to produce butyrate; and then ethanol with equivalent quantity of butyrate to produce caproate through reverse β-oxidation cycles (Agler et al., 2012).

At 30 d, the dilution rate was increased from 0.50 to 0.75 d^{-1}. This did not have an effect of acetate productivity that was maintained at 3.7 $gCOD.d^{-1}$ from 14 to 37 d, and methane production continued to increase slightly, indicating that a dilution rate of 0.75 d^{-1} in these conditions was not enough to get rid of methanogens. Concentrations of butyrate and caproate were stabilized to 3 and 2 mM respectively, indicating that chain elongating bacteria were limited during this period, either by the ethanol production, or the dilution rate, as the more elongated product, the longer time is needed for the reaction to be achieved.

At 38 d, the gas outflow was very low, indicating that the system was limited by the gas supply. H_2 and CO_2 concentrations in the gas phase decreased, while CH_4 concentration increased (Figure 45). To avoid substrate limitation, gas supply was doubled to overcome the mass transfer limitation and promote acetate production. Figure 44 and Figure 43 show that acetate production increased to 4.9 $gCOD.d^{-1}$ by this time, so did methane production (Figure 46) and chain elongation.

Finally, pH was decreased from 6 to 5.5 at 47 d, leading to a decrease of acetate production to

1.9 $gCOD.d^{-1}$, and butyrate and caproate concentrations decreased to 2 mM. Methane production also decreased, but still remained at 0.2 $mL.min^{-1}$.

The increase of D didn't have an effect on acetate and methane productivities, until 0.75 d^{-1}. This value is higher than the D_{crit} zones identified around 0.3 d^{-1} at 35 °C. This could be due to a temperature effect, but also to the mineral medium that was more complete for this assay. However, the increase of D contributed to stabilise chain elongation at low rates of butyrate and caproate production. When the gas inflow was doubled, H_2 consumption rate increased twice, indicating that the system was not mass transfer limited, but limited by the gas inflow. pH decrease from 6 to 5.5 had a significant effect on acetate and methane productivities. However, Figure 46 show that methane production decreases while H_2 and CO_2 increases until the end of the assay. Hence, HM seem to have suffered more from the decrease of pH than HAC that could still produce acetate, but at a lower rate. During this phase, HAC growth must have been limited by thermodynamics which explains lower productivity then before the pH change.

Figure 47 shows the composition of the MMC along the assay at 25 °C. *Clostridium sensu stricto 12*, a group containing HAC, was successfully selected in the CSTR at 25 °C. It is possible that HAC as well as chain elongating bacteria species were selected in this groups, however, the sequencing didn't allow this level of precision. However, the relative abundance of *Clostridium sensu stricto 12* decreased between 41 d, 62 d, and 68 d (83, 70 and 63 % respectively), which is attributed to the pH change from 6 to 5.5. *Methanobrevibacter* was the HM genus selected, and remained in the MMC until the end of the experiment, but at low relative abundance (2, 8 and 11 % at 41, 62 and 68 d respectively), which is consistent with the CH_4 yield of 17 % during the experiment (Figure 43). *Ruminoclostridium 9* and *Oscillibacter* were also detected in significant proportion. These are commonly found in chain elongation

systems at pH 5, either from acetate and ethanol, or from syngas directly (Joshi et al., 2021). *Oscillibacter* is generally associated to known chain elongators such as *C. kluyveri*, and its role in the system remains ununderstood. Their relative abundance increased after the pH change. But this is most likely due to a wash out of HM and HAC than to an increase of chain elongation, as the concentrations of elongated products decreased after the pH changed (Figure 44).

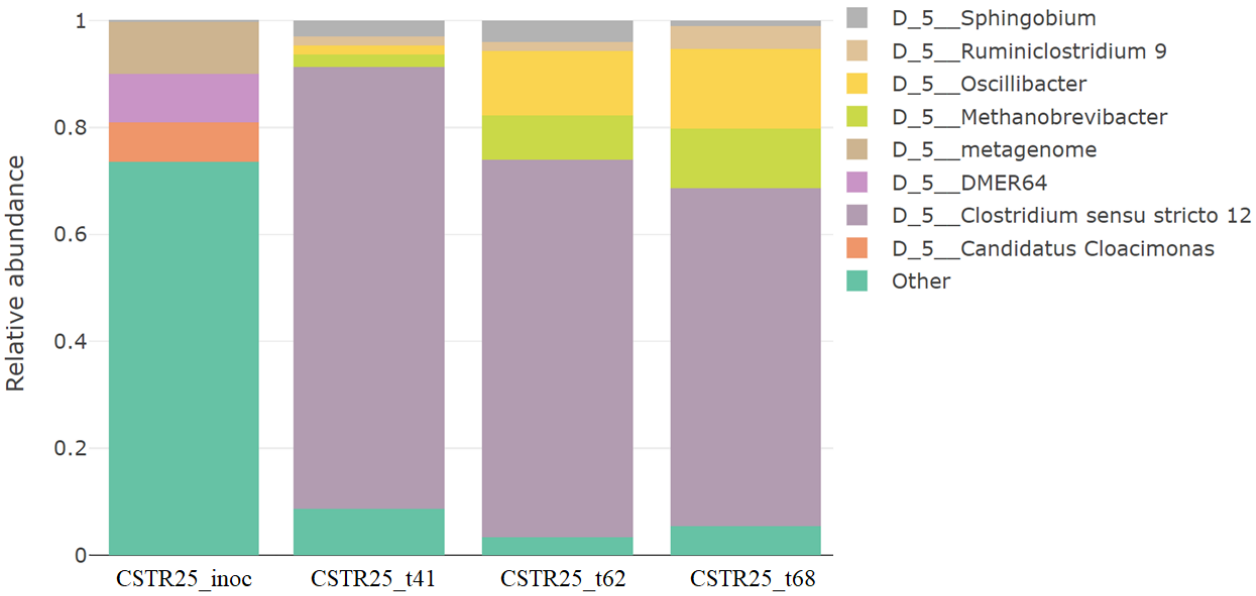

Figure 47: Relative abundance at the genus level during the CSTR test at 25 °C, at t0 and after 41, 62 and 68 d.

3 Conclusion

In this last chapter, a continuous reactor was developed specifically for the study of the microbial competition between HM and HAC. The results obtained during CSTR1 were satisfying, and allowed to validate the system for the study. Then, the effects of pH between 5 and 7 and D between 0.2 and 1 d^{-1} were studied with four CSTRs at 35 °C. The parameters were kept constant for each CSTR, with the exception of D variations because of pH regulation.

Methane production was observed at pH 7 and 5. However at pH 5, and equivalent D of 0.2 d^{-1}, HM were not maintained after 25 d. At pH 5, the productivities of both HM and HAC were lower than at pH 7, by 15 times for HAC. The simulations of the CSTRs demonstrated that this was mainly due to thermodynamic limitation, as the integration of F_T was satisfying to describe the experimental acetate production profile. Therefore, the increase of pH allows to reach higher concentrations, and this has been previously observed in continuous hollow fibre membrane reactor for the production of acetate from H_2/CO_2 (Wang et al., 2017). The authors observed that the decrease of acetate concentration when increasing D, increased their acetate productivities. However, this has to be relativized considering the downstream processes and applications, as it may require a minimal concentration. The effect of pH was also observed on the microbial selection. At neutral pH, the genus *Acetobacterium* was mainly enriched, and this was also the case in the SBs at pH 6 in chapter 2. At pH 5 though, Clostridium sp. were preferentially enriched, with *Clostridium sensu stricto 12* being found in all the assays at 35 °C and pH 5, and in the one at 25 °C and pH 6. After the addition of vitamins in CSTR4, the MMC was enriched of up to 75 % of *C. autoethanogenum*, and acetate maximal concentration was recovered. These results of microbial diversity demonstrate the functional redundancy that MMCs contain depending on the environmental conditions applied.

The effect of D was also studied regarding the microbial competition between HM and HAC. HM had lower specific growth rates than HAC in this study, probably due to the range of

temperature chosen between 25 and 35 °C. Therefore, a D_{crit} zone for HM wash out was determined around 0.3 d^{-1} at neutral pH, and around 0.2 at pH 5. The D_{crit} of HAC though was not reached in this study, indicating that it was higher than 1 d^{-1}. However, thermodynamic limitation of HAC as mentioned before, and nutrient deficiency were identified during this campaign of continuous reactors. Indeed, the mineral medium used was the one of biological methanation described in chapter 1. In CSTR2 at neutral pH and D of 0.4 d^{-1}, acetate production stopped immediately after 6 d, and methane concentration in the gas phase slightly increased until 14 d. This confirmed that HM had fewer nutrient requirements than HAC, and they could have regained the advantage again if the assay lasted longer.

General discussion about the microbial competition between homoacetogens and hydrogenotrophic methanogens

General context

This thesis work focused on the production of acetate from gaseous H_2/CO_2 by engineering anaerobic MMCs. It contributed to the study and the development of interesting catalysts. Ideal catalysts should be easy to produce all around the world, and also inexpensive and nontoxic. From this regard, anaerobic MMC are interesting catalysts because they are found in numerous natural environments. Also, as microorganisms multiply, they are considered autocatalysts and can be maintained to supply catalysts when needed. Due to their microbial diversity, MMCs have high adaptability potential in terms of operational conditions, but also substrates products. Consortium engineering aims at orienting the metabolic function of a MMC. This metabolic function can involve different types of microorganisms that will cooperate for example to degrade complex organic materials (Anaerobic digestion) in a single stage process. On the other hand, MMC engineering also consists to specialize a MMC for a more constraint reaction involving one type of population. However, the advantage compared to pure cultures, is that there could be different populations selected, all capable of the target function, but in different conditions. This is called functional redundancy and contributes to make MMC adaptable and robust catalysts.

Thesis objectives and methodology

In this thesis, the possibility to produce acetate from H_2/CO_2 with MMC was investigated. The main challenge is the competition between the microorganisms of interest, HAC, and HM. Chemical inhibitors or heat treatments can be used, but here it was proposed to evaluate the possibility of eliminating them by engineering of the consortium. Hence, this thesis project aimed

at evaluate in what extent acetate could be produced naturally, by controlling the process parameters. To do so, the mechanisms ruling the system have to be thoroughly understood. In particular, microbial kinetics, thermodynamics of the reactions, and physical-chemical processes such as acid-base equilibria and pH, and gas to liquid mass transfer. However, there is a great variability, and uncertainty about microbial kinetics, making difficult to predict the outcome of the competition in specific culture conditions. From this regard, this work had for objective to highlight key points of attention in the control of the microbial competition between HAC and HM, to specifically promote HAC. The work focused on process parameters as levers to orient the MMC toward acetate production. Among these parameters, temperature, gas to liquid mass transfer rate and pH were investigated. The effect of the cultivation mode on microbial interactions was also addressed, in SBs or CSTRs. The knowledge of biological methanation helped to understand HM features, and VFA accumulation in a thermophilic methanation reactor was studied to formulate first hypothesis. A model was developed and used with a microbial kinetic parameters review. Lowering the temperature in a range of 20-35 °C of the reactors, and maintain high gas partial pressures appeared as determinant for acetate production. Considering the variability of these parameters, physical-chemical and thermodynamic aspects were integrated in the model, in order to bring more accuracy in the system description. This first work allowed to identify the substrate limitation as the main factor governing the competition between HM and HAC.

Overcoming substrate limitation is key for HAC selection

HM have better H_2 fixation features, so the competition must be mange to circumvent this particularity and avoid substrate limitation. The simulations showed that batch mode was suitable for HM selection due to substrate depletion along the experiment. However, if mass transfer limitation was overcome, both HM and HAC grow. The strategy to promote HAC is then to

choose environmental conditions where they can outcompete HM base on their specific growth rate. Then, the possibility of implementing SBs, by transferring at specific times before mass transfer limitation is reached, contributes to the selection of HAC. Going through continuous gas supply is even more interesting, and can be used for the microbial selection. However, the consumption rates must be kept below mass transfer rate, so the use of high transfer capacity system is recommended to allow higher biomass concentrations and increase productivities. Additionally, provided that HAC have higher specific growth rates in certain condition, in particular low temperatures, it is possible to eliminate HM by opening the liquid phase as well and properly choose the dilution rate.

Lowering temperature in a range of 25 – 35 °C contributes to promote HAC

One lever to operate in conditions where HAC have better specific growth rates is temperature. Biological methanation was operated at 55 °C, and low VFA productivities were observed in the reactor. According to these data, and to kinetic parameters from literature, working under thermophilic temperature will lead to the selection of highly performant HM. However, operating below 40 °C will rebalance the competition with HAC. In this work, the HAC selection could be achieved in SBs at 25 °C, transferring as soon as substrate started to be consumed. This way, HM could be eliminated from the MMC, and HAC were enriched. However, at 35 °C HM were selected in SBs and HAC were progressively eliminated by the end of the experiments.

HAC can handle lower retention times than HM in this range of temperatures

Conversely to what was expected with simulations with the model, which represented conventional theory based on r- or K- strategists, the cohabitation of HM and HAC was lost along the SBs. This indicates that the transfer time might have had an effect and allow the elimination of one or another community depending the conditions, and could have a more significant effect

on the competition than temperature between 25 and 35 °C. This also means that it is possible to reproduce these conditions in a continuous process, applying a specific retention time of the microorganisms. The average time of the batches for the selection of HAC and the elimination of HM was 5.3 ± 1 d. Hence, continuous reactors with high mass transfer capacities, compared to SBs vials, have been investigated, by maintaining high gas partial pressures to overcome thermodynamic limitation, under 25 – 35 °C, and a dilution rate between HM and HAC specific growth rates.

The results obtained in continuous reactors were promising. Indeed, HAC could be selected in all the reactors, at 25 °C, but also at 35 °C, at dilution rates ranging from 0.2 to 1 d^{-1} (HRT between 1 and 5 days). The results showed that the D_{crit} of HM must be around 0.3 d^{-1} at neutral pH, and 0.2 d^{-1} at pH 5, corresponding to HRT of 3 and 5 d respectively. This demonstrates that overcoming substrate limitation by supplying gas in semi-continuous, or continuous mode, was more impacting the microbial competition than temperature in this range, as HAC were selected both at 25 °C and 35 °C in CSTRs, which was not the case in the SBs presented in this study. However, in other types of reactors, with higher mass transfer capacities, the enrichment strategy in SBs remains a relevant reactor design for the selection of HAC in MMCs.

HAC recover faster than HM after exposure to O_2

The hydraulic retention time (HRT) of the first CSTR at 35 °C was 5, this allows to confront results from the SBs in a continuous reactor. This first assay (CSTR1) at neutral pH led to a stable cohabitation of HM and HAC, indicating that this HRT was too high to eliminate one or the other community. A part of this controversial result with what was projected from the SBs can be attributed to a pH effect, as SBs were carried out at pH 6 while CSTR1 was regulated at pH 7. But above all, these results support the hypothesis of the longer lag phase of HM than that of HAC during SBs. This contributed to their progressive loss at a batch time of 5.3 ± 1 d. What could

explain this longer lag phase is a sensitivity to oxygen during the transfers from a batch to another. However, going through a continuous process, HM were never in contact with oxygen after inoculation, at the exception of traces amounts that could enter the system. Furthermore, as sulphide was used as reducing agent, HM were likely protected from oxygen toxicity in the CSTRs. Hence, the minimal HRT required by HM was lower. In other terms, the maximal dilution rate (D_{crit}) of HM was higher.

pH decrease from 6 – 7 to 5 led to thermodynamic limitations and significant drop of acetate productivities

pH is a complex physico-chemical, and biological parameter. Indeed, it affects a lot of processes in the system such as thermodynamics of the reactions, cellular physiology, CO_2 solubility and so on. In this study, the effect of pH was observed on thermodynamics of the reaction. In particular at pH 5, productivities were up to 15 times lower than at neutral pH in the CSTRs at 35 °C. The stabilisation of the gas partial pressures in the CSTRs, by applying gas inflows above mass transfer capacities of the system, allowed to accurately represent the maximal acetate concentrations obtained in these assays by integrated F_T. However, this was not the case at pH 7, where thermodynamic limitation was way above the maximal concentrations of acetate obtained. This indicates that physiological limitations must be limiting the production at neutral pH. Hence, maximal acetate concentration reached was 0.74 molC.L^{-1}, at pH 6.5 and 35 °C.

In literature, twice this concentration, under H_2/CO_2 and with MMC treated with BES at 55 °C, could be obtained (Wang et al., 2017) (Table 5). These results were obtained in a hollow fibre membrane reactor (HFMBR). Indeed, in this type of reactor, biomass is fixed to the membranes through which the gas is supplied. This biofilm formation can explain that the physiological toxicity concentration is higher, as a gradient of acetate concentration can be established through the biofilm. Additionally, increasing D leads to acetate dilution in the liquid, while biomass

retention time is decoupled due to the biofilm formation, contributing to increasing productivities to up to 0.356 molC.L^{-1}.d^{-1} with a D of 1 d^{-1}.

Dynamic change of parameters such as pH in continuous processes contributes to the wash out of HM in the MMC

During the last CSTR assay at 25 °C, and pH 6, the cohabitation of HM and HAC was observed again, and so even until D of 0.75 d^{-1}. However, pH was decreased from 6 to 5.5 during the operations and had a significant negative effect on methane production. Yet, methane production was observed at pH 5 in the CSTRs at 35 °C. However, in these CSTRs, the parameters were never changed in a same experiment, implicating that the stabilization of the process was done in the conditions of the selection. Consistently with the functional redundancy of MMCs, HM and HAC could be selected this way. However, changing the environmental conditions during a continuous process, especially after the microbial selection, can affect the microbial communities, depending on their sensitivity to parameters changes. As the functional redundancy have been lost during the selection phase, this have contributed to decrease methanogenic activity in the reactor by using this strategy. This can be done with pH in this case, but it could also be envisaged with other parameters, or nutrients. This way, continuous reactors tend toward production processes for MMCs biotechnology, as they allow the microbial selection, and a continuous production in the same reactor. This work contributed to give some key findings for the implementation of acetate production from H_2/CO_2 with MMCs.

Reactor development for acetate production

The maintain stable gas partial pressures in this study was ensured by applying high gas inflows in the opened gas phase. This configuration was chosen according to the objective of studying a microbial competition, but is not recommended to implement efficient production processes,

because high amounts of gas are wasted. Nevertheless, what could be interesting is to run the gas phase in fed-batch, that is to say closing the outlet. In order to keep stable gas partial pressures, the H_2 and CO_2 supply should be controlled by the pressure and the composition of the gas phase. The liquid phase should be kept opened, to regulate acetate concentrations and thermodynamic or physiological pH limitations, and also ensure a continuous production process. However, if methane is produced, it will accumulate in the gas phase. This can be avoided if the fed-batch is started after the microbial selection was established, or by flushing the gas regularly. Although it will decrease the conversion yield into acetate, the methane accumulation is not necessarily an issue. Indeed, it is possible that this contributes to limit methanogenic reaction, by thermodynamic constraints. Once this limitation is reached, methane production will stop and acetate production yield recover to its maximal value. This would be interesting to investigate in perspectives of this work. In order to increase even more the performances of the process, a two stages reactor could also be envisaged, with the first one serving to microbial selection, and the second one optimized for production, for example a HFMBR.

General conclusion and outlook

In this thesis project, the possibility of producing acetate from H_2/CO_2 by engineering MMCs was investigated. The research especially focused on the microbial competition between HAC and HM, which is the major hurdle for HAC production. Indeed, methane production benefits of thermodynamic advantages that must be circumvent to promote acetate production.

To do so, a systemic methodology was undertaken in this work. First, a model was constructed, according to classical theories of microbial growth, gas to liquid mass transfer, weak acid dissociation and pH, and thermodynamic factor F_T. The model was used as a tool for projecting on hypothesis, and simulating experimental results. This way, the model helped for the understanding of the different limitation states that can rule such anaerobic gas/liquid systems: thermodynamics, mass transfer and microbial kinetics. Experimental campaigns were conducted within this thesis project. The effect of environmental parameters, such as temperature, pH and HRT, was studied in different reactors: SBs and CSTRs. These two types of reactors developed have in common a semi-continuous, or continuous gas supply, and a dilution rate.

Both reactors were successful for the microbial selection of HAC, provided that substrate limitation was overcome. Therefore, this work provides a proof of concept of the possibility of promoting HAC by MMC engineering for acetate production from H_2/CO_2. This has been achieved in different systems and conditions.

Indeed, an enrichment technique at lab scale was developed in SBs. It consisted in operating at 25 °C, with short batch times of 5 d, transferring as soon as H_2 consumption was detected.

In continuous reactors, rather high acetate productivities (0.296 $molC.L^{-1}.d^{-1}$) and concentrations (0.74 $molC.L^{-1}$) were reached at 35 °C and pH 6.5, while methanogenic function was lost working at D above 0.2 and 0.3 d^{-1} at pH 5 and 7 respectively. However, in continuous reactor at 25 °C, HM could not be washed out until D of 0.75 d^{-1}, and chain elongation was observed. This

difference in D_{crit} according to temperature deserves further investigations, with thermodynamic and physiological analysis. Changing parameters such as pH after microbial selection phase helped to decrease methanogenic activity in the CSTR at 25 °C. Ethanol and chain elongated products such as butyrate and caproate were also detected during this assay. In future studies, promoting chain elongation could be investigated, in order to diversify the product portfolio of the system.

In terms of microbial competition, the wash out of HM led to SRB development in most cases. These microorganisms have to be considered in the competition as their H_2 consumption will affect the acetate production yields. A specific study of the kinetic parameters in appropriate reactors and dedicated experimental set up could be conducted, in order to refine the HAC growth knowledge. The model could be used in order to consider thermodynamics and mass transfer for parameter estimations. The system could also be studied at lower temperature (10 – 20 °C) in order to provide information on the communities and evaluate the potential of HAC in this range of temperature.

In terms of production process, this study provided some key findings for their implementation. It will be interesting in future works to optimize acetate production processes, either in batch mode in a reactor with high mass transfer capacities, or in a hybrid system running in continuous mode on the liquid phase, and in fed-batch on the gas phase. The retention time of acetate and biomass could also be decoupled by the use of fixed biomass reactor, as second stages after microbial selection.

Further investigations on nutrient requirements are also needed. Indeed, a vitamin dependence of *C. autoethanogenum* has been identified in this work, but doesn't seem to be required in the same quantities in the different assays, and so it might be different dependant on the HAC selected. Additionally, substitutes to chemical vitamins are needed to limit the costs of the operations. As the limitation occurred after several HRTs in the CSTRs, it indicates that the inoculum provided

all the requirements for growth, some addition of digestate supernatant could therefore be a solution. When activity was recovered after vitamin addition, acetate concentration didn’t stabilise in the reactor, but oscillated. This can be due to toxicity effects of acetate concentration increase and the reasons of this observation deserve to be further investigated and understood.

References

Agler, M.T., Spirito, C.M., Usack, J.G., Werner, J.J., Angenent, L.T., 2012. Chain elongation with reactor microbiomes: upgrading dilute ethanol to medium-chain carboxylates. Energy Environ. Sci. 5, 8189–8192. https://doi.org/10.1039/C2EE22101B

Agler, M.T., Wrenn, B.A., Zinder, S.H., Angenent, L.T., 2011. Waste to bioproduct conversion with undefined mixed cultures: the carboxylate platform. Trends in Biotechnology 29, 70–78. https://doi.org/10.1016/j.tibtech.2010.11.006

Agneessens, L.M., Ottosen, L.D.M., Andersen, M., Berg Olesen, C., Feilberg, A., Kofoed, M.V.W., 2018. Parameters affecting acetate concentrations during in-situ biological hydrogen methanation. Bioresource Technology 258, 33–40. https://doi.org/10.1016/j.biortech.2018.02.102

Agneessens, L.M., Ottosen, L.D.M., Voigt, N.V., Nielsen, J.L., de Jonge, N., Fischer, C.H., Kofoed, M.V.W., 2017. In-situ biogas upgrading with pulse H2 additions: The relevance of methanogen adaption and inorganic carbon level. Bioresource Technology 233, 256–263. https://doi.org/10.1016/j.biortech.2017.02.016

Alberty, R.A., 2005. Thermodynamics of Biochemical Reactions. John Wiley & Sons.

Amend, J.P., Shock, E.L., 2001. Energetics of overall metabolic reactions of thermophilic and hyperthermophilic Archaea and Bacteria. FEMS Microbiol Rev 25, 175–243. https://doi.org/10.1111/j.1574-6976.2001.tb00576.x

Archer, D.B., Powell, G.E., 1985. Dependence of the specific growth rate of methanogenic mutualistic cocultures on the methanogen. Arch. Microbiol. 141, 133–137. https://doi.org/10.1007/BF00423273

Badziong, W., Ditter, B., Thauer, R.K., 1979. Acetate and carbon dioxide assimilation by Desulfovibrio vulgaris (Marburg), growing on hydrogen and sulfate as sole energy source. Arch. Microbiol. 123, 301–305. https://doi.org/10.1007/BF00406665

Baleeiro, F.C.F., Kleinsteuber, S., Neumann, A., Sträuber, H., 2019. Syngas-aided anaerobic fermentation for medium-chain carboxylate and alcohol production: the case for microbial communities. Appl Microbiol Biotechnol. https://doi.org/10.1007/s00253-019-10086-9

Basile, A., Campanaro, S., Kovalovszki, A., Zampieri, G., Rossi, A., Angelidaki, I., Valle, G., Treu, L., 2020. Revealing metabolic mechanisms of interaction in the anaerobic digestion microbiome by flux balance analysis. Metabolic Engineering 62, 138–149. https://doi.org/10.1016/j.ymben.2020.08.013

Batstone, D.J., Keller, J., Angelidaki, I., Kalyuzhnyi, S.V., Pavlostathis, S.G., Rozzi, A., Sanders, W.T.M., Siegrist, H., Vavilin, V.A., 2002. The IWA Anaerobic Digestion Model No 1 (ADM1). Water Sci Technol 45, 65–73. https://doi.org/10.2166/wst.2002.0292

Bellini, R., Bassani, I., Vizzarro, A., Azim, A.A., Vasile, N.S., Pirri, C.F., Verga, F., Menin, B., 2022. Biological Aspects, Advancements and Techno-Economical Evaluation of Biological Methanation for the Recycling and Valorization of CO2. Energies 15, 4064. https://doi.org/10.3390/en15114064

Bengelsdorf, F.R., Beck, M.H., Erz, C., Hoffmeister, S., Karl, M.M., Riegler, P., Wirth, S., Poehlein, A., Weuster-Botz, D., Dürre, P., 2018. Chapter Four - Bacterial Anaerobic Synthesis Gas (Syngas) and CO2+H2 Fermentation, in: Sariaslani, S., Gadd, G.M. (Eds.), Advances in Applied Microbiology. Academic Press, pp. 143–221. https://doi.org/10.1016/bs.aambs.2018.01.002

Benjaminsson, G., Benjaminsson , Johan, Boogh Rudberg, Robert, 2013. Power to Gas – a Technical Review.

Berg, I.A., Kockelkorn, D., Ramos-Vera, W.H., Say, R.F., Zarzycki, J., Hügler, M., Alber, B.E., Fuchs, G., 2010. Autotrophic carbon fixation in archaea. Nature Reviews Microbiology 8, 447–460. https://doi.org/10.1038/nrmicro2365

Bertsch, J., Müller, V., 2015. CO Metabolism in the Acetogen Acetobacterium woodii. Appl. Environ. Microbiol. 81, 5949–5956. https://doi.org/10.1128/AEM.01772-15

Bioprocess Engineering Principles - 2nd Edition [WWW Document], n.d. URL https://www.elsevier.com/books/bioprocess-engineering-principles/doran/978-0-08-091770-2 (accessed 1.22.19).

Braga Nan, L., Trably, E., Santa-Catalina, G., Bernet, N., Delgenès, J.-P., Escudié, R., 2020. Biomethanation processes: new insights on the effect of a high H2 partial pressure on microbial communities. Biotechnology for Biofuels 13, 141. https://doi.org/10.1186/s13068-020-01776-y

Conrad, R., Bak, F., Seitz, H.J., Thebrath, B., Mayer, H.P., Schütz, H., 1989. Hydrogen turnover by psychrotrophic homoacetogenic and mesophilic methanogenic bacteria in anoxic paddy soil and lake sediment. FEMS Microbiology Ecology 5, 285–293. https://doi.org/10.1111/j.1574-6968.1989.tb03382.x

Cord-Ruwisch, R., Seitz, H.-J., Conrad, R., 1988. The capacity of hydrogenotrophic anaerobic bacteria to compete for traces of hydrogen depends on the redox potential of the terminal electron acceptor. Arch Microbiol 149, 350–357. https://doi.org/10.1007/BF00411655

Daniel, S.L., Hsu, T., Dean, S.I., Drake, H.L., 1990. Characterization of the H2- and CO-dependent chemolithotrophic potentials of the acetogens Clostridium thermoaceticum and Acetogenium kivui. Journal of Bacteriology. https://doi.org/10.1128/jb.172.8.4464-4471.1990

Desmond-Le Quéméner, E., Bouchez, T., 2014. A thermodynamic theory of microbial growth. ISME J 8, 1747–1751. https://doi.org/10.1038/ismej.2014.7

Diender, M., Stams, A.J.M., Sousa, D.Z., 2015. Pathways and Bioenergetics of Anaerobic Carbon Monoxide Fermentation. Frontiers in Microbiology 6. https://doi.org/10.3389/fmicb.2015.01275

Drake, H.L., Gößner, A.S., Daniel, S.L., 2008. Old Acetogens, New Light. Annals of the New York Academy of Sciences 1125, 100–128. https://doi.org/10.1196/annals.1419.016

Dumergues, L., 2016. Valorisation du CO2. Techniques de l'Ingénieur.

Egli, T., 2010. How to live at very low substrate concentration. Water Research, Microbial ecology of drinking water and waste water treatment processes 44, 4826–4837. https://doi.org/10.1016/j.watres.2010.07.023

Esteban, D.J., Hysa, B., Bartow-McKenney, C., 2015. Temporal and Spatial Distribution of the Microbial Community of Winogradsky Columns. PLOS ONE 10, e0134588. https://doi.org/10.1371/journal.pone.0134588

Fontecave, M., 2015. Que faire du CO2 ? De la chimie ! | Mediachimie. Presented at the Colloque Chimie et changement climatique.

Fu, B., Jin, X., Conrad, R., Liu, Hongbo, Liu, He, 2019. Competition Between Chemolithotrophic Acetogenesis and Hydrogenotrophic Methanogenesis for Exogenous H2/CO2 in Anaerobically Digested Sludge: Impact of Temperature. Front. Microbiol. 10. https://doi.org/10.3389/fmicb.2019.02418

Fuentes, L., Palomo-Briones, R., de Jesús Montoya-Rosales, J., Braga, L., Castelló, E., Vesga, A., Tapia-Venegas, E., Razo-Flores, E., Ecthebehere, C., 2021. Knowing the enemy: homoacetogens in hydrogen production reactors. Appl Microbiol Biotechnol 105, 8989–9002. https://doi.org/10.1007/s00253-021-11656-6

Ganigué, R., Ramió-Pujol, S., Sánchez, P., Bañeras, L., Colprim, J., 2015. Conversion of sewage sludge to commodity chemicals via syngas fermentation. Water Sci Technol 72, 415–420. https://doi.org/10.2166/wst.2015.222

Ganigué, R., Sánchez-Paredes, P., Bañeras, L., Colprim, J., 2016. Low Fermentation pH Is a Trigger to Alcohol Production, but a Killer to Chain Elongation. Front. Microbiol. 7. https://doi.org/10.3389/fmicb.2016.00702

Gao, D., Liu, L., Liang, H., Wu, W.-M., 2011. Aerobic granular sludge: characterization, mechanism of granulation and application to wastewater treatment. Critical Reviews in Biotechnology 31, 137–152. https://doi.org/10.3109/07388551.2010.497961

Gao, J., Atiyeh, H.K., Phillips, J.R., Wilkins, M.R., Huhnke, R.L., 2013. Development of low cost medium for ethanol production from syngas by Clostridium ragsdalei. Bioresource Technology 147, 508–515. https://doi.org/10.1016/j.biortech.2013.08.075

Girbal, L., Örlygsson, J., Reinders, B.J., Gottschal, J.C., 1997. Why Does Clostridium acetireducens Not Use Interspecies Hydrogen Transfer for Growth on Leucine? Curr Microbiol 35, 155–160. https://doi.org/10.1007/s002849900230

Grim, R.G., Huang, Z., Guarnieri, M.T., Ferrell, J.R., Tao, L., Schaidle, J.A., 2020. Transforming the carbon economy: challenges and opportunities in the convergence of low-cost electricity and reductive CO2 utilization. Energy Environ. Sci. 13, 472–494. https://doi.org/10.1039/C9EE02410G

Grimalt-Alemany, A., Asimakopoulos, K., Skiadas, I.V., Gavala, H.N., 2020. Modeling of syngas biomethanation and catabolic route control in mesophilic and thermophilic mixed microbial consortia. Applied Energy 262, 114502. https://doi.org/10.1016/j.apenergy.2020.114502

Grimalt-Alemany, A., Etler, C., Asimakopoulos, K., Skiadas, I.V., Gavala, H.N., 2021. ORP control for boosting ethanol productivity in gas fermentation systems and dynamics of redox cofactor NADH/NAD+ under oxidative stress. Journal of CO2 Utilization 50, 101589. https://doi.org/10.1016/j.jcou.2021.101589

Grimalt-Alemany, A., Łężyk, M., Kennes-Veiga, D.M., Skiadas, I.V., Gavala, H.N., 2019. Enrichment of Mesophilic and Thermophilic Mixed Microbial Consortia for Syngas Biomethanation: The Role of Kinetic and Thermodynamic Competition. Waste Biomass Valor. https://doi.org/10.1007/s12649-019-00595-z

Grimalt-Alemany, A., Łężyk, M., Lange, L., Skiadas, I.V., Gavala, H.N., 2018. Enrichment of syngas-converting mixed microbial consortia for ethanol production and thermodynamics-based design of enrichment strategies. Biotechnology for Biofuels 11, 198. https://doi.org/10.1186/s13068-018-1189-6

Groher, A., Weuster-Botz, D., 2016. General medium for the autotrophic cultivation of acetogens. Bioprocess Biosyst Eng 39, 1645–1650. https://doi.org/10.1007/s00449-016-1634-5

GRT gaz, 2019. Conditions techniques et économiques d'injection d'hydrogène dans les réseaux de gaz naturel.

Guillou, L., 2005. SYNTHESE DE FISCHER-TROPSCH EN REACTEURS STRUCTURES A CATALYSE SUPPORTEE EN PAROI (Génie des procédés). Ecole Centrale de Lille ; Université de Technologie de Compiègne.

Gujer, W., Zehnder, A.J.B., 1983. Conversion Processes in Anaerobic Digestion. Water Science and Technology 15, 127–167. https://doi.org/10.2166/wst.1983.0164

Hall, M., Beiko, R.G., 2018. 16S rRNA Gene Analysis with QIIME2, in: Beiko, R.G., Hsiao, W., Parkinson, J. (Eds.), Microbiome Analysis: Methods and Protocols, Methods in Molecular Biology. Springer, New York, NY, pp. 113–129. https://doi.org/10.1007/978-1-4939-8728-3_8

Hanselmann, K.W., 1991. Microbial energetics applied to waste repositories. Experientia 47, 645–687. https://doi.org/10.1007/BF01958816

Heffernan, J.K., Valgepea, K., de Souza Pinto Lemgruber, R., Casini, I., Plan, M., Tappel, R., Simpson, S.D., Köpke, M., Nielsen, L.K., Marcellin, E., 2020. Enhancing CO2-Valorization Using Clostridium autoethanogenum for Sustainable Fuel and Chemicals

Production. Frontiers in Bioengineering and Biotechnology 8, 204. https://doi.org/10.3389/fbioe.2020.00204

Henze, M., Gujer, W., Mino, T., van Loosdrecht, M.C.M., 2000. Activated sludge models ASM1, ASM2, ASM2d and ASM3. IWA Publishing, London.

Hu, P., Bowen, S.H., Lewis, R.S., 2011. A thermodynamic analysis of electron production during syngas fermentation. Bioresource Technology 102, 8071–8076. https://doi.org/10.1016/j.biortech.2011.05.080

Jacobi, H.F., Moschner, C.R., Hartung, E., 2009. Use of near infrared spectroscopy in monitoring of volatile fatty acids in anaerobic digestion. Water Science and Technology 60, 339–346. https://doi.org/10.2166/wst.2009.345

Jan, C., 2012. The metagenomic approach of chemosynthesis in deep oceanic hydrothermal systems : the case of bacterial symbiosis associated with shrimp Rimicaris exoculata (Theses). Université de Bretagne occidentale - Brest.

Jarrell, K.F., Kalmokoff, M.L., 1988. Nutritional requirements of the methanogenic archaebacteria. Can. J. Microbiol. 34, 557–576. https://doi.org/10.1139/m88-095

Jeoung, J.-H., Dobbek, H., 2007. Carbon Dioxide Activation at the Ni,Fe-Cluster of Anaerobic Carbon Monoxide Dehydrogenase. Science 318, 1461–1464. https://doi.org/10.1126/science.1148481

Jetten, M.S.M., Stams, A.J.M., Zehnder, A.J.B., 1992. Methanogenesis from acetate: a comparison of the acetate metabolism in Methanothrix soehngenii and Methanosarcina spp. FEMS Microbiol Rev 8, 181–197. https://doi.org/10.1111/j.1574-6968.1992.tb04987.x

Jin, Q., Bethke, C.M., 2007. The thermodynamics and kinetics of microbial metabolism. Am J Sci 307, 643–677. https://doi.org/10.2475/04.2007.01

Joshi, S., Robles, A., Aguiar, S., Delgado, A.G., 2021. The occurrence and ecology of microbial chain elongation of carboxylates in soils. ISME J 15, 1907–1918. https://doi.org/10.1038/s41396-021-00893-2

Kantzow, C., Mayer, A., Weuster-Botz, D., 2015. Continuous gas fermentation by Acetobacterium woodii in a submerged membrane reactor with full cell retention. Journal of Biotechnology 212, 11–18. https://doi.org/10.1016/j.jbiotec.2015.07.020

Karekar, S., Stefanini, R., Ahring, B., 2022. Homo-Acetogens: Their Metabolism and Competitive Relationship with Hydrogenotrophic Methanogens. Microorganisms 10, 397. https://doi.org/10.3390/microorganisms10020397

Kotsyurbenko, O.R., Glagolev, M.V., Nozhevnikova, A.N., Conrad, R., 2001. Competition between homoacetogenic bacteria and methanogenic archaea for hydrogen at low temperature. FEMS Microbiol Ecol 38, 153–159. https://doi.org/10.1111/j.1574-6941.2001.tb00893.x

Laguillaumie, L., Peyre-Lavigne, M., Grimalt-Alemany, A., Gavala, H.N., Skiadas, I.V., Paul, E., Dumas, C., 2023. Controlling the microbial competition between hydrogenotrophic methanogens and homoacetogens using mass transfer and thermodynamic constraints. Journal of Cleaner Production 414, 137549. https://doi.org/10.1016/j.jclepro.2023.137549

Laguillaumie, L., Rafrafi, Y., Moya-Leclair, E., Delagnes, D., Dubos, S., Spérandio, M., Paul, E., Dumas, C., 2022. Stability of ex situ biological methanation of H2/CO2 with a mixed microbial culture in a pilot scale bubble column reactor. Bioresource Technology 354, 127180. https://doi.org/10.1016/j.biortech.2022.127180

Lambie, S.C., Kelly, W.J., Leahy, S.C., Li, D., Reilly, K., McAllister, T.A., Valle, E.R., Attwood, G.T., Altermann, E., 2015. The complete genome sequence of the rumen methanogen Methanosarcina barkeri CM1. Standards in Genomic Sciences 10, 57. https://doi.org/10.1186/s40793-015-0038-5

Lee, M.J., Zinder, S.H., 1988. Isolation and Characterization of a Thermophilic Bacterium Which Oxidizes Acetate in Syntrophic Association with a Methanogen and Which Grows Acetogenically on H2-CO2. Appl. Environ. Microbiol. 54, 124–129.

Lewis, K., Epstein, S., D'Onofrio, A., Ling, L.L., 2010. Uncultured microorganisms as a source of secondary metabolites. J Antibiot 63, 468–476. https://doi.org/10.1038/ja.2010.87

Liew, F., Henstra, A.M., Winzer, K., Köpke, M., Simpson, S.D., Minton, N.P., 2016. Insights into CO2 Fixation Pathway of Clostridium autoethanogenum by Targeted Mutagenesis. mBio 7, e00427-16. https://doi.org/10.1128/mBio.00427-16

Liou, J.S.-C., Balkwill, D.L., Drake, G.R., Tanner, R.S.Y. 2005, 2005. Clostridium carboxidivorans sp. nov., a solvent-producing clostridium isolated from an agricultural settling lagoon, and reclassification of the acetogen Clostridium scatologenes strain SL1 as Clostridium drakei sp. nov. International Journal of Systematic and Evolutionary Microbiology 55, 2085–2091. https://doi.org/10.1099/ijs.0.63482-0

Liu, F., Monroe, E., Davis, R.W., 2018. Engineering Microbial Consortia for Bioconversion of Multisubstrate Biomass Streams to Biofuels. Biofuels - Challenges and opportunities. https://doi.org/10.5772/intechopen.80534

Liu, H., Wang, J., Wang, A., Chen, J., 2011. Chemical inhibitors of methanogenesis and putative applications. Appl Microbiol Biotechnol 89, 1333–1340. https://doi.org/10.1007/s00253-010-3066-5

Liu, K., Atiyeh, H.K., Tanner, R.S., Wilkins, M.R., Huhnke, R.L., 2012. Fermentative production of ethanol from syngas using novel moderately alkaliphilic strains of Alkalibaculum bacchi. Bioresource Technology 104, 336–341. https://doi.org/10.1016/j.biortech.2011.10.054

Luo, G., Jing, Y., Lin, Y., Zhang, S., An, D., 2018. A novel concept for syngas biomethanation by two-stage process: Focusing on the selective conversion of syngas to acetate. Science of The Total Environment 645, 1194–1200. https://doi.org/10.1016/j.scitotenv.2018.07.263

Madigan, M., Martinko, J., 2007. Brock Biologie des micro-organismes. Pearson Education France.

McInerney, M.J., Bryant, M.P., 1981. Basic Principles of Bioconversions in Anaerobic Digestion and Methanogenesis, in: Sofer, S.S., Zaborsky, O.R. (Eds.), Biomass Conversion Processes for Energy and Fuels. Springer US, Boston, MA, pp. 277–296. https://doi.org/10.1007/978-1-4757-0301-6_15

Ministère de la transition écologique et solidaire, 2020. Stratégie Nationale Bas-Carbone - Mars 2020.

Mohammadi, M., Mohamed, A.R., Najafpour, G.D., Younesi, H., Uzir, M.H., 2014. Kinetic Studies on Fermentative Production of Biofuel from Synthesis Gas Using Clostridium ljungdahlii [WWW Document]. The Scientific World Journal. https://doi.org/10.1155/2014/910590

Moletta, R., 2008. La méthanisation (2e ed.). Lavoisier.

Monod, J., 1942. Recherches sur la croissance des cultures bactériennes. Hermann.

Mordor Intelligence, 2020. Marché de l'acide acétique | 2022 - 27 | Part de l'industrie, taille, croissance - Mordor Intelligence [WWW Document]. URL https://www.mordorintelligence.com/fr/industry-reports/acetic-acid-market (accessed 4.27.22).

Moscoviz, R., Trably, E., Bernet, N., Carrère, H., 2018. The environmental biorefinery: state-of-the-art on the production of hydrogen and value-added biomolecules in mixed-culture fermentation. Green Chem. 20, 3159–3179. https://doi.org/10.1039/C8GC00572A

Nagarajan, H., Sahin, M., Nogales, J., Latif, H., Lovley, D.R., Ebrahim, A., Zengler, K., 2013. Characterizing acetogenic metabolism using a genome-scale metabolic reconstruction of

Clostridium ljungdahlii. Microbial Cell Factories 12, 118. https://doi.org/10.1186/1475-2859-12-118

Omar, B., Abou-Shanab, R., El-Gammal, M., Fotidis, I.A., Kougias, P.G., Zhang, Y., Angelidaki, I., 2018. Simultaneous biogas upgrading and biochemicals production using anaerobic bacterial mixed cultures. Water Research 142, 86–95. https://doi.org/10.1016/j.watres.2018.05.049

Park, J.O., Liu, N., Holinski, K.M., Emerson, D.F., Qiao, K., Woolston, B.M., Xu, J., Lazar, Z., Islam, M.A., Vidoudez, C., Girguis, P.R., Stephanopoulos, G., 2019. Synergistic substrate cofeeding stimulates reductive metabolism. Nat Metab 1, 643–651. https://doi.org/10.1038/s42255-019-0077-0

Paul, E., Bessière, Y., Dumas, C., Girbal-Neuhauser, E., 2021. Biopolymers Production from Wastes and Wastewaters by Mixed Microbial Cultures: Strategies for Microbial Selection. Waste Biomass Valor 12, 4213–4237. https://doi.org/10.1007/s12649-020-01252-6

Pavlostathis, S.G., Giraldo-Gomez, E., 1991. Kinetics of anaerobic treatment: A critical review. Critical Reviews in Environmental Control 21, 411–490. https://doi.org/10.1080/10643389109388424

Phillips, J.R., Clausen, E.C., Gaddy, J.L., 1994. Synthesis gas as substrate for the biological production of fuels and chemicals. Appl Biochem Biotechnol 45, 145–157. https://doi.org/10.1007/BF02941794

Prakash, D., Wu, Y., Suh, S.-J., Duin, E.C., 2014. Elucidating the Process of Activation of Methyl-Coenzyme M Reductase. Journal of Bacteriology 196, 2491–2498. https://doi.org/10.1128/JB.01658-14

Pratt, S., Liew, D., Batstone, D.J., Werker, A.G., Morgan-Sagastume, F., Lant, P.A., 2012. Inhibition by fatty acids during fermentation of pre-treated waste activated sludge. Journal of Biotechnology 159, 38–43. https://doi.org/10.1016/j.jbiotec.2012.02.001

Ragsdale, S.W., Pierce, E., 2008. Acetogenesis and the Wood–Ljungdahl pathway of CO2 fixation. Biochimica et Biophysica Acta (BBA) - Proteins and Proteomics 1784, 1873–1898. https://doi.org/10.1016/j.bbapap.2008.08.012

Ramió-Pujol, S., Ganigué, R., Bañeras, L., Colprim, J., 2015. Incubation at 25°C prevents acid crash and enhances alcohol production in Clostridium carboxidivorans P7. Bioresource Technology 192, 296–303. https://doi.org/10.1016/j.biortech.2015.05.077

Regueira, A., González-Cabaleiro, R., Ofițeru, I.D., Rodríguez, J., Lema, J.M., 2018. Electron bifurcation mechanism and homoacetogenesis explain products yields in mixed culture anaerobic fermentations. Water Research 141, 349–356. https://doi.org/10.1016/j.watres.2018.05.013

Reichert, P., 1994. AQUASIM – A TOOL FOR SIMULATION AND DATA ANALYSIS OF AQUATIC SYSTEMS. Water Science and Technology 30, 21–30. https://doi.org/10.2166/wst.1994.0025

RIVIERE, J., 1975. LES APPLICATIONS INDUSTRIELLES DE LA MICROBIOLOGIE.

Rodríguez, J., Kleerebezem, R., Lema, J.M., Loosdrecht, M.C.M. van, 2006a. Modeling product formation in anaerobic mixed culture fermentations. Biotechnology and Bioengineering 93, 592–606. https://doi.org/10.1002/bit.20765

Rodríguez, J., Lema, J.M., Kleerebezem, R., 2008. Energy-based models for environmental biotechnology. Trends in Biotechnology 26, 366–374. https://doi.org/10.1016/j.tibtech.2008.04.003

Rodríguez, J., Lema, J.M., van Loosdrecht, M.C.M., Kleerebezem, R., 2006b. Variable stoichiometry with thermodynamic control in ADM1. Water Science and Technology 54, 101–110. https://doi.org/10.2166/wst.2006.531

Roustan, M., 2003. Transferts gaz-liquide dans les procédés de traitement des eaux et des effluents gazeux - Michel Roustan, Lavoisiers. ed.

Salehizadeh, H., Yan, N., Farnood, R., 2020. Recent advances in microbial CO2 fixation and conversion to value-added products. Chemical Engineering Journal 124584. https://doi.org/10.1016/j.cej.2020.124584

Sánchez-Andrea, I., Guedes, I.A., Hornung, B., Boeren, S., Lawson, C.E., Sousa, D.Z., Bar-Even, A., Claassens, N.J., Stams, A.J.M., 2020. The reductive glycine pathway allows autotrophic growth of Desulfovibrio desulfuricans. Nat Commun 11, 5090. https://doi.org/10.1038/s41467-020-18906-7

Sander, R., 2015. Compilation of Henry's law constants (version 4.0) for water as solvent. Atmos. Chem. Phys. 15, 4399–4981. https://doi.org/10.5194/acp-15-4399-2015

Schönheit, P., Moll, J., Thauer, R.K., 1980. Growth parameters (Ks, μmax, Ys) of Methanobacterium thermoautotrophicum. Arch. Microbiol. 127, 59–65. https://doi.org/10.1007/BF00414356

Schuchmann, K., Müller, V., 2014. Autotrophy at the thermodynamic limit of life: a model for energy conservation in acetogenic bacteria. Nature Reviews Microbiology 12, 809–821. https://doi.org/10.1038/nrmicro3365

Shen, N., Dai, K., Xia, X.-Y., Zeng, R.J., Zhang, F., 2018. Conversion of syngas (CO and H2) to biochemicals by mixed culture fermentation in mesophilic and thermophilic hollow-fiber membrane biofilm reactors. Journal of Cleaner Production 202, 536–542. https://doi.org/10.1016/j.jclepro.2018.08.162

Simpson, S.D., Forster, R.L.S., Rowe, M., 2007. Microbial fermentation of gaseous substrates to produce alcohols. WO2007117157A1.

Spring, S., Rosenzweig, F., 2006. The Genera Desulfitobacterium and Desulfosporosinus: Taxonomy, in: Dworkin, M., Falkow, S., Rosenberg, E., Schleifer, K.-H., Stackebrandt, E. (Eds.), The Prokaryotes: Volume 4: Bacteria: Firmicutes, Cyanobacteria. Springer US, New York, NY, pp. 771–786. https://doi.org/10.1007/0-387-30744-3_24

Steinbusch, K.J.J., Hamelers, H.V.M., Plugge, C.M., Buisman, C.J.N., 2011. Biological formation of caproate and caprylate from acetate: fuel and chemical production from low grade biomass. Energy Environ. Sci. 4, 216–224. https://doi.org/10.1039/C0EE00282H

Thauer, R.K., Jungermann, K., Decker, K., 1977. Energy conservation in chemotrophic anaerobic bacteria. Bacteriol Rev 41, 100–180.

Theil, S., Rifa, E., 2021. rANOMALY: AmplicoN wOrkflow for Microbial community AnaLYsis. F1000Res 10, 7. https://doi.org/10.12688/f1000research.27268.1

Tlili, A., Frogneux, X., Blondiaux, E., Cantat, T., 2014. Creating Added Value with a Waste: Methylation of Amines with CO2 and H2. Angewandte Chemie International Edition 53, 2543–2545. https://doi.org/10.1002/anie.201310337

Toulouse-Blagnac (Haute-Garonne - France) | Relevés météo en temps réel - Infoclimat [WWW Document], n.d. URL https://www.infoclimat.fr/observations-meteo/temps-reel/toulouse-blagnac/07630.html (accessed 4.20.22).

Valgepea, K., de Souza Pinto Lemgruber, R., Abdalla, T., Binos, S., Takemori, N., Takemori, A., Tanaka, Y., Tappel, R., Köpke, M., Simpson, S.D., Nielsen, L.K., Marcellin, E., 2018. H2 drives metabolic rearrangements in gas-fermenting Clostridium autoethanogenum. Biotechnology for Biofuels 11, 55. https://doi.org/10.1186/s13068-018-1052-9

Valgepea, K., de Souza Pinto Lemgruber, R., Meaghan, K., Palfreyman, R.W., Abdalla, T., Heijstra, B.D., Behrendorff, J.B., Tappel, R., Köpke, M., Simpson, S.D., Nielsen, L.K., Marcellin, E., 2017. Maintenance of ATP Homeostasis Triggers Metabolic Shifts in Gas-Fermenting Acetogens. Cell Systems 4, 505-515.e5. https://doi.org/10.1016/j.cels.2017.04.008

Vavilin, V.A., Lokshina, L.Ya., Rytov, S.V., Kotsyurbenko, O.R., Nozhevnikova, A.N., 2000. Description of two-step kinetics in methane formation during psychrophilic H2/CO2 and mesophilic glucose conversions. Bioresource Technology 71, 195–209. https://doi.org/p

Vigliar, E., Malapelle, U., de Luca, C., Bellevicine, C., Troncone, G., 2015. Challenges and opportunities of next-generation sequencing: a cytopathologist's perspective. Cytopathology 26, 271–283. https://doi.org/10.1111/cyt.12265

Villemur, R., Lanthier, M., Beaudet, R., Lépine, F., 2006. The Desulfitobacterium genus. FEMS Microbiology Reviews 30, 706–733. https://doi.org/10.1111/j.1574-6976.2006.00029.x

Wahid, R., Mulat, D.G., Gaby, J.C., Horn, S.J., 2019. Effects of H2:CO2 ratio and H2 supply fluctuation on methane content and microbial community composition during in-situ biological biogas upgrading. Biotechnol Biofuels 12, 104. https://doi.org/10.1186/s13068-019-1443-6

Walters, W., Hyde, E.R., Berg-Lyons, D., Ackermann, G., Humphrey, G., Parada, A., Gilbert, J.A., Jansson, J.K., Caporaso, J.G., Fuhrman, J.A., Apprill, A., Knight, R., 2015. Improved Bacterial 16S rRNA Gene (V4 and V4-5) and Fungal Internal Transcribed Spacer Marker Gene Primers for Microbial Community Surveys. mSystems 1, e00009-15. https://doi.org/10.1128/mSystems.00009-15

Wang, Y., Zhang, Y., Wang, J., Meng, L., 2009. Effects of volatile fatty acid concentrations on methane yield and methanogenic bacteria. Biomass and Bioenergy 33, 848–853. https://doi.org/10.1016/j.biombioe.2009.01.007

Wang, Y.-Q., Yu, S.-J., Zhang, F., Xia, X.-Y., Zeng, R.J., 2017. Enhancement of acetate productivity in a thermophilic (55 °C) hollow-fiber membrane biofilm reactor with mixed culture syngas (H2/CO2) fermentation. Appl Microbiol Biotechnol 101, 2619–2627. https://doi.org/10.1007/s00253-017-8124-9

Wang, Y.-Q., Zhang, F., Zhang, W., Dai, K., Wang, H.-J., Li, X., Zeng, R.J., 2018. Hydrogen and carbon dioxide mixed culture fermentation in a hollow-fiber membrane biofilm reactor at 25 °C. Bioresource Technology 249, 659–665. https://doi.org/10.1016/j.biortech.2017.10.054

Weijma, J., Gubbels, F., Hulshoff Pol, L.W., Stams, A.J.M., Lens, P., Lettinga, G., 2002. Competition for H2 between sulfate reducers, methanogens and homoacetogens in a gas-lift reactor. Water Sci Technol 45, 75–80. https://doi.org/10.2166/wst.2002.0294

Welsby, D., Price, J., Pye, S., Ekins, P., 2021. Unextractable fossil fuels in a 1.5 °C world. Nature 597, 230–234. https://doi.org/10.1038/s41586-021-03821-8

Westerholm, M., Dolfing, J., Schnürer, A., 2019. Growth Characteristics and Thermodynamics of Syntrophic Acetate Oxidizers. Environ. Sci. Technol. 53, 5512–5520. https://doi.org/10.1021/acs.est.9b00288

Wood, H.G., Ragsdale, S.W., Pezacka, E., 1986. The acetyl-CoA pathway of autotrophic growth. FEMS Microbiology Reviews 2, 345–362. https://doi.org/10.1111/j.1574-6968.1986.tb01865.x

Yan, B.H., Selvam, A., Xu, S.Y., Wong, J.W.C., 2014. A novel way to utilize hydrogen and carbon dioxide in acidogenic reactor through homoacetogenesis. Bioresource Technology 159, 249–257. https://doi.org/10.1016/j.biortech.2014.02.014

Younesi, H., Najafpour, G., Mohamed, A.R., 2005. Ethanol and acetate production from synthesis gas via fermentation processes using anaerobic bacterium, Clostridium ljungdahlii. Biochemical Engineering Journal 27, 110–119. https://doi.org/10.1016/j.bej.2005.08.015

Zhang, F., Ding, J., Shen, N., Zhang, Y., Ding, Z., Dai, K., Zeng, R.J., 2013a. In situ hydrogen utilization for high fraction acetate production in mixed culture hollow-fiber membrane biofilm reactor. Appl Microbiol Biotechnol 97, 10233–10240. https://doi.org/10.1007/s00253-013-5281-3

Zhang, F., Ding, J., Zhang, Y., Chen, M., Ding, Z.-W., van Loosdrecht, M.C.M., Zeng, R.J., 2013b. Fatty acids production from hydrogen and carbon dioxide by mixed culture in the membrane biofilm reactor. Water Research 47, 6122–6129. https://doi.org/10.1016/j.watres.2013.07.033